Tissue distribution of Influenza virus receptors in mammalian hosts using Tissue Microarrays

Andreas Papanikolaou, Supervisor: **Kim M. Bouwman**, Principal investigator: **Dr. M. Hélène Verheije**
Department of Pathobiology, Faculty of Veterinary Medicine, Utrecht University, Utrecht, The Netherlands

Abstract

Susceptibility of a host to a virus requires the expression of virus-specific receptors. These are host molecules present on the cell surface that support the binding of specific viral attachment proteins. The receptors for many viruses, including influenza A virus, have previously been elucidated. However, their tissue and host distribution contributing to the susceptibility of species is often not well understood. In order to broaden our knowledge on the expression of these host molecules, we aimed at creating tissue microarrays (TMA) of various mammalian species. In particular, TMAs represent the true complexity of cell surface molecules present in a host and are therefore excellent tools to study virus-host interactions. This technique still faced several technical drawbacks. Here, we first technically optimized the TMA construction method such that tissue-slides were easier easier and more intact generated. Subsequently, a variety of tissues of pig, dog and horse of animals that were submitted to the necropsy hall of the Pathobiology department. Formalin-fixed, paraffin embedded tissues were analyzed and healthy tissues from these animals were selected based on microscopic evaluation of tissue slides. Tissue cores of each of the tissues were combined in one tissue block to generate (monospecies or multispecies) porcine, canine and equine TMAs, respectively. From these TMA blocks, tissue-slides were generated to study viral receptor expression. First, the tissue distribution of the sialic acids Neu5Acα2-3Gal (α2-3 linked sialic acid) and Neu5Acα2-6Gal (α2-6 linked sialic acid), was studied using the plant-derived lectins; Maackia amurensis lectins I & II and the Sambucus nigra lectin. These sialic acids constitute the viral receptors of avian and human influenza A viruses, respectively. Next, we studied the binding of the viral attachment proteins HA of various influenza A subtypes using protein histochemistry assays. To study interspecies variation of these different IVA receptors, a monospecies TMA composed of tissues of six anatomic locations of the respiratory tracts from six animals were compared. We observed that the variability of sialic acid expression in the same regions was low, indicating that TMAs composed of tissues of one animal already provide sufficient information in order to draw valid conclusions for larger animal groups. Interestingly, in the porcine respiratory tract, co-expression of Neu5Acα2-3Gal and Neu5Acα2-6Gal was only detected in the lower regions of the respiratory tract, and was absent in the trachea, suggesting that the current hypothesis that pigs can function as a 'mixing vessel' for IAVs, is disputable. In order to gain insight to the interspecies transmission of equine IAVs to the canine population, we analyzed the presence of Neu5Acα2-3Gal & Neu5Gcα2-3Gal receptor expression in equine and canine tissues. Lectin staining revealed that Neu5Acα2-3Gal was expressed in various canine and equine tissues, which was confirmed by the specific binding of HA-H3, of equine IAV subtype, to respiratory tract tissue of both species. In contrast, Neu5Gcα2-3Gal expression could only be detected in equine tissues upon staining of TMA slides with a specific antibody, which was in agreement with the protein binding of HA-H7 of equine IAV subtype to equine, but not canine tissues. These results might explain that H3 IAVs of equine origin have crossed the species barrier to dogs, while this has not been observed for H7 IAVs. Taken together, the generated TMAs of various mammalian species provide an excellent tool for the analysis of the distribution of viral receptors in multiple host species, thereby increasing our understanding of host susceptibility and interspecies transmission for particular viruses.

Introduction

The lack of knowledge regarding the distribution of viral receptors on host tissues and the binding properties of viral proteins lead to difficulty in predicting, preventing and managing outbreaks. Susceptibility of an individual to a virus, either human or not, is determined by various factors. One of them is the successful interaction between the host and the virus allowing the subsequent infection of a cell. The interaction is defined by the attachment of a viral particle to a host molecule expressed on the cellular surface, which is called a receptor. Since the first step to susceptible host tissues is the expression of the viral-specific receptor, is it is important to know which molecules are used by the viruses as receptors and what the distribution is on the host's tissues. Viral receptor preference is extensively studied around the globe and therefore most of the viral receptors have been described. However, the tissue distribution of viral receptors is not a popular research subject, leading to uncertainties about host and tissue susceptibility.

Analyzing the tissues of a species can be facilitated by the use of a tissue microarray. It demonstrates the complexity of the cellular surface in an accurate manner, allowing the comparison of the data to the in vivo situation, but also allowing the use of multiple tissues simultaneously. The first idea of incorporating multiple tissue-cores in one paraffin block was envisioned by Hector Battifora in 1986. He described a method of embedding 100 or more different tissue samples in a paraffin block, which he dubbed the multitumor tissue block (MTTB). The MTTB was constructed by wrapping tissue cores into a sheet of small mammal intestine before being imbedded in paraffin blocks in order to be cut. Battifora developed the MTTB for immunohistochemical antibody testing and as a quality control for routine procedures, as it diminished most of the variation causes between tissue samples (Battifora 1986). The technique was adapted by Kononen in 1998 (Kononen, Bubendorf et al. 1998), and was used to rapidly analyze hundreds of molecular markers of human tumor tissues. Kononen revised the construction procedure, developing a custom instrument which consisted of a thin-walled stainless steel tube, a stainless steel wire that acted as a stylet and a precision guide, which could move in the x-y axis. The punched tissue cores were placed in a pre-formed recipient paraffin blocks. In this procedure as many as 1000 different specimens could be placed on one array block. As a result, the analysis of morphological and molecular aspects of tumors was revolutionized and simplified for future generations (Kononen, Bubendorf et al. 1998). The usefulness of TMAs is demonstrated by numerous publications (Camp, Charette et al. 2000, Packeisen, Buerger et al. 2002, Hans, Weisenburger et al. 2004), following the publication of Kononen, and it is most commonly used to analyze molecular markers, such as RNA, DNA and proteins, and less commonly used in immunohistochemical procedures.

The usefulness of such array in infection biology has been demonstrated by our research group, using avian coronaviruses recombinant attachment proteins on an avian multispecies TMA (Wickramasinghe, de Vries et al. 2015) and proved to be an excellent tool for elucidating the tissue distribution of viral receptors. The multi-species avian TMA was used in combination with the attachment glycoprotein spike (S1) of avian coronavirus (infectious bronchitis virus) and the hemagglutinin protein of influenza A virus H5N1, in order to compare attachment characteristics between the different avian species. In addition, single species TMAs were used to study tissue and glycan binding profiles of spike glycoproteins of different avian coronaviruses revealing a novel receptor for the turkey coronavirus (TCoV) (Wickramasinghe, de Vries et al. 2015). The conclusion was that the tissue microarrays provide a fast and cost effective way to elucidate host and tissue binding profiles of viral attachment proteins (Wickramasinghe, de Vries et al. 2015). In this study, mammalian hosts were chosen in order to gain insights about the expression of viral receptors, and in particular, receptors of the Influenza genus. The receptor preference is unquestionably well described, but that is not the case for the tissue distribution of the receptor in susceptible hosts.

Firstly, we wanted to investigate the Influenza A virus (IAV) receptor in particular. The virus belongs to the Orthmyxoviridae family, which are enveloped, segmented, negative-stranded RNA viruses, and tend to form a short-lived relationship with their infected host. One of the proteins incorporated in the virion, the attachment protein hemagglutinin (HA), determines the receptor binding ability of each viral strain (Skehel, Wiley 2000). It is a type I membrane glycoprotein, and is comprised of three identical subunits (Russell, Gamblin et al. 2013). The receptor binding site is present on the most membrane-distal part of the trimer, and is capable of recognizing cell-bound glycoproteins which are used as the viral receptor (Russell, Gamblin et al. 2013). N-acetylneuraminic acid, or sialic acid, is a terminal saccharide of the carbohydrate side-chains of cell surface glycoproteins, and is known to be the receptor of most of the IAVs (Skehel, Wiley 2000). As mentioned before, the attachment of the virion to the host cell receptor comprises a fundamental first step needed for the journey which leads to an infected cell. Influenza A has been described in humans, aquatic birds, domestic poultry, equids, suids, canids, felids and also in many aquatic mammals. Avian and equine IAVs preferentially bind α2,3 linked sialic acids, human IAVs prefer the α2,6 linkage, and porcine IAVs can bind to both linkages (Russell, Gamblin et al. 2013). The expression of different linked sialic acids, and their presence on different anatomic regions might comprise a relatively strong barrier against large outbreaks of one virus type in all species, but does not necessarily mean that it cannot cause a large epidemic in one of the susceptible species. The zoonotic potential of the IAV is underlined by the capability of the virus to switch receptor specificity, thus redefining which species are susceptible for a particular strain.

Secondly, another distant member of the Influenza genus, the newly described influenza D virus (IDV), is also an interesting candidate for further investigation of the host susceptibility and tissue preference. IDV shares only ±50% overall amino acid identity with its closest relatives of the influenza C genus, and was therefore classified as a new genus within the Orthmyxoviridae family (Hause, Collin et al. 2014, Ducatez, Pelletier et al. 2015). The primary infected species consist of suids and bovines (Hause, Ducatez et al. 2013). One of the striking differences between IAVs and IDVs is the composition of the attachment protein. The IDV possesses a major surface bound glycoprotein, the hemagglutinin-esterase-fusion (HEF) protein, which is capable of receptor binding, receptor destroying and membrane fusion activities (Song, Qi et al. 2016). These functions are separated in Influenza A viruses, with the hemagglutinin protein being responsible for the receptor binding properties and the neuraminidase protein for the receptor destroying properties. The IDV uses 9-O-Acetylated sialic acids as its receptor, and protein binding studies reveal attachment to bovine, porcine and human tracheas (Song, Qi et al. 2016). This is confirmed by seroprevalence studies in the pigs and humans (Hause, Ducatez et al. 2013). IDV is also commonly seen in combination with various viral and bacterial pathogens causing the multifactorial bovine respiratory disease complex, mostly seen in post-weaning calves (Collin, Sheng et al. 2015). Little information is available on the tissue distribution of the 9-O-Acetylated sialic acids in different species. In addition, the fact that humans can be seropostitive for IDV antibodies, can be isolated from humans (Hause, Ducatez et al. 2013), thus demonstrating zoonotic characteristics, makes it wise to investigate the localization of the viral receptor in the susceptible species reservoir in order to gain more knowledge about the susceptibility and interspecies transmission characteristics.

To expand our knowledge about tissue distribution of viral receptors in mammalian hosts, we aimed at the development of mammalian TMAs and combining them with protein histochemistry. Firstly, the procedure of creating the TMA was optimized, making the creation of TMA blocks and the generation of tissue slides easier. This facilitates the use for non-specialized researchers. First, we analyzed the presence of Neu5Acα2-3Gal and Neu5Acα2-6Gal in the porcine, canine and equine respiratory tract with plant derived lectins and confirmed the data with the use of recombinant produced hemagglutinin proteins. We also analyzed the presence of Neu5Gcα2-3Gal in the canine and equine tissues since it plays a major role in the infection cycle of several equine IAVs. Next, we developed a bovine TMA consisting of various tissues in order to analyze the presence of 9-O-Acetylated sialic acids. We opted to analyze the distribution of this type of sialic acid by recombinantly producing and using the attachment protein of Influenza D virus, (HEF-1). We observed that Neu5Acα2-3Gal and Neu5Acα2-6Gal are both present in the lower porcine respiratory tract, but not in the upper regions. Furthermore, we detected presence of Neu5Acα2-3Gal in both the equine and the canine respiratory tract, but Neu5Gcα2-3Gal was only detected in the equine tract. The use of tissue microarrays will strengthen the concept that they are excellent tools for obtaining more information about host-virus interaction in the early steps of an infection and that they facilitate the fast analysis of tissues.

Materials & methods

Ethics statement

The tissues used for this study were collected from animals that were submitted to the Pathology Department or Dutch Wildlife Health Center of the Faculty Veterinary Medicine (Department of Pathobiology, Faculty of Veterinary Medicine, Utrecht University, The Netherlands). Furthermore, tissues were collected from euthanized animals from ongoing animal experiments executed by other research groups within the faculty. The use of tissues of already deceased animals does not require the permission of the Committee on the Ethics of Animal Experiment. Moreover, human tissues were obtained from the University Medical Centre Utrecht (UMCU). Anonymous use of human tissue does not require the permission of the Medical research Ethics Committee.

Animal tissues & Processing

Tissues were collected at the necropsy facilities of the Pathobiology department at the Veterinary medicine faculty of Utrecht University, or send to us via collaborators (table 1).

Table 1. Characteristics of the animals collected.

Species	No. of animals	Age	Sex	Reason of submission	Source
Pig -Sus scrofa	7	6-8mo	F/M	Negative control group DECnr: n/a	Pathology dept.
Horse -Equus ferus caballus	1	1y 7mo	F	Diagnostic reasons GLIMSnr: 316112103601	Pathology dept.
Dog -Canis familiaris	1	1y 7mo	F	Negative control group DECnr: 2014.II.08.064.	Pathology dept.
Cow -Bos taurus	3	unknown	F/M	Negative control group DECnr: n/a	Collaborators

The porcine tissues were collected through an ongoing animal experiment. The pigs were euthanized and submitted to the pathology department for further sampling. Tissues were collected while the carcass was still fresh. The H&E staining showed minimal damage to the epithelium and to subsequent layers. The morphology was well preserved in all tissues, and were devoid of immunological reactions, except of minor presence of inflammatory cells in the lower gastrointestinal tract.

The mare was submitted to the clinic of the faculty of Veterinary medicine with severe abdominal pain. After euthanazation, the horse was submitted to the pathology department for diagnostic procedures. All tissues, except of parts of the caecum and colon, were in good morphological condition without immunological responses. The caecum and colon were damaged through an intussusception of the caecum in colon and could not be used completely. Macroscopically undamaged samples were collected of that area.

The canine tissues were submitted to the pathology department as part of an ongoing animal experiment within the faculty. No macroscopic or microscopic changes were noted.

Bovine tissues were received from an ongoing animal experiment of our collaborator Dr. M. Ducatez from the École nationale vétérinaire de Toulouse. The tissues were submitted in the form of pre-sampled specimens, preserved in 70% alcohol in airtight locked containers. The majority of the samples were in good morphological condition and could be used for further processing.

In total we obtained tissues from 12 different animals and 4 different species.

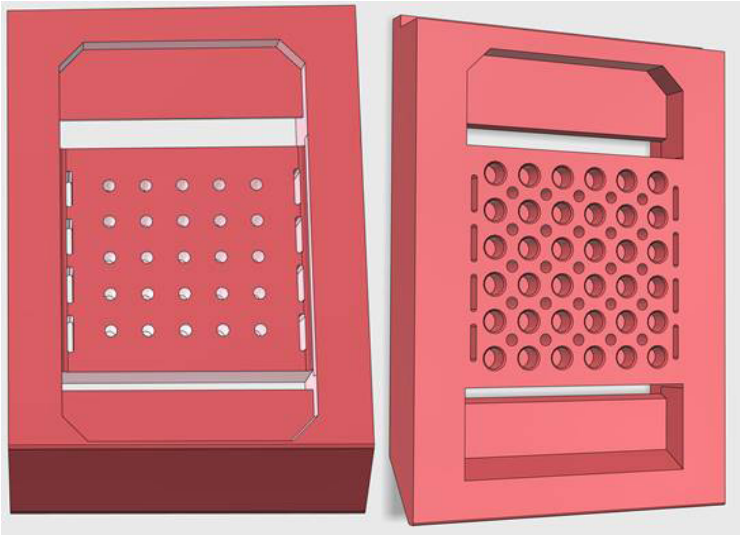

Figure 1. Tissue microarray, depicted schematically. Designed with 123D Design, Autodesk.

The tissues were trimmed in appropriate sizes (max. 3x2 cm length and 3 mm width) and placed into organ-specific labelled cassettes. The tissues were fixed in 4% neutral buffered formaldehyde (Klinipath BV, cat#4078-9020, The Netherlands) overnight with a minimal formaldehyde to tissue ratio of 10:1. Further processing included dehydration in different concentrations of alcohol (50%, 70%, 85%, 96% and 100%) and intermediate clearing with xylene (cat#: 4055-9005, Klinipath BV, The Netherlands). Once dehydrated, they were embedded in paraffin (Paraclean Histology Wax, cat#: 2079, Klinipath BV, The Netherlands). The paraffin blocks were sectioned to 4 µm thick sections, using a Reichert/Leica 2030 Microtome, and placed on microscope slides (KP frost slides / KP plus printer slides, Klinipath BV, The

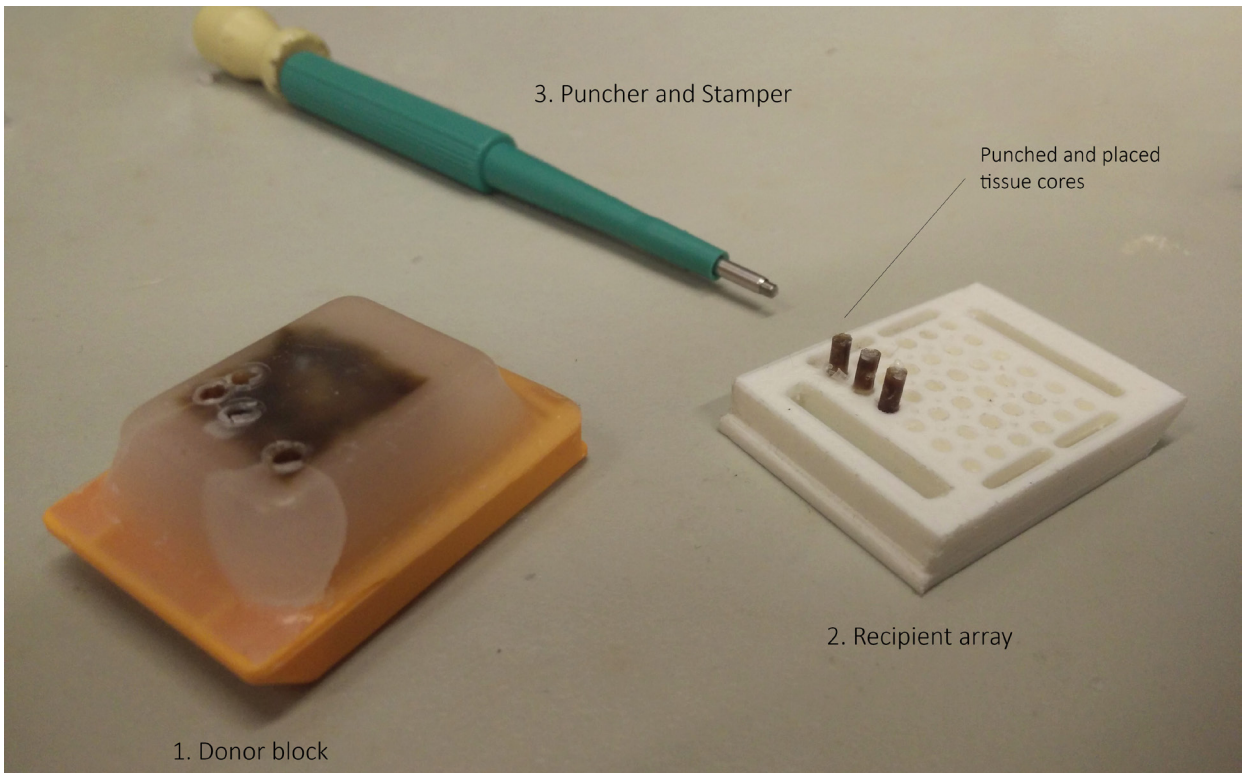

Figure 2. Overview of the placing procedure. 1: Donor tissue block, 2: Recipient array, 3: Puncher and stamper.

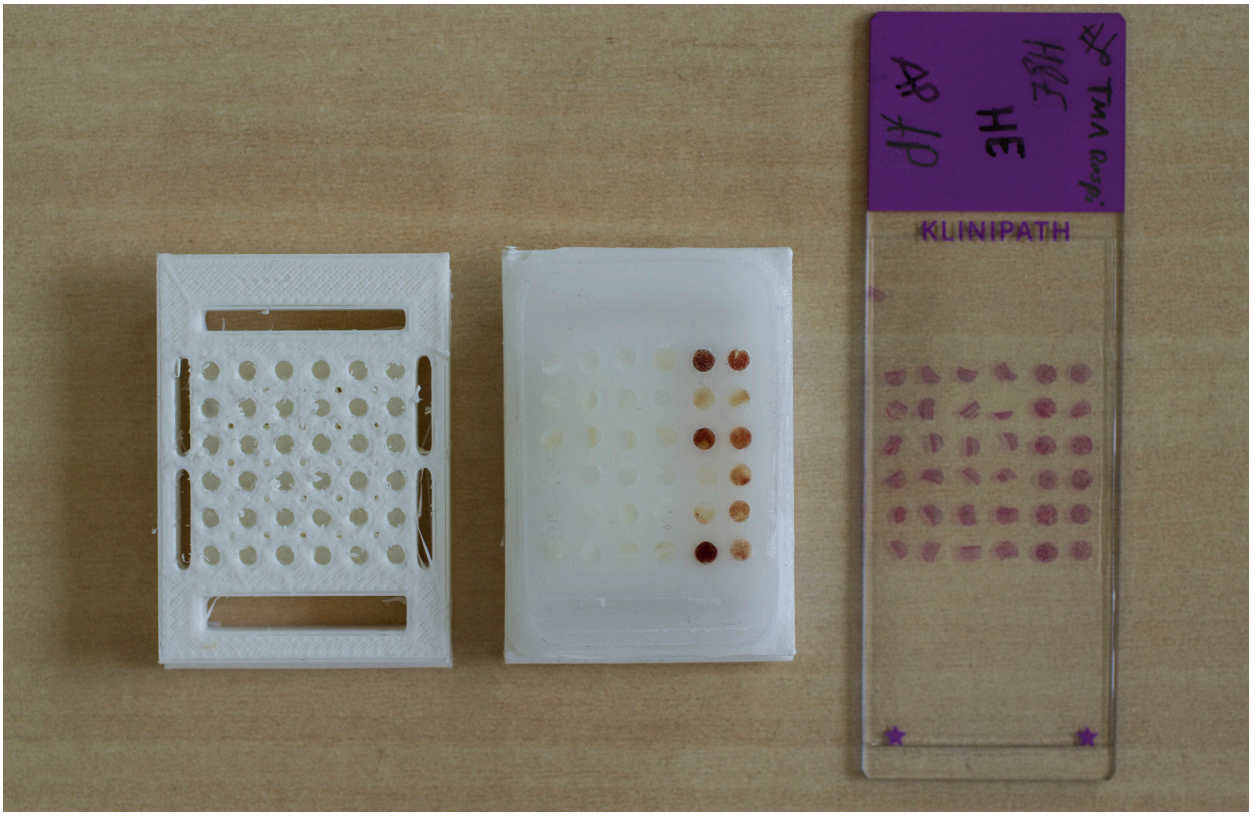

Figure 3. Overview of the different preparation steps. From empty array plate to filled array paraffin block to H&E stained tissue section.

Netherlands). Sections were stained with hematoxylin and eosin (H&E), and assessed microscopically for histological analysis performed by a certified pathologist. The analysis consisted of the selection of areas with a morphology analogous to the specific organ, devoid of pathological changes and absence of immune reactions. The positions were marked in order to be punched for the preparation of a tissue microarray.

Preparation of tissue microarray (TMA)

Preparation of a tissue microarray (TMA) was previously performed using the procedure described in (Wickramasinghe, de Vries et al. 2015). The described procedure resulted, unfortunately, in loss of tissue during the process of sectioning and the following protein histochemistry.
To improve the procedure, an array plate was designed (software 123D Design, Autodesk Inc.) and printed with a 3D-printer (Sigma, BCN3D Technologies, Spain), using polylactic acid filament (PLA, thickness 2.85mm). The plate was designed to contain 36 holes of ±1,9-mm diameter (fig. 1), in which tissue cores could be placed. Subsequently to printing, tissue cores were punched from the donor paraffin blocks and placed into the holes of the plate (fig. 2). The plate was embedded in paraffin and after solidification (±24 hours), 4µm sections were sectioned from these TMA's. The array blocks were then sectioned into 4 µm TMA serial sections and mounted on numbered microscopes slides (KP frost slides / KP plus printer slides, Klinipath BV, The Netherlands). One slide of each array block was stained with H&E, for quality control and identification of different cell types in each tissue (fig. 3). The remaining slides were stored at 4°C until further processing such as lectin and protein histochemistry. Where possible, serial sections were used in order to ensure maximum similarity of the tissues. Three TMA blocks were created (for species & placement map, see annex I; table 1 to 3); a TMA consisting of a selection of various organs of one porcine individual, a TMA consisting of respiratory tract tissues of six different non-related porcine individuals and a TMA consisting of respiratory tract tissues of canine and equine individuals. The organs of the TMA of one porcine individual were as followed: the respiratory tract was represented by the nasal epithelium, nasopharynx, primary bronchus, upper and lower trachea, and lung. The gastrointestinal tract was represented by the soft palate, epiglottis, larynx, oesophagus, stomach, duodenum, jejunum, ileum, caecum and colon. Additional organs were the liver, kidney, heart, spleen, pancreas, thymus, bladder, adrenal gland, lymphnodes, pharyngeal tonsil, conjunctiva and the ovarium with the uterus. At last, the central nervous system was represented by the following parts: cerebrum, cerebellum, hypophysis, bulbus olphactorius, brain stem and the sciatic nerve. The tissues used from the six non-related porcines were the upper-, mid-, and lower trachea, primary bronchus, bronchiole and alveoli. The equine-canine combination TMA consisted of the bulbus olphactorius, kidney, laryngeal epithelium, lower trachea epithelium, lung, nasal epithelium, oropharynx, primary bronchus, upper trachea epithelium and the soft palate.

Lectin staining

Lectin stainings (lectins MALI (Maackia amurensis lectin I, cat#: B-1315), MALII (Maackia amurensis lectin

II, cat#: B-1265) and SNA (Sambucus nigra lectin, cat#: B-1305) (Vector Laboratories, USA) were performed on one section of each TMA. The lectins were used in the following concentrations: SNA with a concentration of 10 µg/ml, MALII with 10µg/ml and MALI with 15 µg/ml. The tissue sections were deparaffinized with xylene (cat#: 4055-9005, Klinipath BV, The Netherlands), twice for 5 minutes followed by dehydratation with 100%, 96% and 70% alcohol (cat#: 4096-9005, Klinipath BV, The Netherlands), twice for 3 minutes in each concentration. After rinsing in distilled water, antigen retrieval was performed in preheated 10 mM sodium citrate (cat#: 100244 , Merck KGaA, Germany) (pH adjusted to 6.0 with 10 mM NaOH, cat#: 106462, Merck KGaA, Germany) for 10 minutes. Cooling down the slides to ±20˚C, was followed by inactivating the endogenous peroxidase by incubating the slides in 1% hydrogen peroxide (cat#: 108600, Merck KGaA, Germany) in methanol (cat#: 106009, Merck KGaA, Germany) for 30 minutes at room temperature. After washing with Phosphate-Buffered Saline – Tween 20 (PBS-T), 0,1%, the slides were treated with 1x Carbo-free blocking solution (cat#: SP-5040, Vector laboratories Inc., USA) for 60 minutes at room temperature. After removing the blocking solution, the slides were incubated with bionylated lectins for 30 minutes at room temperature in a humidity chamber. After rinsing thrice with PBS-T 0,1%, the tissue slides were incubated with avidin-biotin complex HRP (ABC-kit, cat#: PK6100, Vectastain, Vector laboratories Inc., USA) for 30 minutes at room temperature, followed by rinsing thrice with PBS. To visualize the staining, slides were incubated with 3-amino-9-ethyl-carbazole (AEC, cat#: K3469, Dako, Denmark A/S) for 15 minutes at room temperature in a dark humidity chamber and subsequently counterstained with hematoxylin for 45 seconds. Presence of the peroxidase of the ABC-kit would react with the AEC and result in red color staining, thus revealing the presence of the lectin, whilst hematoxylin associates and stains the nucleus blue. After rinsing with tap water, the tissue slides were mounted with aquatex (cat#: 108562, Merck KGaA, Germany). Images were captured using a charge-coupled device (CCD) camera, and an Olympus BX41 microscope linked to Cell^B imaging software (Soft Imaging Solutions GmbH, Münster, Germany). Stained slides were assessed for positivity by the student first and were subsequently discussed with the complete research group.

Genes and expression vectors

The sequence encoding for the Influenza D attachment protein, HEF-1, was obtained from our collaborators in France (virus isolate: IDV/bovine/France/5920/2014). Using that sequence, a codon optimized sequence was ordered from GenScript and was cloned into a pCD5 expression vector by restriction enzyme digestion, using the upstream NheI and downstream PacI restriction sites. At the N-terminus, the CD5 signal peptide was followed by the HEF-1 gene (2049 bp, 683 amino acids) and at the C-terminus, a GCN4 trimerization domain (GCN4; RMKQIEDKIEEIESKQKKIENEIARIKK-LVPRGSLE) was followed by a Strep-Tag II (ST; WSHPQFEK, IBA GmbH, Germany), resulting in pCD5-HEF-EctoDomain-GCN4T-ST. Also, three mutations were introduced into the sequence in order to reduce the esterase activity of the protein (on positions S57, D356 and H359). In addition, 2 smaller construct were designed, based on a previous publication on the HEF-1 structure (Song, Qi et al. 2016). The first additional construct, coded for the amino acids 1 to 605 and the second for the amino acids 1 to 439. All three mentioned constructs were also cloned into a pCD5 plasmid by Dr. R. P. de Vries. These constructs contained a Strep-Tag II and a superfolding GFP-protein (MSKGEELFTGVVPILVELDGDVNGHKFSVRGEGEGDATNGKLTLKFICTTGKLPVPWPTLVTTLTYGVQCFSRYPDHMKRHDFFKSAMPEGYVQERTISFKDDGTYKTRAEVKFEGDTLVNRIELKGIDFKEDGNILGHKLEYNFNSHNVYITADKQKNGIKANFKIRHNVEDGSVQLADHYQQNTPIGDGPVLLPDNHYLSTQSVLSKDPNEKRDHMVLLEFVTAAGITHGM, (Pédelacq, Cabantous et al. 2006)). Table 2 gives an overview of the created constructs including their characteristics.

Table 2. Characteristics of the designed HEF constructs.

Construct name	Sequence length	Vector	Strep-Tag	GFP sequence	Multimeric form
pCD5-HEF-ED-GCN4-ST	1-683	pCD5	1	-	Trimer
pCD5-HEF-1-605-GCN4-ST	1-605	pCD5	1	-	Trimer
pCD5-HEF-1-439-GCN4-ST	1-439	pCD5	1	-	Trimer
pCD5-HEF-ED-GCN4-Di-GFP-STST	1-683	pCD5	2	present	Dimer
pCD5-HEF-1-605-GCN4-Di-GFP-STST	1-605	pCD5	2	present	Dimer
pCD5-HEF-1-439-GCN4-Di-GFP-STST	1-439	pCD5	2	present	Dimer
pCD5-HEF-ED-GCN4-Tri-GFP-STST	1-683	pCD5	2	present	Trimer
pCD5-HEF-1-605-GCN4-Tri-GFP-STST	1-605	pCD5	2	present	Trimer
pCD5-HEF-1-439-GCN4-Tri-GFP-STST	1-439	pCD5	2	present	Trimer

Table 3. Hemagluttinin proteins received from Dr. R. P. de Vries, including virus strains, described host, modifications and receptor binding preference.

Virus Strain	Multimeric form	Described Host	Modifications*	Preference	Publication
A/Puerto Rico/8/1934 (H1N1)	Trimer (GCN4-trimerization domain - C-terminus)	Human	E190D mutation	α2,6 linked Neu5Ac	(Xu, McBride et al. 2012)
A/California/04/2009 (H1N1)*	Trimer (GCN4-trimerization domain - C-terminus)	Human	D190E, I219A, G225D, and E227A mutations	α2,3 linked Neu5Ac	(Lakdawala, Jayaraman et al. 2015)
A/Vietnam/1203/2004 (H5N1)	Trimer (GCN4-trimerization domain - C-terminus)	Human	none	α2,3 linked Neu5Ac	(de Vries, Zhu et al. 2014)
A/Kanazawa/1/2007 (H3N8)	Trimer (GCN4-trimerization domain - C-terminus)	Equine	none	α2,3 linked Neu5Ac	(Ito, Nagai et al. 2008)
A/Vietnam/1203/2004* (H5N1)	Trimer (GCN4-trimerization domain - C-terminus)	Human	T160A and Y161A mutations	α2,3 linked Neu5Gc	(Wang, Tscherne et al. 2012)
A/Santiago/1/1977 (H7N7)	Trimer (GCN4-trimerization domain - C-terminus)	Equine	none	α2,3 linked Neu5Gc	(Gambaryan, Matrosovich et al. 2012)
A/Texas/1/2004 (H3N8)	Trimer (GCN4-trimerization domain - C-terminus)	Canine	none	α2,3 linked Neu5Ac	(Yamanaka, Tsujimura et al. 2010)

Expression and purification of proteins

The pCD5 expression vectors containing the HEF-1 domain-encoding sequences were transfected into HEK293T cells, grown in Dulbecco's Modified Eagle's Medium (DMEM, cat#: BE12-709F, Lonza) supplemented with L-Glutamine (cat#: 17-605F, Lonza), fetal bovine serum (FBS, cat#: F7524, Sigma-Aldrich) and penicillin/streptomycin (cat#: 15140122, Gibco). For transfection, polyethyleneimine I (PEI) was used in a 1:8 ratio of µL DNA to µL PEI (both stock concentrations of 1µg/µL). At 16 h post transfection, the growth medium was replaced by 293 SFM II medium (cat#: 11686-029, Gibco), supplemented with 3,7 g/L Sodium hydrogencarbonate NaHCO3 (cat#: 106329, Merck, KGaA), 2 g/L D-(+)-Glucose (cat#: G-7021, Sigma-Aldrich), 3 g/L Primatone RL (cat#: P4963, Kerry Bio-science), 10 mL/L penicillin/streptomycin (cat#: 15140122, Gibco), 10 mL/L glutaMAX (Gibco), 15 mL/L Dimethyl sulfoxide (cat#:154938, Sigma-Aldrich) and 0,33 g/L Valproic acid sodium salt (cat#: P4543, Sigma-Aldrich). Cell culture supernatant was harvested 6-7 days post transfection and 30 µL of it was analyzed by western blot. The proteins were purified by gravity flow purification using Strep-Tactin Sepharose 50% suspension (cat#: 2-1201-010, IBA GmbH, Germany) (approx. 200µL Sepharose suspension to 50 mL supernatant) and eluted with Strep-Tactin elution buffer containing desthiobiotin (cat#: 2-1000-025, IBA GmbH, Germany) according to manufacturer's instructions. The concentration was determined by a NanoDrop 1000 spectrophotometer (Thermo Fisher Scientific Inc.).

All Influenza A proteins were obtained through the collaboration with Dr. R. P. de Vries (Utrecht Institute for Pharmaceutical Sciences, Utrecht University). Table 3 shows the received proteins and their characteristics. The protein production process has been described previously (de Vries, de Vries et al. 2010, de Vries, de Vries et al. 2011, de Vries, de Vries et al. 2013). In brief, codon optimized sequences for the mentioned hemagglutinins (table 3) were obtained from GenScript, and cloned into pCD5 vectors. The pCD5 vectors contained also a GCN4 trimerization domain and a Strep-Tag II. The plasmids were transfected into HEK293T cells and cultured for 7 days, before harvesting the cell culture supernatant. The proteins were purified by Strep-Tactin Sepharose 50% suspension and the supernatant was analyzed by SDS-PAGE and western blotting.

Western blotting

The expression and purification of proteins were analyzed by sodium dodecyl sulfate-polyacrylamide gel (10%) electrophoresis (SDS-PAGE) followed by western blotting using the horseradish peroxidase (HRPO)-conjugated Strep-Tactin antibody (cat#: 2-1502-001, IBA GmbH) and the Amersham Enhanced Chemiluminscence prime western blotting detection reagent (ECL, cat#: RPN2232, GE Healthcare) for visualization. Protein samples loaded with a 3x loading buffer and preheated for 5 minutes at 98˚C before loading onto the gel. The PageRuler plus prestained protein ladder (cat#: 26619, Thermo Fisher Scientific Inc.) was used for determining protein size. Proteins were blotted to PVDF membrane (cat#: 162-0177, Bio-Rad Laboratories Inc.) for 60 min at 100V. After Western blotting, the membranes were first blocked with 3% milk powder in PBS (cat#: 170-6404, Bio-Rad Laboratories Inc.) for 60 minutes, and stained with the horseradish peroxidase (HRPO)-conjugated Strep-Tactin antibody (1:2000) for another 60 minutes. The membrane was then washed with PBS-T and twice with PBS, before incubating for 5 minutes with ECL. Proteins were visualized using an Odyssey Fc Imaging System (LI-COR, Inc.). The electrophoresis and western blotting was done with the Mini-PROTEAN Tetra Cell vertical electrophoresis system (cat#: 1658001, Bio-Rad Laboratories Inc.)

Protein histochemistry

The TMAs were sectioned at a thickness of 4 µm and stored at 5 ˚C. The tissue sections were deparaffinized and antigen retrieval was performed as mentioned previously (lectin staining section). Endogenous peroxidase was inactivated by incubating the slides in 1% hydrogen peroxide in methanol for 30 minutes at room temperature. After washing with PBS-T, the sections were blocked with 3% bovine serum albumin (cat#: A3294, Sigma-Aldrich) at 4°C, overnight. To visualize binding to the tissues, the proteins (ranging from 5-50 µg/mL) were pre-complexed with StrepMAB-Classic, HRP conjugate mouse antibody (cat#: 2-1509-001, IBA GmbH) and Goat anti-Mouse IgG (H+L) Secondary Antibody-HRP (1:125 dilution) (cat#: 31430, Thermo Fisher Scientific Inc.) for 20 minutes at room temperature before being applied on the tissue sections. The protein-antibody complex was incubated on the tissues for 90 minutes at room temperature and rinsed three times in PBS, before applying AEC for visualization of protein binding. Presence of the protein and subsequently the peroxidase enzyme of the antibodies would react with the AEC and result in red color staining. The sections were counterstained with Hematoxylin and were mounted with Aquatex. Images were captured using a charge-coupled device (CCD) camera, as mentioned previously. The positive signal was determined as in lectin staining.

Antibody staining

The antibody staining was performed similar to the protein histochemistry. However, in the deparaffinization process, the endogenous peroxidase block was performed between the steps of 100% and 96% alcohol. Furthermore, the procedure was unchanged. The incubation with the primary antibody, specific against α2,3 linked N-Glycolylneuraminic sialic acid (Chicken polyclonal IgY isotype, cat#: 146903, BioLegend, Inc.) was performed with a concentration of 1 µg/ml for 60 minutes at room temperature. The secondary antibody, rabbit anti-Chicken IgG (H+L) Secondary Antibody-HRP (diluted 1:100, cat#: 61-3120, Zymed), was for 30 minutes at room temperature. The visualization, counterstaining & signal scoring remained unchanged (see lectin staining & protein histochemistry).

Results

The novel creation procedure of the TMA leads to improved tissue preservation

The change in the making procedure of the TMA, from using a commercial pre-formed recipient paraffin block, used in previous experiments (Wickramasinghe, de Vries et al. 2015), to creating a TMA using the 3D-printed array plate, led to an overall improvement of the procedure. First and foremost, optimal sectioning of the TMA was achieved. The sections showed minimal tissue damage and less irretrievable loss of tissue cores when compared with the procedure used previously. Second, the cores were more tightly attached to the slides which was confirmed during the protein histochemistry process. Particularly during the antigen retrieval step, in which the tissues are treated with sub-boiling citrate, tissue cores tended to detach from the glass slides. However, this specific issue was diminished with the slides produced with the altered procedure. Nonetheless, the procedure showed disadvantages, and the suboptimal placement of the cores was one of them. It is technically challenging to place the cores into the holes, but also to arrange the cores in similar heights. When ignored, the differences in core heights resulted in tissue sections with variable presence of the tissues, which can be retraced to the sectioning. In this project, three TMA blocks were created (for species & placement map, see annex I; table 1 to 3), from which 98% of all sectioned slides were in very good to perfect condition. One representative section was stained with H&E and was evaluated and compared to the morphology of the donor tissues. The stained slides were, as expected, well preserved and no significant changes were observed, which allowed the use of the remaining slides. H&E stainings of all TMAs can be found in annex 1 (figures 10 to 12).

Organ-specific expression of sialic acids in porcines

Porcine monospecies TMA

A porcine monospecies TMA was equipped to determine the specific tissue distribution of sialic acids not only in the respiratory tract but also in other organs and major systems of this species. As sialic acids are known to be the receptors for various viruses, including influenza A, it is important to know which organs are susceptible to attachment and to possible infection. The lectins used were the Maackia amurensis lectin I (MALI), Maackia amurensis lectin II (MALII) and Sambucus nigra lectin (SNA). MAL I recognizes the SAα2,3-Galβ(1-4)GlcNAc sialic acids, while MAL II recognizes the SAα2,3-Galβ(1-3)GlcNAc (Konami, Yamamoto et al. 1994). On the contrary, SNA lectins are described to bind SAα2,6-Gal sialic acids (Shibuya, Goldstein et al. 1987). Table 4 gives an overview of the signal detected in all tissues. All images can be found in annex I, figures 1, 2 and 3. In the respiratory tract, SNA was the most obvious signal, mostly seen in the upper and lower trachea and in the primary bronchus. The signal was primarily seen in goblet cells and ciliated epithelium. Towards the lung, the signal was clearly seen at the bronchiole and at the alveolar lining of the lung. The submucosal tissues were also positive for SNA at the full length of the trachea. The MALII staining was mostly seen in the submucosal layers of the respiratory tract. However, near the end of the respiratory tract, MALII staining was also present on goblet and epithelial cells, and the submucosal signal was more positive than the upper respiratory part of the pig. In the bronchiole and alveolar lining, the signal resembled that of the SNA signal. MALI staining was not detected in

any part of the respiratory tract. In the gastrointestinal tract, SNA staining was strongly detected in the stomach, duodenum, jejunum, ileum, caecum and colon. Both epithelium and goblet cells were strongly stained. MALII was also detected in most parts of the gastrointestinal tract. The strongest signal of MALII was detected in the epithelial and goblet cells in the duodenum, jejunum, ileum and the colon. Weak staining signal was seen in the stomach and no signal at all was seen in the caecum. The signal in the caecum was restricted to the submucosal layers of the tissue. MALI was not present at any part of the gastrointestinal tract. All three lectins were detected in the central nervous system, with co-localization in most parts of the brain but with different intensity. SNA and MALII were also detected in the glomeruli and in some extend in the connective tissue of the kidney. In most of the organs, the connective tissue was positive for SNA and MALII. The described stainings indicate that the SAα2,6-Gal are primarily located at the respiratory and digestive system, whereas the SAα2,3-Galβ(1-3)GlcNAc was located only at the lower part of the respiratory system and in all parts of the digestive system, except of the caecum. SAα2,3-Galβ(1-4)GlcNAc was only located at the central nervous system (CNS) and parts of the urogenital tract.

Table 4. Overview of lectin staining results on porcine tissues present on the TMA. ++, very strong positive signal; +, positive signal; +/-, partly positive signal; -, no signal detected. See also annex I for pictures.

	Organ	MALI	MALII	SNA
Respiratory system	Nasal epithelium	-	-	+/-
	Nasopharynx	-	+	+
	Upper trachea	-	+/-	+
	Lower trachea	-	+/-	+
	Primary bronchus	-	+	+
	Lung	-	+	+
Digestive system	Soft palate	-	-	-
	Epiglottis	-	-	+
	Larynx	-	-	-
	Oesophagus	-	-	-
	Stomach	-	+/-	+
	Duodenum	-	+	++
	Jejunum	-	++	++
	Ileum	-	+	++
	Caecum	-	-	++
	Colon	-	++	++
	Liver	-	-	+
	Kidney	+/-	+	+
	Heart	-	+/-	-
	Spleen	-	-	-
	Pancreas	-	-	-
	Thymus	-	-	+
	Bladder	-	-	-
	Adrenal gland	-	+/-	-
	Lymphnode	-	-	-
	Pharyngeal tonsil	-	+/-	+/-
	Conjunctiva	-	-	+
	Ovarium	+/-	+/-	-
	Uterus	+/-	-	-
CNS	Cerebrum	+/-	+/-	+/-
	Cerebellum	+	+	+/-
	Hypophysis	+/-	+/-	-
	Bulbus olphactorius	-	+/-	-
	Brain stem	+/-	+/-	+/-
	Sciatic nerve	+/-	+/-	+/-

Low intraspecies variation in the expression of sialic acids in the porcine respiratory tract

Porcine respiratory TMA

In order to study the intraspecies variation of sialic acids expression, a TMA was created holding respiratory tract tissuesvfrom pigs. The tissues originated from six different non-related individuals and consisted of six different anatomic regions. Tissues of the upper-, mid-, and lower trachea, primary bronchus, bronchiole and alveoli were collected and placed into the TMA. None of the cores of all six animals showed MALI staining. MALII staining was only detected in the submucosal layers of the respiratory tract of all the individuals, without any signal on the epithelial cells. However, in the lungs, MALII staining was clearly present in the bronchiole and alveolar lining. SNA staining on the other hand, was present on the ciliated epithelium and goblet cells in most of the tract, starting from the upper-trachea towards the deeper parts of the respiratory tract. The submucosal layers were dominated by the presence of the MALII in the whole length of the tract. The SNA signal was restricted to submucosal glands of that region. See also figures 4, 5 and 6 in Annex 1. These data suggest that there is some co-localization of SAα2,3-Galβ(1-3)GlcNAc and SAα2,6-Gal in the respiratory tract of the pig. However, this appears to happen only in the lower parts of the respiratory, as in the bronchiole and alveolar lining. Analyzing the binding pattern of the lectins on the different individuals, it is clear that the expression of sialic acids is similar in between the individuals and suggests that the intraspecies variation is minimal.

Recombinant viral attachment proteins reveal similar expression of their receptor in the same regions of the respiratory tract of multiple pigs

Human H1 hemagglutinin staining

The hemagglutinin of a human H1N1 Influenza A strain (A/Puerto Rico/8/1934 - PR8D) was used in a soluble form to determine the presence of SAα2,6-Gal on the porcine tissues. The chosen strain possesses a E190D mutation which switches the specificity from SAα2,3-Gal to SAα2,6-Gal (Xu, McBride et al. 2012). Staining

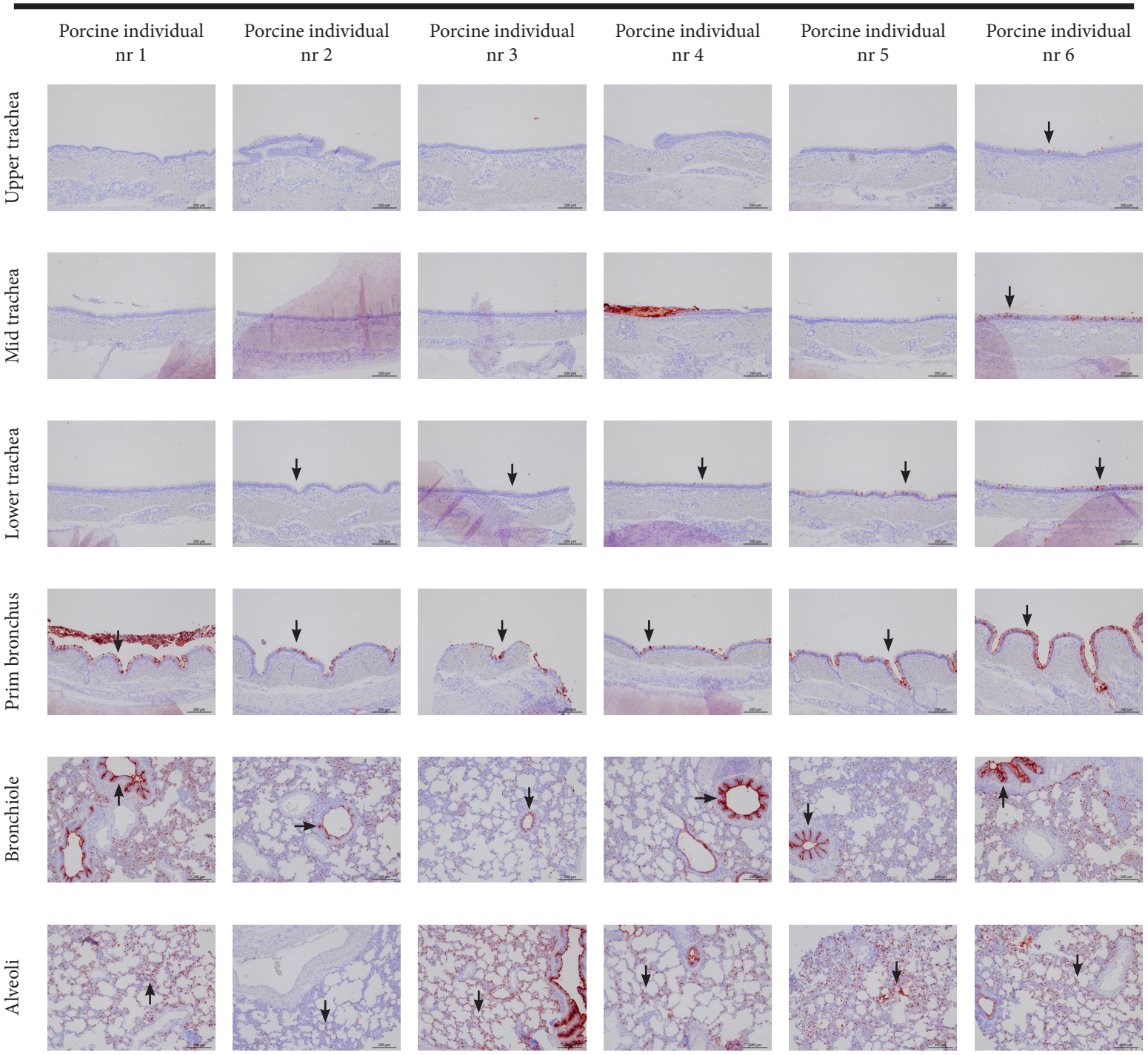

Figure 4. Staining results of the H1 attachment protein of the H1N1 Influenza A strain (A/Puerto Rico/8/1934 - PR8D) on the porcine respiratory tract TMA. Samples are depicted, from top to bottom, of the upper, mid and lower trachea, primary bronchus, bronchioli and alveoli. All tissues were collected from six individuals, depicted from left to right. Arrows indicate positions where positive signal (red color) was observed. Signal was observed predominantly seen in the mid and lower parts of the respiratory tract.

signal was mostly seen at the lower respiratory tract. Signal was already present at the mid trachea, but became more evident at the lower trachea and primary bronchus. This pattern continued to the bronchiole and the alveolar lining. The positive signal was predominantly located at the epithelial border, including the goblet cell population present. The submucosal layers were not stained with the protein. Table 5 gives an overview of the signal along the respiratory tract of the individuals. Figure 4 depicts the staining results on all individuals. The presence of SAα2,6-Gal on all six individuals was more pronounced at the end of the respiratory tract, however the most proximal staining location differed in two of the six samples.

Human H1 hemagglutinin mutant staining

The hemagglutinin 1 of the pandemic H1N1, which emerged in 2009 (A/California/04/2009(H1N1)), was obtained as a recombinant soluble trimeric protein in order to study the binding pattern on the respiratory tract of the pig. The coding gene was however altered at four sites which translated to four different amino acids near the receptor binding site of the hemagglutinin. This resulted to the change of receptor specificity from SAα2,6-Gal to SAα2,3-Gal, which correspondents to the avian influenza A receptor (Lakdawala, Jayaraman et al. 2015). The staining results observed in the porcine respiratory tract are summarized in table 5, and figure 5 depicts the staining results on all individ-

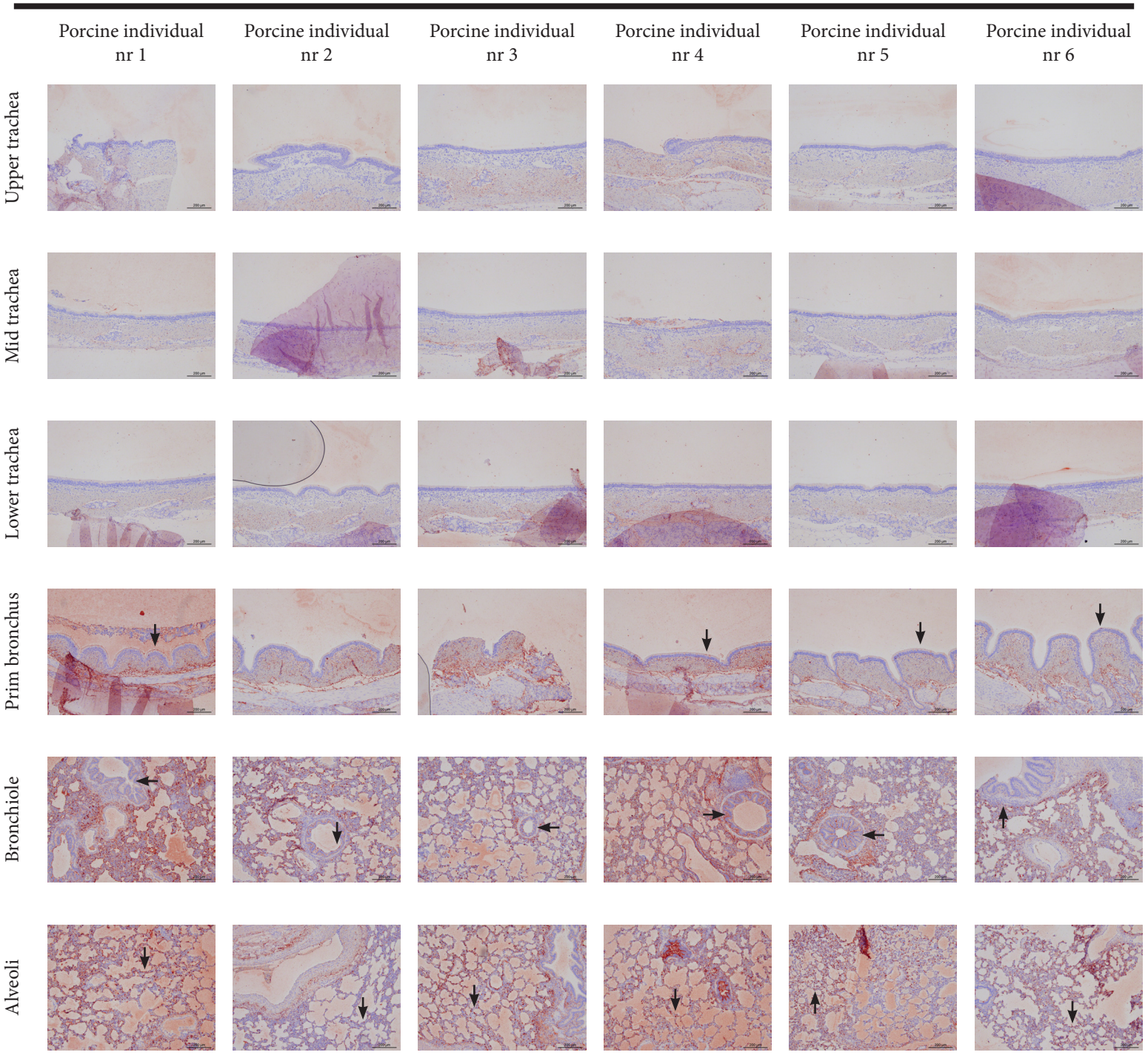

Figure 5. Staining results of the mutated H1 attachment protein of the H1N1 Influenza A (A/California/04/2009) on the porcine respiratory tract TMA. Samples are depicted, from top to bottom, of the upper, mid and lower trachea, primary bronchus, bronchioli and alveoli. All tissues were collected from six individuals, depicted from left to right. Arrows indicate positions where positive signal (red color) was observed. Signal was observed predominantly seen in the lower parts of the respiratory tract.

uals. The respiratory tract, from the upper trachea to the lower trachea were not stained. The primary bronchus showed weak positive signal, predominantly on the goblet cells rather than the epithelial cells. The bronchiole and the alveolar lining showed stronger signal, more evident in the alveoli than the bronchiole. The presence of signal in the deeper parts of the respiratory tract proves the expression of SAα2,3-Gal in that area. Furthermore, the scarce variation of detectable signal between the different individuals underlines the comparable existence of the specific sialic acids.

Human H5 hemagglutinin staining

The hemagglutinin protein of the human influenza A H5N1 strain (A/human/Vietnam/1203/2004) was used to stain the respiratory tract of the pig. This specific virus strain has been described to use SAα2,3-Gal as the receptor (de Vries, Zhu et al. 2014). An overview of the staining results can be found in table 5. The upper trachea did not reveal any signal on any of the six cores. The mid- and lower trachea however, showed slight positive signal at three of the five cores. The sixth core of the mid- and lower trachea was damaged during staining and no data is obtained. All of the six primary bronchi, the broncheoli and alveoli were stained positive. The staining had a significant amount of background noise with no apparent explanation. In the lungs, the signal was unmistakable present at all cores. Figure 6 depicts the staining results on all individu-

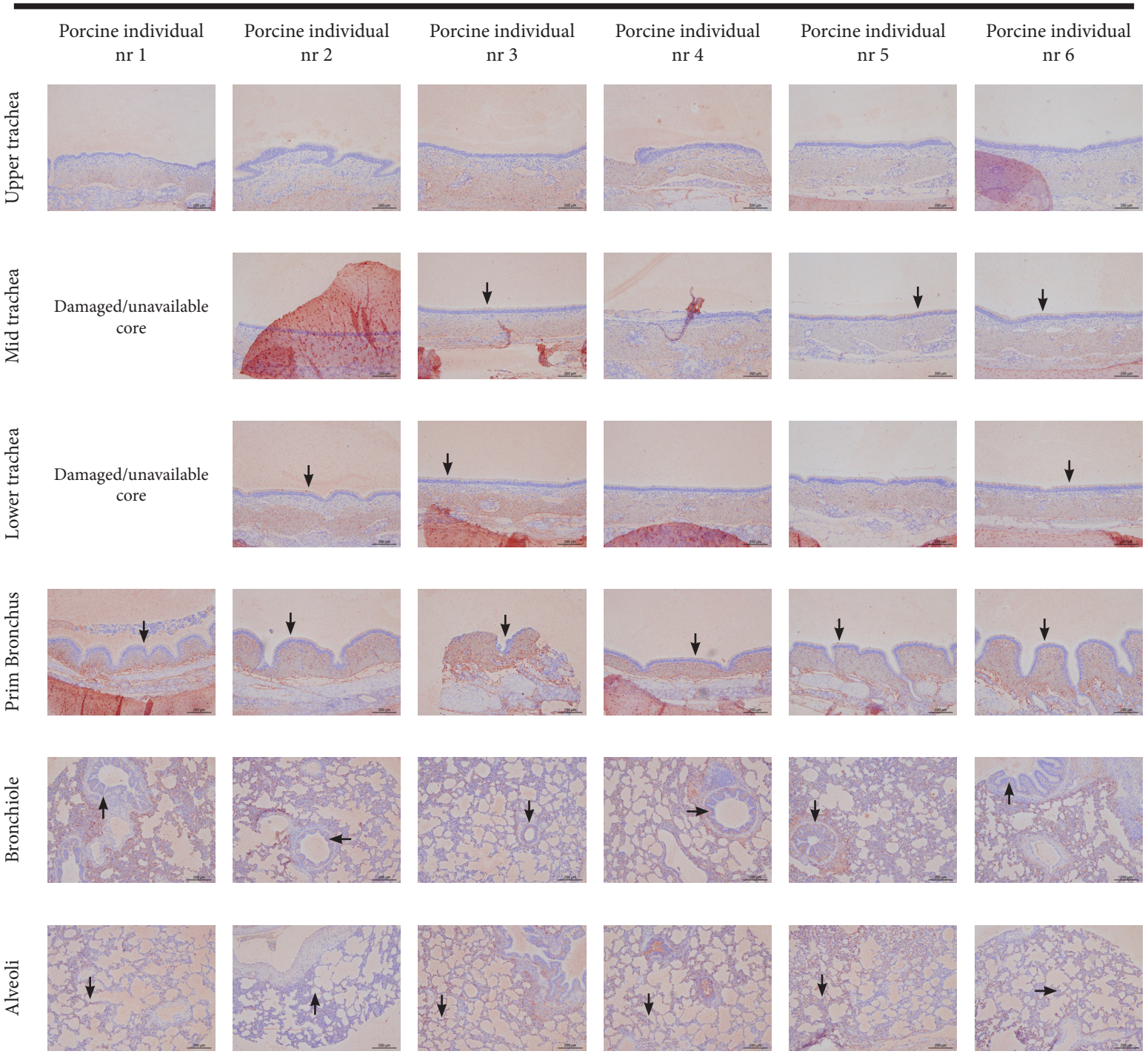

Figure 6. Staining results of the H5 attachment protein of the H5N1 Influenza A strain (A/Vietnam/1203/2004) on the porcine respiratory tract TMA. Samples are depicted, from top to bottom, of the upper, mid and lower trachea, primary bronchus, bronchioli and alveoli. All tissues were collected from six individuals, depicted from left to right. Arrows indicate positions where positive signal (red color) was observed. Signal was observed predominantly seen in the mid and lower parts of the respiratory tract.

Table 5. Overview of the staining results of the hemagglutinins on the different location of the respiratory tract present on the TMA. The score indicates the presence of clear signal in the six porcine individuals and the intensity is categorized as: ++, very strong positive signal; +, positive signal; +/-, partly positive signal; -, no signal detected.

Hemagglutinin source	H1N1 PR8D		H1N1 Cal04 4x		H5N1 Vietnam	
Respiratory tract location	Pos signal	Intensity	Pos signal	Intensity	Pos signal	Intensity
Upper trachea	1/6	+/-	0/6	-	0/6	-
Mid trachea	1/6	+	0/6	-	3/5	+/-
Lower trachea	5/6	+	0/6	-	3/5	+/-
Primary bronchus	6/6	++	4/6	+/-	6/6	+
Bronchiole	6/6	++	6/6	+	6/6	+
Alveoli	6/6	++	6/6	++	6/6	+

als. Thus, presence of SAα2,3-Gal was predominantly present in the lower respiratory tract in all individuals, suggesting low intraspecies variation at that region. However, the intraspecies variation was present in the mid-region of the tract, as the detectable signal variated between individuals.

Differences in tissue distribution of sialic acids in equine and canine respiratory tissues

Equine and canine TMA

In order to understand the tissue distribution of influenza A receptors in equines and canines, and the possible differences of the distribution, an equine-canine TMA was created. The equine-canine combined TMA consisted of ten organs per species, mainly containing respiratory tract tissues of the two species. A summary of the staining results can be found in table 6. MALI binds preferably to canine tissues. This lectin preferentially bind the epithelial and goblet cells of the lower trachea and nasal epithelium. Also the bronchiole appeared to give a slight positive signal. Most of the equine tissues were negative for MALI, except for the nasal epithelium and the glands in the subsequent submucosal layers. MALI also stained the submucosal layers of the upper and lower trachea but not the epithelial or goblet cells of these parts. MALII was detected in a different pattern. Strong signal was seen in the nasal epithelium of both species. However, only the lower canine trachea showed staining on the epithelium, whereas the equine trachea and bronchus showed signal in the submucosal layers. The binding pattern that was observed in the lungs of the species, was similar to each other in the alveolar lining and the bronchiole. The glomeruli of the canine kidneys were also positive for MALII, but the signal was more intense in the equine tissues. The epithelial cells of the equine nasal area, the complete trachea, including the primary bronchus, were positive for the SNA lectin. The equine lung and kidney showed stronger signal when compared to the canine lung and kidney. The canine nasal epithelium revealed positive signal, along with the lower part of the trachea. These stainings indicate that the two species share the presence of the sialic acids in their respiratory tract. SAα2,3-Galβ(1-4)GlcNAc, recognized by MALI, was predominantly seen in the canine tissues, and especially in the trachea, but not in the equine tissues. SAα2,3-Galβ(1-3)GlcNAc, recognized by MALII, was seen in both of the kidneys and both of the nasal epithelium. However, only the canine trachea epithelial cells were positive to SAα2,3-Galβ(1-3)GlcNAc. The SAα2,6-Gal staining resembled the SAα2,3-Galβ(1-3) GlcNAc data in the kidneys, but differed in the tracheal epithelium. Both animals shared the SAα2,6-Gal signal on the trachea and in the lungs. Taken together, the data indicate that equine and canine hosts, share the presence of SAα2,3-Gal in their kidneys but not in the respiratory tract. Furthermore, the SAα2,6-Gal moiety is shared in the respiratory tract and kidney of the two species.

Species related differences in the expression and distribution of virus-specific receptors in the equine and canine respiratory tract

Equine H3 staining

The hemagglutinin attachment protein of a H3N8 (A/equine/Kanazawa/1/2007) (Ito, Nagai et al. 2008) was obtained and used to study the tissue tropism on the TMA. The hemagglutinin has previously shown a strong avidity for α2,3 linked N-acetyl neuraminic acids (Neu5Ac) on a glycan array (R.P. de Vries, unpublished data). The protein staining on the tissue sections revealed signal on tissues of both species, at various parts of the respiratory tract, an overview is given by table 7. The lungs of both species were stained positively, including the bronchiole and alveoli. The epithelial and goblet cells of the nasal epithelium of both species were positive. The laryngeal epithelium of both species was negative. The oropharynx of the equine sample was stained positive, as were the kid-

Table 6. Overview of lectin staining results on the tissues present on the equine-canine combined TMA. ++, very strong positive signal; +, positive signal; +/-, partly positive signal; -, no signal detected. See also annex I for pictures.

		MALI		MALII		SNA	
Organ	**Species**	Equine	Canine	Equine	Canine	Equine	Canine
Bulbus olphactorius		-	+/-	+/-	+/-	+/-	+/-
Kidney		-	-	+	+	++	+
Laryngeal epithelium		-	-	-	-	-	-
Lower trachea epithelium		-	+	-	+	+/-	+
Lung		-	+/-	+/-	+/-	++	+
Nasal epithelium		+/-	+	+	++	+	+
Oropharynx		-	-	-	-	+	+
Primary bronchus		-	n/a	-	n/a	+	n/a
Upper trachea epithelium		-	n/a	-	n/a	+	n/a
Soft palate		n/a	-	n/a	+/-	n/a	-

neys of both species. The lungs showed similar binding patterns, however, the canine core was slightly more positive. The canine lower trachea was undoubtedly positive, but the equine cores did not give not a similar intensity. Figure 7 displays the staining images. The data show that the α2,3 linked Neu5Ac, which is used by the H3 attachment protein, is present on both equine and canine hosts, but is expressed at different amounts.

Human H5 Vietnam 161.160 staining

The attachment protein of the human influenza A H5N1 strain (A/human/Vietnam/1203/2004) was obtained as a soluble protein in order to elucidate binding tropism on mammalian tissues. The H5 was mutated at two distinct positions (T160A and Y161A) in order to change the specificity of the protein. The mutated H5 160.161 protein, bound preferentially to α2,3 linked N-glycolyl neuraminic acids (Neu5Gc) instead of

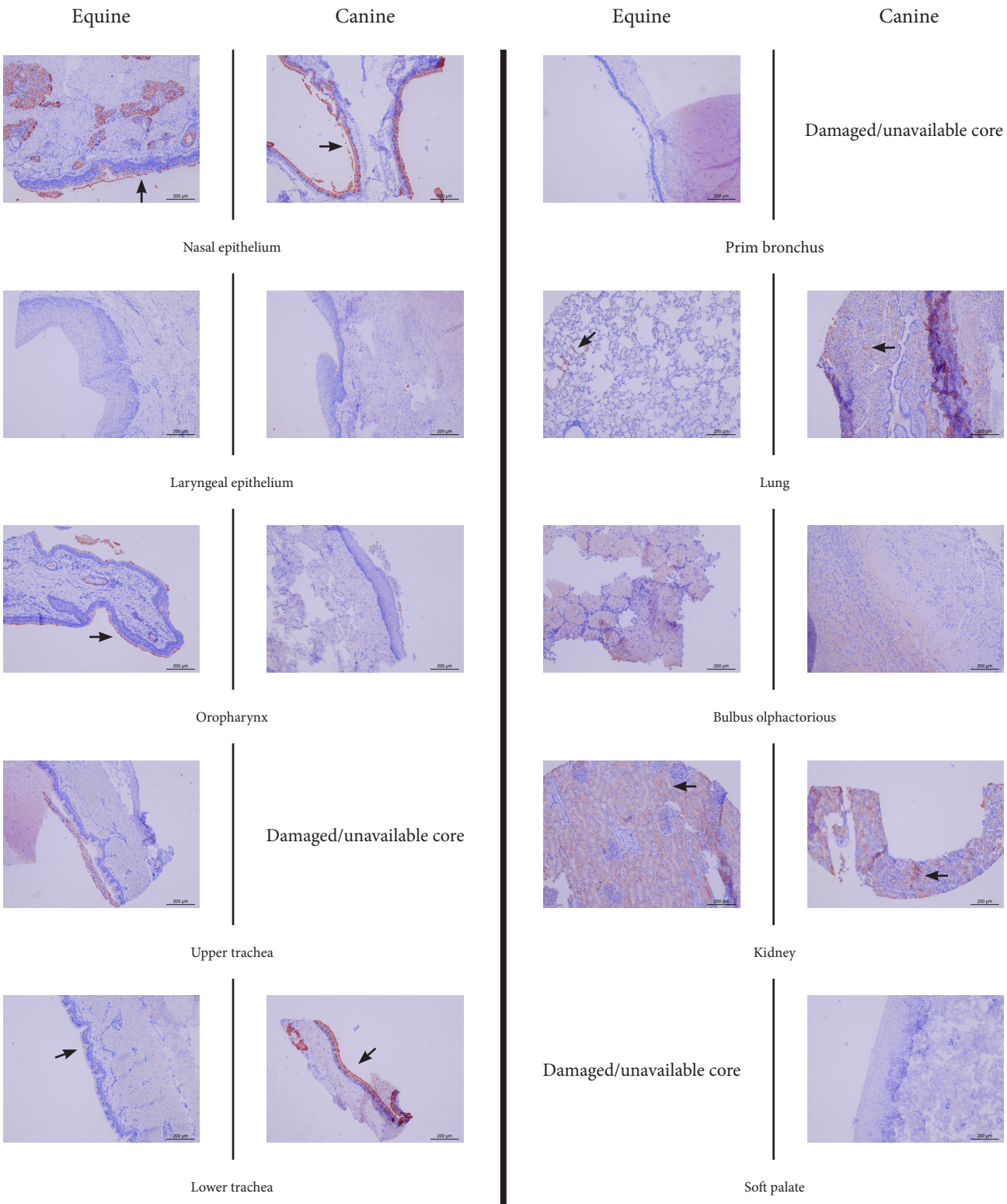

Figure 7. Staining results of the H3 hemagglutinin of influenza A H3N8 (A/equine/Kanazawa/1/2007) on respiratory tissues and kidney of equine and canine individuals. This specific H3 recognizes predominantly Neu5Ac sialic acids. Arrows indicate positions where positive signal (red color) was observed. Signal, which reveals that expression of Neu5Ac sialic acid, was detected in both species.

N-acetyl neuraminic acids (Neu5Ac) (Wang, Tscherne et al. 2012). The staining showed clear differences between the equine and canine tissues. All of the canine tissues were negative, except for a slightly positive signal in the bronchiole and kidney. Most of the equine tissues were evidently positive for the binding. The epithelial and goblet cells of the oropharynx, upper and lower trachea, nasal area and primary bronchus were positively stained. Furthermore, the glomeruli of the kidney and the alveoli of the lung revealed positive staining. See also figure 8 for images of the staining. The data indicate the absence of Neu5Gc in canine tissues and the unmistakable presence of the receptor in equine tissues.

Equine H7 staining

The attachment protein of the equine influenza A strain H7N7 (A/equine/Santiago/1/1977) was expressed as a soluble protein by the collabolatirs and was used for

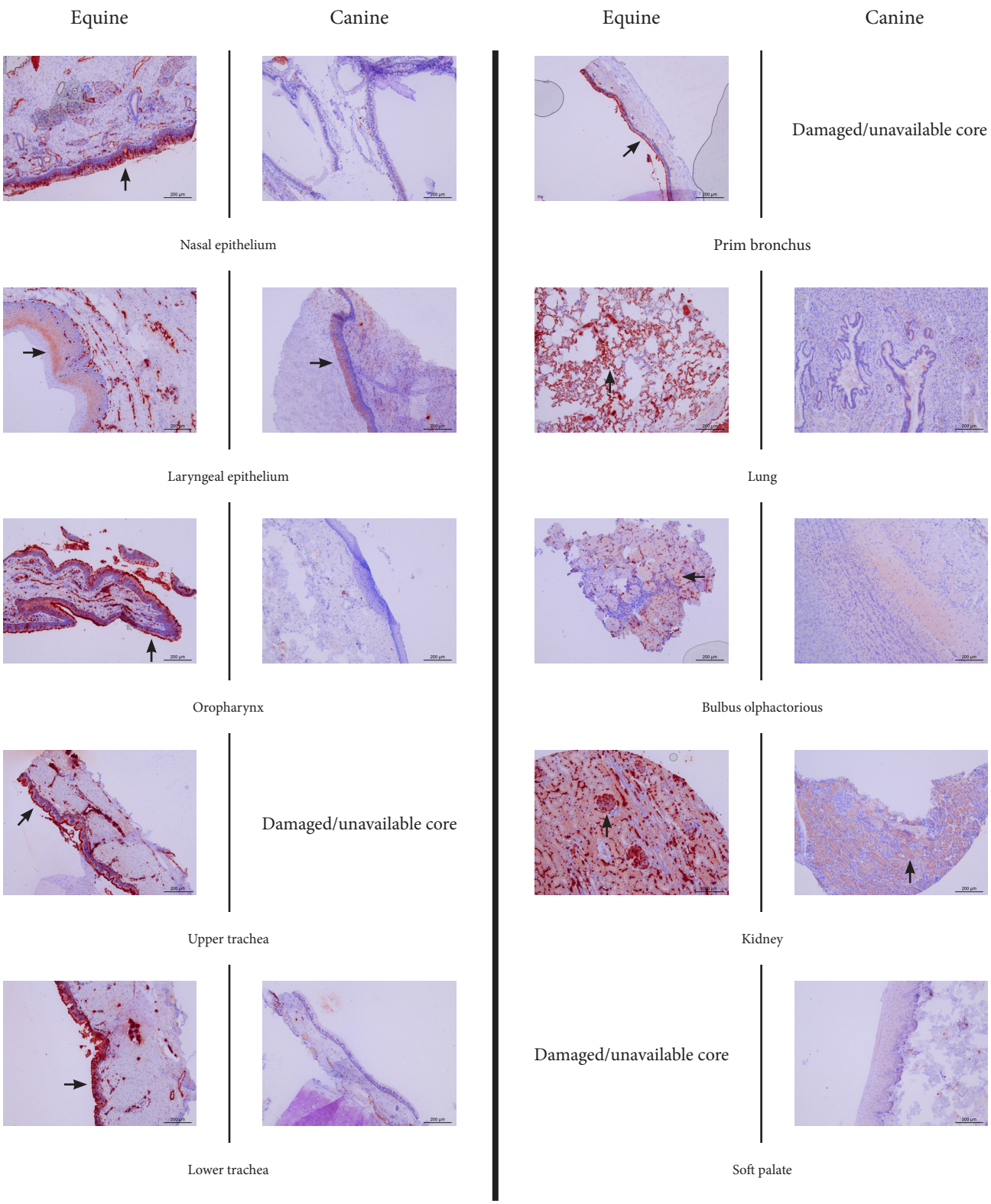

Figure 8. Staining results of the mutated hemagglutinin protein influenza A H5N1 strain (A/human/Vietnam/1203/2004) on equine and canine tissues. This mutant H5 recognizes predominantly Neu5Gc sialic acids. Arrows indicate positions where positive signal (red color) was observed. Signal was detected only in the equine tissues, which reveals the expression of Neu5Gc sialic acid.

the analysis of tissue tropism on equine and canine hosts. The binding preference has been described previously (Gambaryan, Matrosovich et al. 2012), and has been established that there is a significantly higher avidity for Neu5Gc sialic acids than for Neu5Ac. The binding pattern on the sections revealed strong preference for the equine tissues, and specifically, the epithelium of the respiratory tract. The staining was clearly positive on the oropharynx, the complete length of the trachea, including the primary bronchus and the alveolar lining. Slightly positive signal has been observed in the kidney of the equine. The canine tissues however, were mostly negative. The canine kidney and lung revealed slight positive binding but not as evident as in the equine samples. For images of the staining see figure 9 and for an overview of the staining results table 7. The general binding pattern reveals that the receptor of the H7 attachment protein is predominantly present on equine tissues and scantily present on canine tissues.

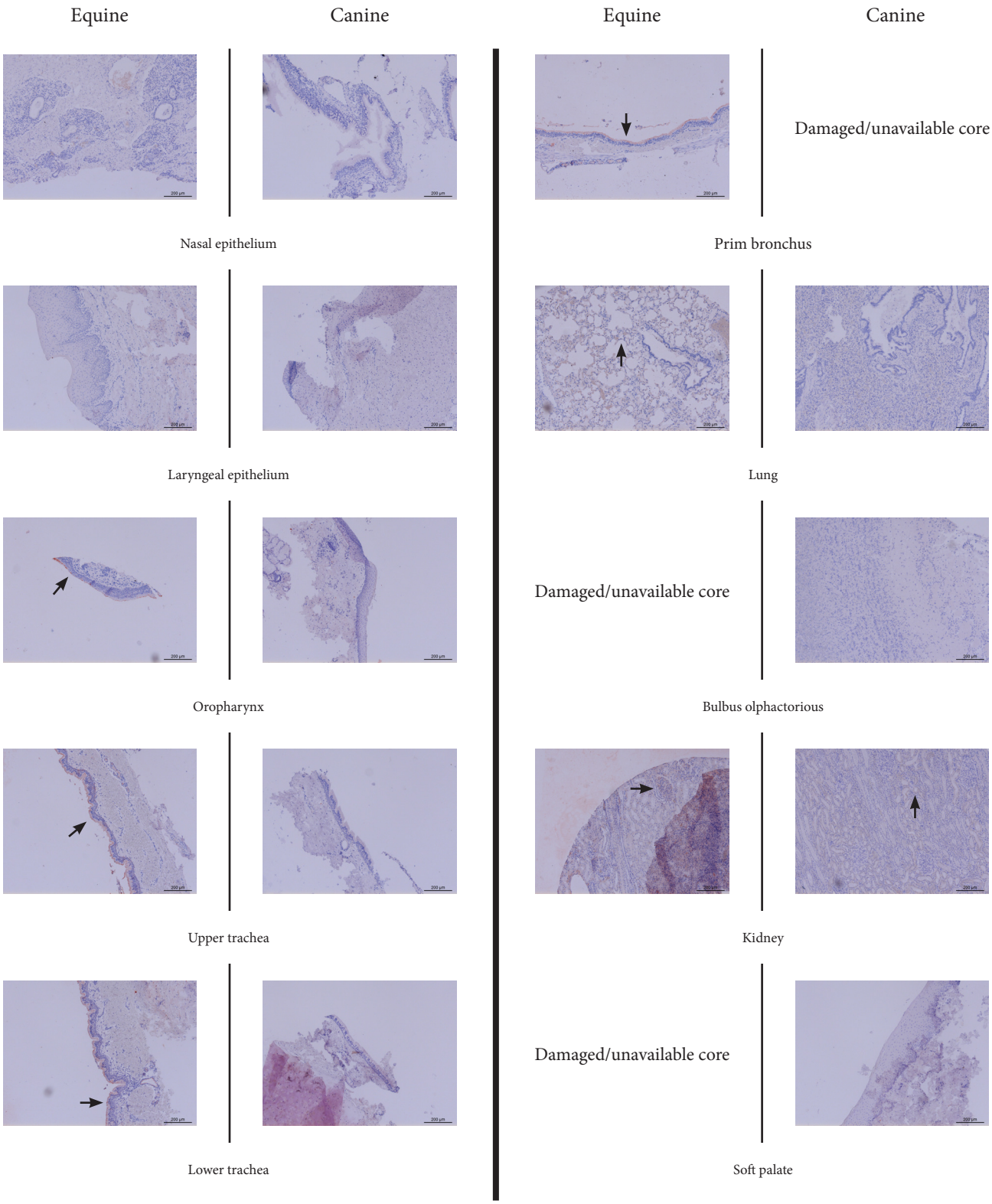

Figure 9. Staining results of the attachment protein of the equine influenza A strain H7N7 (A/equine/Santiago/1/1977) on equine and canine tissues. This H7 recognizes predominantly Neu5Gc sialic acids. Arrows indicate positions where positive signal (red color) was observed. Signal, which reveals that expression of Neu5Gc sialic acid, was only detected in equine tissues.

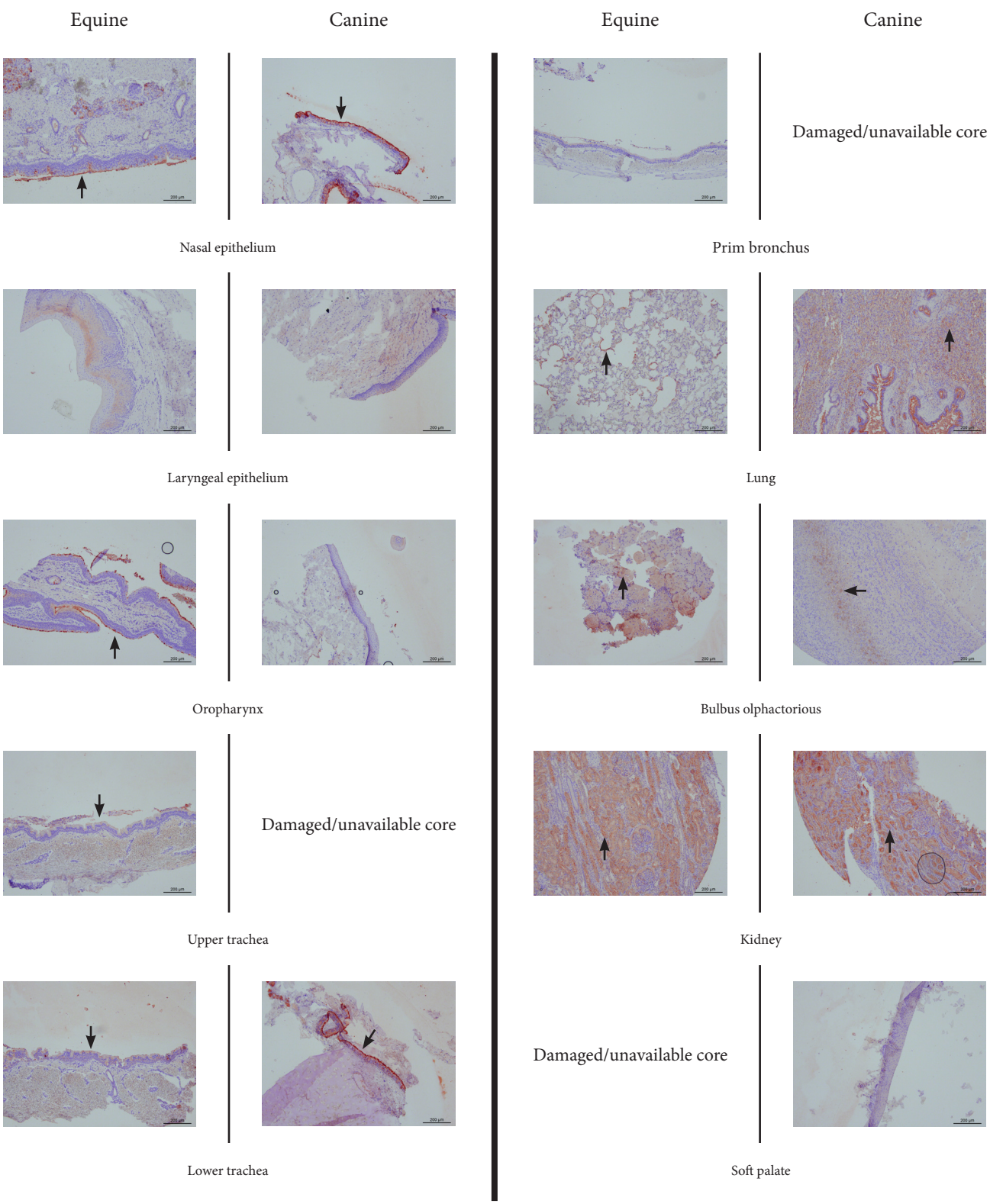

Figure 10. Staining results of the hemagglutinin protein of the influenza A H3N8 strain (A/Canine/Texas/1/2004) (H3N8) on equine and canine tissues. This mutant H3 recognizes predominantly Neu5Ac sialic acids. Arrows indicate positions where positive signal (red color) was observed. Signal, which reveals that expression of Neu5Ac sialic acid, was detected in both species.

H3 canine texas

The hemagglutinin protein of the canine H3N8 collected in Texas in 2004 (A/canine/Texas/1/2004) was obtained as a soluble form and used to stain the respiratory tract of equine and canine individuals. The receptor preference has been described previously (Yamanaka, Tsujimura et al. 2010) and the hemagglutinin binds preferentially to α2,3 linked Neu5Ac. Table 7 gives an overview of the staining results. The staining showed signal at the nasal epithelium of the canine and the equine host. However, the laryngeal epithelium of both species did not show positive signal. The equine oropharynx was positive but the canine one did not reveal any signal. The kidney of both species showed similar staining pattern in and around of the glomeruli. The staining in the canine lower trachea was strongly present, which differed in the equine trachea. The equine trachea was positively stained but not as strongly as the canine one. The equine primary

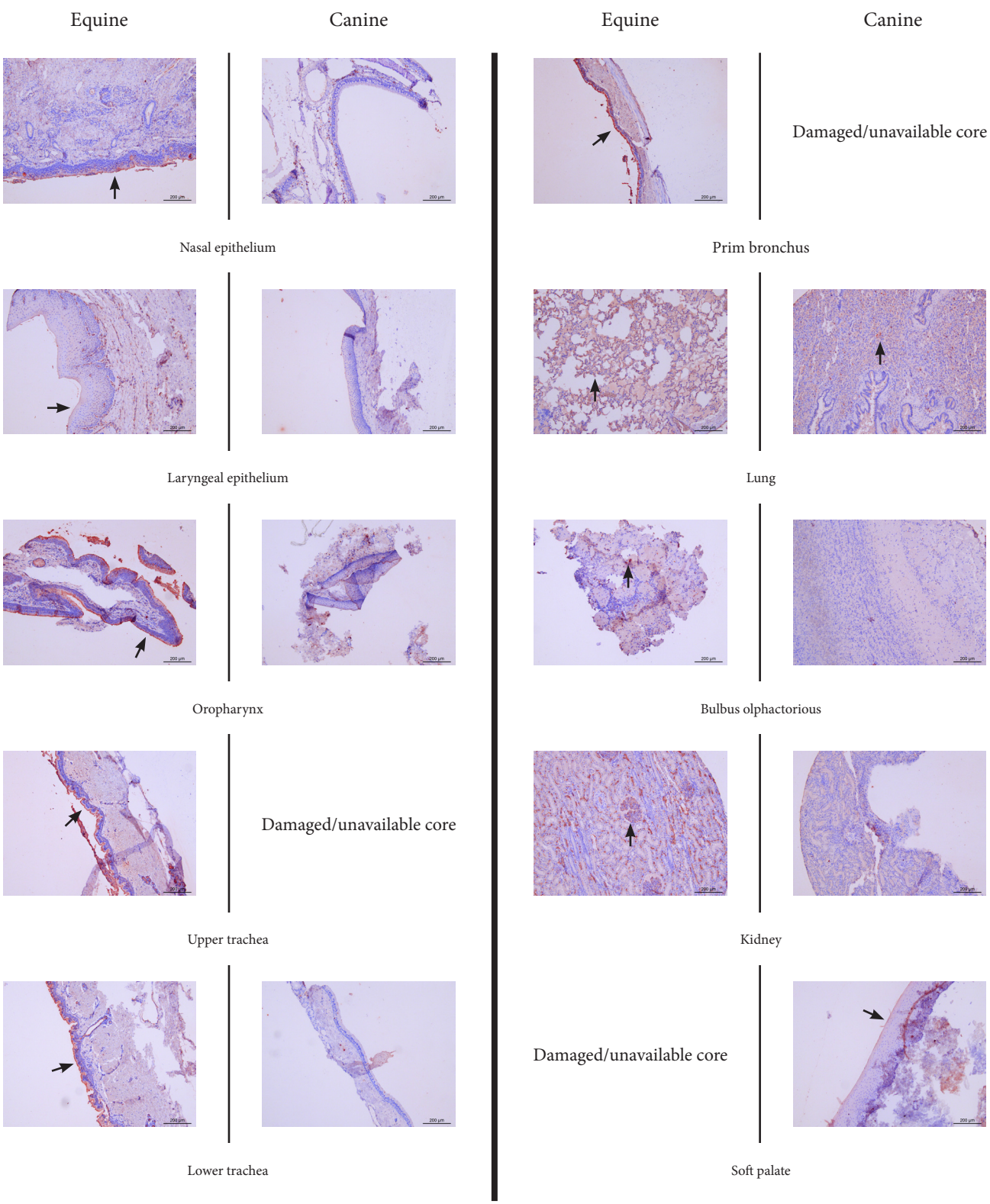

Figure 11. Staining results of the antibody specific against the Neu5Gc sialic acids on equine and canine tissues. Arrows indicate positions where positive signal (red color) was observed. Signal, which reveals that expression of Neu5Gc sialic acid, was only detected in equine tissues.

bronchus staining was similar to the equine lower trachea. Both of the lung cores, were positively stained, with a similar pattern. See also figure 10 for the staining images. The data suggest that the receptor used by the canine H3 protein is present on both species, however it might be with a different density present on the tissues.

Anti-Neu5Gc antibody staining

In order to confirm the presence of α2,3 linked N-glycolyl neuraminic sialic acid on the tissues, a straining was performed using an anti-Neu5Gc antibody. Table 7 gives an overview of the staining results. The staining revealed signal at most tissues of the equine but not on the canine tissues. Strong positive signal was detected on the epithelial and goblet cells of the equine upper and lower trachea, nasal area, the oropharynx, and primary bronchus. In addition, binding was observed in the kidney and the alveoli of the horse. On the contrary, the canine trachea and oropharynx were not stained. However, a slight positive signal was de-

Table 7. Overview of protein histochemistry stainings results on the tissues present on the equine-canine combined TMA. ++, very strong positive signal; +, positive signal; +/-, partly positive signal; -, no signal detected. See also annex I for pictures.

	H3N8 equine		H5N1 161.160		H7N7 equine		H3N8 canine		Neu5Gc	
Organ/Species	Equine	Canine	Equine	Canine	Equine	Canine	Equine	Canine	Equine	Canine
Bulbus olphactorius	-	-	+	-	n/a	-	+/-	+/-	+/-	-
Kidney	+	+	+	+/-	+/-	+/-	+	+	+	-
Laryngeal epithelium	-	-	+/-	+/-	-	-	-	-	+/-	-
Lower trachea	+/-	++	+	-	+	-	+	++	+	-
Lung	+/-	+	+	-	+	-	+	+	+	+/-
Nasal epithelium	+	+	+	-	n/a	-	+	+	+	-
Oropharynx	+	-	+	-	+	-	+	-	+	-
Primary bronchus	-	n/a	+	n/a	+	n/a	-	n/a	+	n/a
Upper trachea	-	n/a	+	n/a	+	-	+/-	n/a	+	n/a
Soft palate	n/a	-	n/a	-	n/a	-	n/a	-	n/a	+/-

tected in the lung and the kidney of the canine. See also figure 11 for images of the staining. This information shows that canines lack the Neu5Gc sialic acids in their respiratory tract, but is greatly represented in the equine tract.

Complications during the expression of the hemagglutinin-esterase-fusion (HEF) protein of the Influenza D virus

To allow analysis of the tissue distribution of receptors for IDV, we cloned the gene encoding for its viral attachment protein HEF into the pCD5 expression vector. In this way, we aimed at producing the HEF ectodomain as a soluble protein that was fused to a C-terminal GCN4 trimerisation tag, followed by a GFP superfolder and streptag. Transfection of this construct (HEF ectodomain-683aa) into 293T cells did however, not result in the production of soluble proteins, as Western blot analysis of the cell culture supernatant using streptag antibodies did not show a band of the correct size. Next, site-directed mutagenesis was performed to generate two new constructs, both encoding smaller N-terminal domains of HEF (aa1-439 and aa1-605). The expression and purification of the HEF protein consisted of multiple steps due to the inability isolating a soluble protein. The pCD5 vector containing the codon optimized gene that encoded for the ectodomain (683 aa) of the HEF-1, a GCN4 trimerization domain and a Strep-Tag was transfected into HEK293T cells. In addition, two more constructs were transfected into cells, a smaller part of the ectodomain (605 aa) and the part were the receptor binding domain is located (439 aa) (Song, Qi et al. 2016). 7 days after transfection, supernatant was collected and analyzed for the production of recombinant protein by western blot, using anti-strepTAG antibodies. As no proteins appeared to be produced (data not shown), the ORFs were cloned into another expression vector, which included a GFP sequence (Pédelacq, Cabantous et al. 2006), a GCN4 trimerization and dimerization domain, followed by a strepTAG. Unfortunately, no visible signal was detected when analyzing the cell culture supernatant (data not shown). To ensure that the transfection was succesful, a GFP containg plasmide was transfected alongside with the vectors of interest and assesed under a cell imaging microscope. All constructs including a GFP sequence gave a strong positive signal intracellularly, which indicates that the transfection was a success, however the translated protein was not being excreted from cells. Analyzing the lyzate of the cells revealed positive signal for the three trimer constructs. The dimer constructs were not detected (figure 12).

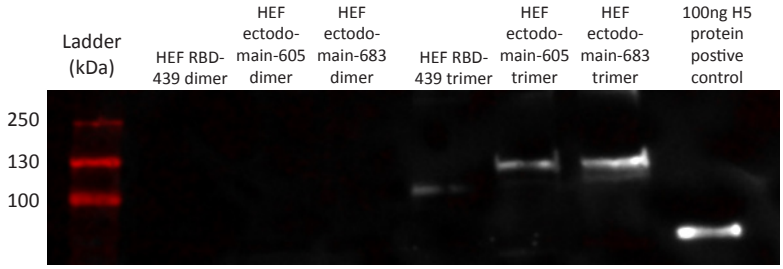

Figure 12. Westernblot results of the lyzate of the transfected cells. From left to right: HEF receptor binding domain 439aa dimer, HEF ectodomain 605aa dimer, HEF ectodomain 683aa dimer, HEF receptor binding domain 439aa trimer, HEF ectodomain 605aa trimer, HEF ectodomain 683aa trimer, and 100ng H5 (A/Vietnam/1203/2004) as a control. The dimer constructs did not show any signal on the westernblot, while the trimer constructs showed clear postive signal. All used HEF constructs included a GFP in their coding sequence.

Discussion

In this study, we generated TMAS of various mammalian species to allow visualization of the interaction between host specific viral receptors and viral attachment proteins. Furthermore, the optimization of the TMA creation allowed the construction of blocks consisting of porcine, equine & canine tissues, and obtaining well-preserved tissue sections for further use. Sampling specific anatomic locations gave us the possibility of looking more precisely to the interaction on the tissues of interest, such as organs of the respiratory tract. In addition, sampling tissues from more than one individual of a species enabled us to investigate the intraspecies variation of expressed viral receptors. Our results reveal that intraspecies variation in viral

receptor expression in the porcine respiratory tract is low. Binding tropism of viral attachment proteins of influenza A was in accordance with the respective lectin stainings in the porcine respiratory tract and revealed the presence of Neu5Acα2-3Gal & Neu5Acα2-6Gal in the lower porcine respiratory tract (from the primary bronchus and downwards). Furthermore, we observed the expression of Neu5Acα2-3Gal in the respiratory tract of equids and canids, although the canines tissue lacked the Neu5Gcα2-3Gal.

We described that TMAs are a fast and reliable tool for analyzing tissue distribution of cell bound molecules. Through the combination of the TMA technique with mammalian tissues and recombinant viral attachment proteins, we were able to look further into the first and foremost step of the infection cycle. The TMA technique was previously used by our group, predominantly to study host and tissue binding specificities of viral attachment proteins on avian hosts (Wickramasinghe, de Vries et al. 2015). The procedure gives clear advantages over the conventional method of analyzing various markers, through the readily availability of numerous samples on one slide. This also leads to the elimination of indivudual tissue variation. It was first used by H. Battifora (Battifora 1986), in order to standardize the immunohistological procedures and to ensure similar tissue treatment during immunostainings. As stated before TMAs have also facilitated the rapid analysis of molecular markers in cancer research studies (Kononen, Bubendorf et al. 1998). Analyzing each tissue sample individually would be unnecessarily time- and fund consuming, which furhter accentuates the advantages of the TMAs. These advantages can be extrapolated to the infection biology field, with the same reasoning. Staining and analyzing the attachment preferences of viral proteins on numerous tissues of interest individually is not the most favorable option. Other techniques that can be used to analyze the binding patterns of viral proteins include hemagglutination assays in combination with specific re-sialylation (Glaser, Stevens et al. 2005), and glycan microarrays (McBride, Paulson et al. 2016). Both of the mentioned techniques are undoubtedly valuable and can be used alongside the TMA, even though they have their own restrictions. The combined use of all three methods would allow a more complete analysis of viral receptors. The TMA represents the in vivo situation of an animal at a desirable level, combining the complex structures and wide variation of glycans present on the cell surface with the anatomic location in the species of interest. However, a considerable point of discussion is the use of a small, representative core of an organ to draw valid conclusions about the impact on the whole organ, and perhaps the whole species. Regarding the intraspecies variation, sampling more than one animal would already shed light on answering that important question, and this issue will be discussed later on. We can conclude that the TMA technique is an excellent and cost-effective tool to elucidate the presence of cell bound molecules that can serve as viral receptor, applicable to various tissues and species. In addition, the technique creates similar circumstances to that of an in vivo model without its disadvantages.

Our data indicate that the intraspecies variation in viral receptor expression is low. These data suggest that sampling one animal can be sufficient to extrapolate the obtained results to be represetantive for a large group of the same species. Our study demonstrated that within the porcine species, expression of sialic acids are similar to each other on identical anatomical locations of the respiratory tract. Nelli and coworkers also investigated the tissue distribution of sialic acids in the porcine species, sampling numerous organs from four pigs (Nelli, Kuchipudi et al. 2010). Unfortunately, there is no mention of accessing the variation between the samples, which could indicate the absence of variation or the absence of accessing the variation in general. Another recent study (Trebbien, Larsen et al. 2011), reflected on the expression of sialic acids in porcines, but also did not describe any significant variation between the used tissues. However, both studies are in agreement when it comes to differences in expression along the respiratory tract. In order to capture a complete image of the sialic acid distribution it is highly recommended to sample multiple sites of the tract. Taken together, the evidence points to the fact that the differences in expressing sialic acids molecules in the respiratory tract of pigs, is insignificant and that one animal can be taken as representative.

In our study, we observed a lack of expression of 2,3 sialic acids in the pig upper respiratory tract. Both lectins and HA proteins detecting this specific sialic acid did not stain the trachea of pigs, but could reveal the presence of this molecule in the lungs. It is believed that swines express both the human (Neu5Acα2,6-Gal) and avian type (Neu5Acα2-3Gal) in their trachea, constituting them an ideal host for the emergence of pandemic Influenza viruses (Ito, Couceiro et al. 1998). However, the truth about sialic acid expression in swine's respiratory tract is a bit distorted. More recent studies report that the epithelial cells of the porcine trachea express Neu5Acα2-3Gal in a more modest fashion than previously reported. Nelli et al. described the presence of Neu5Acα2-6Gal in the entire respiratory tract, with a gradual rise of expression of the Neu5Acα2-3Gal towards the lower respiratory lining (Nelli, Kuchipudi et al. 2010). Similar results were reported by Trebbien et al., who demonstrated that Neu5Acα2-6Gal was present in the epithelial cells of the trachea, bronchi, bronchiole and alveoli (Trebbien, Larsen et al. 2011). They likewise described the presence of Neu5Acα2-3Gal by lectin histochemistry, and concluded that Neu5Acα2-3Gal was present in the bronchiole and alveoli of the lung but not in the trachea (Trebbien, Larsen et al. 2011). Van Poucke et al. approached the receptor location using respiratory explants, and again, the results pointed to the predominant presence of Neu5Acα2-6Gal in the tracheal, bronchial and lung explants, while

scarce presence of Neu5Acα2-3Gal in the tracheal and bronchial explants and moderate presence in the lung explants was detected (Van Poucke, Nicholls et al. 2010). Our data from the lectin stainings are in agreement with the abovementioned studies. However, we were not able to confirm the presence of Neu5Acα2-6Gal in the lung cores, which could be attributed to the concentration of the used lectins, or the means of visualization. Nelli et al. used the same concentration of lectins for the SNA and MALII lectin and less for MALI, but used FITC labelled lectins. Visualization of fluorescence signals might be more sensitive than the peroxidase labelled lectins used in our study. The studies of Trebbien and van Boucke used a digoxin labelled SNA lectin, which could explain the difference in staining intensity, as we used peroxidase labelled lectins. Considering our data from two 'avian type' Influenza A strains, H1N1 Cal04 4x & H5N1 Vietnam, Neu5Acα2-3Gal is not present in the trachea of the swine. However, presence of Neu5Acα2-3Gal in the bronchiole and alveoli is unassailable and in agreement with the results of the lectin histochemistry of our study and the previous reports. The discrepancy of our results from the protein histochemistry compared to the SNA lectin histochemistry, could be the result of varying preference for the small ifferences in glycosylation present at the Neu5Acα2,6-Gal. Our results are in contrast with those of Ito et al., that both human and avian type are present in the porcine trachea, and that we agree that the Neu5Acα2-3Gal presence in the porcine trachea is little to not existent like the recent studies of Nelli et al., Trebbien et al. and van Poucke et al. suggest. The presence of Neu5Acα2-6Gal is undeniable in the lower parts of the respiratory tract, but there are some discrepancies regarding the upper part. Without the expression of Neu5Acα2-3Gal in the trachea of the pig, it is not suggestive that the suids can function as an ideal 'mixing vessel', as avian type of influenza viruses could not attach to the epithelial cells of the trachea, where the human types would be present.

Interspecies transmission of certain equine influenza A viruses to the canine population could be limited by the lack of expression of Neu5Gcα2-3Gal in the canine respiratory tract. There are multiple cases described where canine individuals were infected with an equine-origin Influenza A virus, which underline the possibility of interspecies transmission of the equine viruses (Crawford, Dubovi et al. 2005, Daly, Blunden et al. 2008, Kirkland, Finlaison et al. 2010). As attachment of the virus is the first and most important step of the infection cycle, interaction between the hemagglutinin and the preferred receptor is a fundamental necessity. It is described that most of the equine and avian H3 Influenza A viruses prefer Neu5Acα2-3Gal as their receptor (Connor, Kawaoka et al. 1994, Zhu, Hughes et al. 2015), therefore presence of this type of sialic acids is expected in equine tissues. The first reported equine-related canine Influenza A virus carrying the H3 subtype, has been described to be directly related to equine H3N8 viruses, since all eight genomic segments were from equine origin (Virus strain: A/canine/Florida/43/04, H3N8) (Crawford, Dubovi et al. 2005). Along with equine viruses that bear the H3 subtype, it is reported that there is, or was, another equine Influenza virus, the previously called equine-1 and now known as H7N7, which has never been described in canids. It is the very first isolate of equine Influenza, dating back to 1956 (Sovinova, Tumova et al. 1958). However, the H7N7 variant is believed to have disappeared from the general horse population, as it was last isolated in 1979 (Webster 1993). Interestingly, Gambaryan et al. described two H7N7 strains which recognized predominantly Neu5Gcα2-3Gal as their receptor, showing little affinity to Neu5Acα2-3Gal (Gambaryan, Matrosovich et al. 2012). We have already seen that H3 bearing equine Influenza subtypes prefer the Neu5Acα2-3Gal isoform, thus affinity for Neu5Gcα2-3Gal reveals a key difference between the two equine-specific viruses. There are no reports on interspecies transmission of the H7N7 virus from equids to canids, but to go as far as to insinuate that receptor-specificity was the only restricting factor is too much of a speculation. It is, however, interesting to investigate the relation of attachment specificity and receptor distribution on the two species. Regarding the presence of Neu5Acα2-3Gal in canine tissues, all recent reports are in accordance with our findings (Daly, Blunden et al. 2008, Song, Kang et al. 2008, Muranaka, Yamanaka et al. 2011, Ning, Wu et al. 2012). However, the expression of Neu5Acα2-3Gal in the equine host varies between similar studies (Scocco, Pedini 2008, Daly, Blunden et al. 2008, Muranaka, Yamanaka et al. 2011). Taking into consideration the data of the staining with the recombinantly expressed H3 from equine and canine origin, it is possible that Neu5Acα2-3Gal is more vividly expressed in canine tissues rather than the equine ones, which could explain the inconsistent reports. The ratio between Neu5Acα2-3Gal and Neu5Gcα2-3Gal expression in equine tissues is 1 to 9 (Suzuki, Ito et al. 2000), which could further explain the stronger signal of the hemagglutinins on the canine trachea, in which Neu5Acα2-3Gal is the predominant moiety. This hypothesis also supports the interspecies transmission of H3 bearing influenza subtypes on two unrelated occasions, one on the Asian and one on the American continent (Crawford, Dubovi et al. 2005, Song, Kang et al. 2008). Beside the presence of the different linked sialic acids, we investigated the presence of the Neu5Gcα2-3Gal sialic acid, which, as indicated before, seems to be the receptor for attachment of equine influenza viruses. The equine respiratory tract undoubtedly showed presence of the Neu5Gcα2-3Gal, and contradictory, the canine tissues did not reveal any signal. Suzuki et al. also described the presence of Neu5Gcα2-3Gal in the equine trachea and established that the analogy of Neu5Acα2-3Gal to Neu5Gcα2-3Gal present in the trachea was at a ratio of 1 to 9 (Suzuki, Ito et al. 2000). In contrast, Yang et al. described the presence of Neu5Gcα2-3Gal in the canine tracheal epithelium, which is opposed to our findings. This can be explained by the use of a western blot analysis used

for the detection of Neu5Gcα2-3Gal in tissue lysate, which is more sensitive than the lectin histochemistry (Yang, Li et al. 2013). However, it is probable that Neu5Gcα2-3Gal is expressed in canine tissues but not as vividly as in the equine species. Taken together, the data supports the theory that H7N7 equine viruses were never transmitted to the canine population, since the first step of infection could not take place in natural environmental conditions. In conclusion, canids and equids share the Neu5Acα2-3Gal moiety in their respiratory tract, which would greatly benefit an interspecies transmission of equine specific influenza A viruses. The two species differ largely in the expression of the Neu5Gcα2-3Gal in their respiratory tissues, something that could create a barrier for transmission of equine viruses with such a receptor preference.

The expression of Neu5Acα2-3Gal and Neu5Acα2-6Gal in the majority of the porcine organs suggests that they are a potential target for Influenza A virus attachment. In the digestive tract, Neu5Acα2-6Gal expression seemed to be dominant over the Neu5Acα2-3Gal, which is in agreement with previous reports (Nelli, Kuchipudi et al. 2010). Our data are indicative that the gastrointestinal tract can be available for the possible infection of Influenza A viruses from both types. For humans, it is well established that viral replication can occur in the gastrointestinal tract (Uiprasertkul, Puthavathana et al. 2005), and it is well described that gastrointestinal infections play a major role in the avian population as it is also a very efficient spreading mechanism for this species (Olsen, Munster et al. 2006, Breban, Drake et al. 2009). Unfortunately, the described cases in pigs do not clarify whether the gastrointestinal symptoms can be appointed to the Influenza A infection, or to a possible synergy between the virus and other pathogens (Lange, Kalthoff et al. 2009). The general belief is that influenza A in swine is mostly restricted to the respiratory tract and not to the digestive apparatus (Rajao, Anderson et al. 2014). Furthermore, presence of the sialic acids in the central nervous system (CNS) suggests that this system is also vulnerable to a potential infection. The presence of both moieties indicates that both avian and human Influenza A viruses could infect the CNS in case of systemic infection. However, the expression of the receptor in that area does not necessarily mean that the virus can reach and infect it. A similar effect is suggested by the animal experiments described by Munster & de Wit et al., which revealed that no viral load was detected in ferret brains, after inoculation with a pandemic H1N1 and a common seasonal H1N1 (Munster, de Wit et al. 2009). Despite the statement of Munster & de Wit, it seems that this is not applicable for all strains and possibly all species. Gu et al. described cases where an Influenza A virus (H5N1) was isolated in the brain of human individuals, which indicates that Influenza A viruses can replicate in the brain (and other organs) beside the respiratory tract (Gu, Xie et al. 2007). It is described that viral Influenza A RNA was detected in the brainstem of pigs, which, in combination with the lack of viremia, supported the hypothesis of neuronal spreading from the nasal mucosa to the neuronal pathways (De Vleeschauwer, Atanasova et al. 2009). Our findings support such a hypothesis, as the necessary receptors are present on the neuronal tissues. In conclusion, avian and human type sialic acids are expressed in the central nervous system and the gastrointestinal tract of the swine, allowing the attachment of various influenza A viruses, although it seems not applicable to all Influenza A viruses or hosts.

It is important to remember that our study demonstrates the expression of sialic acids/viral receptors on various host tissues, thus confirming the ability of viruses to attach to their preferred sialic acids, though it does not answer any questions about actual cell infection. This has been demonstrated previously using canine Influenza A viruses and equine hosts. Yang et al. reported an amino aciad substitution in canine influenza hemagglutinins, which is not present in equine or avian isoforms, and their data suggested that it comprised a specific host adaptation as it is highly conserved in canine viruses. The mutation appears at a position that is adjacent to the receptor binding site (Yang, Li et al. 2013). Since it enhances the binding affinity to Neu5Acα2-3Gal, it would be probable that it would also enhance binding, and therefore infection, to equine hosts. However, no symptoms, replication or further transmission was observed when equids were inoculated with canine isolates (Quintana, Hussey et al. 2011). This emphasizes the fact that receptor specificity of a hemagglutinin is not the only factor determining the host range of an Influenza A virus. Another study that promotes this theory revealed that a single amino acid substitution in the fusion domain of the hemagglutinin of canine but not equine viruses, could interfere with the stability of the hemagglutinin or the fusion process, partly explaining the one-way transmission of the virus (Collins, Vachieri et al. 2014). It is also known that the presence of a cell-secreted protease, which can cleave the inactive hemagglutinin precursor, is essential for the infectivity of a virus, as it allows the conformational change of the hemagglutinin, which is necessary for the membrane fusion in the endosomes and thus for perpetuation of the infection (Klenk, Garten 1994, Chen, Lee et al. 1998, Skehel, Wiley 2000b, Russell, Gamblin et al. 2013). In short, our experiments setting, thus visualizing the binding of a recombinantly expressed hemagglutinin protein to tissues, does not directly ensure cell infection with the virus from where the attachment protein originated. This proces is dependent on various other factors which determine viral pathogenicity, and cannot be fully presented by our approach.

Unfortunately, we were yet unable to produce the HEF-1 proteins of IDV as soluble recombinant proteins. As the method has been previously established and successful for production of IAV HA and other viral attachment proteins (de Vries, de Vries et al. 2010), it is most likely that an intrinsic characteristic of the HEF-1 gene

hampers its production. Song et al. described the recombinant production of the protein, with some alterations in the procedure. The main differences between the two studies are the used cells and vectors, since they used Hi5 insect cells, and a baculovirus transfer vector to produce the soluble HEF-1 proteins (Song, Qi et al. 2016). Interestingly, a gp67 signal sequence was incorporated into the vector, which ensures the secretion of the proteins out of the cells (Whitford, Stewart et al. 1989, Song, Qi et al. 2016). However, insect cells do not ensure the complex N-glycosylations which are present in mammalian expression cells, leaving the question whether the absence of this type of glycosylation would interfere with the biological activity (Altmann, Staudacher et al. 1999, Palmberger, Wilson et al. 2012). Another possibility for the failure of our cells to excrete the protein, is the interference of the esterase-inactivating mutations with the folding of the protein. Inaccurate folded or incomplete folded proteins are withheld and degraded within the cell by proteases (Alberts, Bray et al. 2013), which could explain the absence of the protein in the cell culture supernatant. However, evidence of intracellular HEF-1 protein was presented in this study, which indicates that the issue is located at the secretion of the cells. This would indicate an irregularity in the CD5 sequence, which directs the synthesis and the export of secreted proteins (Aruffo, Stamenkovic et al. 1990, Zeng, Langereis et al. 2008, Wickramasinghe, de Vries et al. 2011). However, no discrepancies were detected in the encoding sequence, leaving the unanswered question as why the protein is not being secreted out of the cells. Another study, investigating the esterase activity of the HEF protein of the Influeza C virus (ICV), described the disability to produce the protein in certain cell types (Pleschka, Klenk et al. 1995). It therefore might be interesting to approach the expression of the HEF-1 protein in different cell types, since the two viruses share ±50% overall amino acid identity (Hause, Collin et al. 2014, Ducatez, Pelleter et al. 2015). In summary, we opted to analyze the tissue distribution of the viral receptor of the HEF-1 attachment protein by recombinantly producing the protein. Unfortunately, no soluble protein could be produced, which sabotaged our further intentions.

Acknowledgements

We would like to thank Dr R. P. de Vries of the Department of Chemical Biology & Drug Discovery, Institute for Pharmaceutical Sciences at Utrecht University, for providing the recombinant hemagglutinins and for the extremely helpful scientific discussions. Also, we would like to thank Dr M. F. Ducatez of the École Nationale Vétérinaire de Toulouse, for the submission of the bovine tissues. Also, we would like to thank S.C. van Essen-van Dorresteijn and Dr R. W. Wubbolts for the optimization of the TMA technique and the 3D-printing expertise. Furthermore, I would like to thank M. de Jong, G. de Vrieze and A. J. Berends for the excellent introduction and assistance in various laboratory procedures & techniques. Also, I would like to thank Drs E. A. W. S. Weerts for his critical opinion and insightful discussions during the project. Also, I would like to thank the members of the Master research committee, for considering and allowing me to be a part of this project. Last but not least, I would like to thank K. Kanhai for the moral support and interesting ideas throughout the project.

I would like to mention that without the guidance and help of my supervisors Dr. M.H. Verheije and Drs K.M. Bouwman, it would not have been possible to start and complete this research project.

References

1. ALBERTS, B., BRAY, D., HOPKIN, K., JOHNSON, A., LEWIS, J., RAFF, M., ROBERTS, K. and WALTER, P., 2013. Essential cell biology. Garland Science.
2. ALTMANN, F., STAUDACHER, E., WILSON, I.B. and MÄRZ, L., 1999. Insect cells as hosts for the expression of recombinant glycoproteins. Glycoconjugate journal, 16(2), pp. 109-123.
3. ARUFFO, A., STAMENKOVIC, I., MELNICK, M., UNDERHILL, C.B. and SEED, B., 1990. CD44 is the principal cell surface receptor for hyaluronate. Cell, 61(7), pp. 1303-1313.
4. BATTIFORA, H., 1986. The multitumor (sausage) tissue block: novel method for immunohistochemical antibody testing. Laboratory investigation; a journal of technical methods and pathology, 55(2), pp. 244-248.
5. BREBAN, R., DRAKE, J.M., STALLKNECHT, D.E. and ROHANI, P., 2009. The role of environmental transmission in recurrent avian influenza epidemics. PLoS computational biology, 5(4), pp. e1000346.
6. CAMP, R.L., CHARETTE, L.A. and RIMM, D.L., 2000. Validation of tissue microarray technology in breast carcinoma. Laboratory investigation, 80(12), pp. 1943.
7. CHEN, J., LEE, K.H., STEINHAUER, D.A., STEVENS, D.J., SKEHEL, J.J. and WILEY, D.C., 1998. Structure of the hemagglutinin precursor cleavage site, a determinant of influenza pathogenicity and the origin of the labile conformation. Cell, 95(3), pp. 409-417.
8. COLLIN, E.A., SHENG, Z., LANG, Y., MA, W., HAUSE, B.M. and LI, F., 2015. Cocirculation of two distinct genetic and antigenic lineages of proposed influenza D virus in cattle. Journal of virology, 89(2), pp. 1036-1042.
9. COLLINS, P.J., VACHIERI, S.G., HAIRE, L.F., OGRODOWICZ, R.W., MARTIN, S.R., WALKER, P.A., XIONG, X., GAMBLIN, S.J. and SKEHEL, J.J., 2014. Recent evolution of equine influenza and the origin of canine influenza. Proceedings of the National Academy of Sciences of the United States of America, 111(30), pp. 11175-11180.
10. CONNOR, R.J., KAWAOKA, Y., WEBSTER, R.G. and PAULSON, J.C., 1994. Receptor specificity in human, avian, and equine H2 and H3 influenza virus isolates. Virology, 205(1), pp. 17-23.
11. CORNELISSEN, L.A., DE VRIES, R.P., DE BOER-LUIJTZE, E.A., RIGTER, A., ROTTIER, P.J. and DE HAAN, C.A., 2010. A single immunization with soluble recombinant trimeric hemagglutinin protects chickens against highly pathogenic avian influenza virus H5N1. PLoS One, 5(5), pp. e10645.
12. CRAWFORD, P.C., DUBOVI, E.J., CASTLEMAN, W.L., STEPHENSON, I., GIBBS, E.P., CHEN, L., SMITH, C., HILL, R.C., FERRO, P., POMPEY, J., BRIGHT, R.A., MEDINA, M.J., JOHNSON, C.M., OLSEN, C.W., COX, N.J., KLIMOV, A.I., KATZ, J.M. and DONIS, R.O., 2005. Transmission of equine influenza virus to dogs. Science (New York, N.Y.), 310(5747), pp. 482-485.
13. DALY, J.M., BLUNDEN, A.S., MACRAE, S., MILLER, J., BOWMAN, S.J., KOLODZIEJEK, J., NOWOTNY, N. and SMITH, K.C., 2008. Transmission of equine influenza virus to English foxhounds. Emerging infectious diseases, 14(3), pp. 461-464.
14. DE VLEESCHAUWER, A., ATANASOVA, K., VAN BORM, S., VAN DEN BERG, T., RASMUSSEN, T.B., UTTENTHAL, Å and VAN REETH, K., 2009. Comparative pathogenesis of an avian H5N2 and a swine H1N1 influenza virus in pigs. PloS one, 4(8), pp. e6662.
15. DE VRIES, R.P., DE VRIES, E., BOSCH, B.J., DE GROOT, R.J., ROTTIER, P.J. and DE HAAN, C.A., 2010. The influenza A virus hemagglutinin glycosylation state affects receptor-binding specificity. Virology, 403(1), pp. 17-25.
16. DE VRIES, R.P., DE VRIES, E., MARTINEZ-ROMERO, C., MCBRIDE, R., VAN KUPPEVELD, F.J., ROTTIER, P.J., GARCIA-SASTRE, A., PAULSON, J.C. and DE HAAN, C.A., 2013. Evolution of the hemagglutinin protein of the new pandemic H1N1 influenza virus: maintaining optimal receptor binding by compensatory substitutions. Journal of virology, 87(24), pp. 13868-13877.
17. DE VRIES, R.P., DE VRIES, E., MOORE, K.S., RIGTER, A., ROTTIER, P.J. and DE HAAN, C.A., 2011. Only two residues are responsible for the dramatic difference in receptor binding between swine and new pandemic H1 hemagglutinin. The Journal of biological chemistry, 286(7), pp. 5868-5875.
18. DE VRIES, R.P., ZHU, X., MCBRIDE, R., RIGTER, A., HANSON, A., ZHONG, G., HATTA, M., XU, R., YU, W., KAWAOKA, Y., DE HAAN, C.A., WILSON, I.A. and PAULSON, J.C., 2014. Hemagglutinin receptor specificity and structural analyses of respiratory droplet-transmissible H5N1 viruses. Journal of virology, 88(1), pp. 768-773.
19. DORTMANS, J.C., DEKKERS, J., WICKRAMASINGHE, I.N., VERHEIJE, M.H., ROTTIER, P.J., VAN KUPPEVELD, F.J., DE VRIES, E. and DE HAAN, C.A., 2013. Adaptation of novel H7N9 influenza A virus to human receptors. Scientific reports, 3, pp. 3058.

20. DUCATEZ, M.F., PELLETIER, C. and MEYER, G., 2015. Influenza D virus in cattle, France, 2011-2014. Emerging infectious diseases, 21(2), pp. 368-371.
21. GAMBARYAN, A.S., MATROSOVICH, T.Y., PHILIPP, J., MUNSTER, V.J., FOUCHIER, R.A., CATTOLI, G., CAPUA, I., KRAUSS, S.L., WEBSTER, R.G., BANKS, J., BOVIN, N.V., KLENK, H.D. and MATROSOVICH, M.N., 2012. Receptor-binding profiles of H7 subtype influenza viruses in different host species. Journal of virology, 86(8), pp. 4370-4379.
22. GLASER, L., STEVENS, J., ZAMARIN, D., WILSON, I.A., GARCIA-SASTRE, A., TUMPEY, T.M., BASLER, C.F., TAUBENBERGER, J.K. and PALESE, P., 2005. A single amino acid substitution in 1918 influenza virus hemagglutinin changes receptor binding specificity. Journal of virology, 79(17), pp. 11533-11536.
23. GREENE, J.L., 2015. Update on the Highly-Pathogenic Avian Influenza Outbreak of 2014-2015. Congressional Res Serv [Internet], .
24. GU, J., XIE, Z., GAO, Z., LIU, J., KORTEWEG, C., YE, J., LAU, L.T., LU, J., GAO, Z. and ZHANG, B., 2007. H5N1 infection of the respiratory tract and beyond: a molecular pathology study. The Lancet, 370(9593), pp. 1137-1145.
25. HANS, C.P., WEISENBURGER, D.D., GREINER, T.C., GASCOYNE, R.D., DELABIE, J., OTT, G., MULLER-HERMELINK, H.K., CAMPO, E., BRAZIEL, R.M., JAFFE, E.S., PAN, Z., FARINHA, P., SMITH, L.M., FALINI, B., BANHAM, A.H., ROSENWALD, A., STAUDT, L.M., CONNORS, J.M., ARMITAGE, J.O. and CHAN, W.C., 2004. Confirmation of the molecular classification of diffuse large B-cell lymphoma by immunohistochemistry using a tissue microarray. Blood, 103(1), pp. 275-282.
26. HAUSE, B.M., DUCATEZ, M., COLLIN, E.A., RAN, Z., LIU, R., SHENG, Z., ARMIEN, A., KAPLAN, B., CHAKRAVARTY, S. and HOPPE, A.D., 2013. Isolation of a novel swine influenza virus from Oklahoma in 2011 which is distantly related to human influenza C viruses. PLoS pathogens, 9(2), pp. e1003176.
27. HAUSE, B.M., COLLIN, E.A., LIU, R., HUANG, B., SHENG, Z., LU, W., WANG, D., NELSON, E.A. and LI, F., 2014. Characterization of a novel influenza virus in cattle and Swine: proposal for a new genus in the Orthomyxoviridae family. mBio, 5(2), pp. e00031-14.
28. ITO, M., NAGAI, M., HAYAKAWA, Y., KOMAE, H., MURAKAMI, N., YOTSUYA, S., ASAKURA, S., SAKODA, Y. and KIDA, H., 2008. Genetic analyses of an H3N8 influenza virus isolate, causative strain of the outbreak of equine influenza at the Kanazawa racecourse in Japan in 2007. Journal of Veterinary Medical Science, 70(9), pp. 899-906.
29. ITO, T., COUCEIRO, J.N., KELM, S., BAUM, L.G., KRAUSS, S., CASTRUCCI, M.R., DONATELLI, I., KIDA, H., PAULSON, J.C., WEBSTER, R.G. and KAWAOKA, Y., 1998. Molecular basis for the generation in pigs of influenza A viruses with pandemic potential. Journal of virology, 72(9), pp. 7367-7373.
30. KIRKLAND, P.D., FINLAISON, D.S., CRISPE, E. and HURT, A.C., 2010. Influenza virus transmission from horses to dogs, Australia. Emerging infectious diseases, 16(4), pp. 699-702.
31. KLENK, H. and GARTEN, W., 1994. Host cell proteases controlling virus pathogenicity. Trends in microbiology, 2(2), pp. 39-43.
32. KONAMI, Y., YAMAMOTO, K., OSAWA, T. and IRIMURA, T., 1994. Strong affinity of Maackia amurensis hemagglutinin (MAH) for sialic acid-containing Ser/Thr-linked carbohydrate chains of N-terminal octapeptides from human glycophorin A. FEBS letters, 342(3), pp. 334-338.
33. KONONEN, J., BUBENDORF, L., KALLIONIMENI, A., BÄRLUND, M., SCHRAML, P., LEIGHTON, S., TORHORST, J., MIHATSCH, M.J., SAUTER, G. and KALLIONIMENI, O., 1998. Tissue microarrays for high-throughput molecular profiling of tumor specimens. Nature medicine, 4(7), pp. 844-847.
34. LAKDAWALA, S.S., JAYARAMAN, A., HALPIN, R.A., LAMIRANDE, E.W., SHIH, A.R., STOCKWELL, T.B., LIN, X., SIMENAUER, A., HANSON, C.T., VOGEL, L., PASKEL, M., MINAI, M., MOORE, I., ORANDLE, M., DAS, S.R., WENTWORTH, D.E., SASISEKHARAN, R. and SUBBARAO, K., 2015. The soft palate is an important site of adaptation for transmissible influenza viruses. Nature, 526(7571), pp. 122-125.
35. LANGE, E., KALTHOFF, D., BLOHM, U., TEIFKE, J.P., BREITHAUPT, A., MARESCH, C., STARICK, E., FEREIDOUNI, S., HOFFMANN, B. and METTENLEITER, T.C., 2009. Pathogenesis and transmission of the novel swine-origin influenza virus A/H1N1 after experimental infection of pigs. Journal of General Virology, 90(9), pp. 2119-2123.
36. LEE, Y., LEE, D., LEE, H., PARK, J., YUK, S., SUNG, H., PARK, H., LEE, J., PARK, S. and CHOI, I., 2012. Serologic evidence of H3N2 canine influenza virus infection before 2007. Vet Rec, 171, pp. 477.
37. LEYSON, C., FRANÇA, M., JACKWOOD, M. and JORDAN, B., 2016. Polymorphisms in the S1 spike glycoprotein of Arkansas-type infectious bronchitis virus (IBV) show differential binding to host tissues and altered antigenicity. Virology, 498, pp. 218-225.

38. LOEFFEN, W., DE VRIES, R., STOCKHOFE, N., VAN ZOELEN-BOS, D., MAAS, R., KOCH, G., MOORMANN, R., ROTTIER, P. and DE HAAN, C., 2011. Vaccination with a soluble recombinant hemagglutinin trimer protects pigs against a challenge with pandemic (H1N1) 2009 influenza virus. Vaccine, 29(8), pp. 1545-1550.
39. MCBRIDE, R., PAULSON, J.C. and DE VRIES, R.P., 2016. A Miniaturized Glycan Microarray Assay for Assessing Avidity and Specificity of Influenza A Virus Hemagglutinins. Journal of visualized experiments : JoVE, (111). doi(111), pp. 10.3791/53847.
40. MUNSTER, V.J., DE WIT, E., VAN DEN BRAND, J.M., HERFST, S., SCHRAUWEN, E.J., BESTEBROER, T.M., VAN DE VIJVER, D., BOUCHER, C.A., KOOPMANS, M., RIMMELZWAAN, G.F., KUIKEN, T., OSTERHAUS, A.D. and FOUCHIER, R.A., 2009. Pathogenesis and transmission of swine-origin 2009 A(H1N1) influenza virus in ferrets. Science (New York, N.Y.), 325(5939), pp. 481-483.
41. MURANAKA, M., YAMANAKA, T., KATAYAMA, Y., HIDARI, K., KANAZAWA, H., SUZUKI, T., OKU, K. and OYAMADA, T., 2011. Distribution of influenza virus sialoreceptors on upper and lower respiratory tract in horses and dogs. Journal of Veterinary Medical Science, 73(1), pp. 125-127.
42. NELLI, R.K., KUCHIPUDI, S.V., WHITE, G.A., PEREZ, B.B., DUNHAM, S.P. and CHANG, K., 2010. Comparative distribution of human and avian type sialic acid influenza receptors in the pig. BMC veterinary research, 6(1), pp. 4.
43. NING, Z., WU, X., CHENG, Y., QI, W., AN, Y., WANG, H., ZHANG, G. and LI, S., 2012. Tissue distribution of sialic acid-linked influenza virus receptors in beagle dogs. Journal of veterinary science, 13(3), pp. 219-222.
44. OLSEN, B., MUNSTER, V.J., WALLENSTEN, A., WALDENSTROM, J., OSTERHAUS, A.D. and FOUCHIER, R.A., 2006. Global patterns of influenza a virus in wild birds. Science (New York, N.Y.), 312(5772), pp. 384-388.
45. PACKEISEN, J., BUERGER, H., KRECH, R. and BOECKER, W., 2002. Tissue microarrays: a new approach for quality control in immunohistochemistry. Journal of clinical pathology, 55(8), pp. 613-615.
46. PALMBERGER, D., WILSON, I.B., BERGER, I., GRABHERR, R. and RENDIC, D., 2012. SweetBac: a new approach for the production of mammalianised glycoproteins in insect cells. PLoS One, 7(4), pp. e34226.
47. PÉDELACQ, J., CABANTOUS, S., TRAN, T., TERWILLIGER, T.C. and WALDO, G.S., 2006. Engineering and characterization of a superfolder green fluorescent protein. Nature biotechnology, 24(1), pp. 79.
48. PLESCHKA, S., KLENK, H.-D., HERRLER, G. 1995. The catalytic triad of the influenza C virus glycoprotein HEF esterase: characterization by site-directed mutagenesis and functional analysis. Journal of general virology, 76(10) pp. 2529-2537.
49. QUINTANA, A.M., HUSSEY, S.B., BURR, E.C., PECORARO, H.L., ANNIS, K.M., RAO, S. and LANDOLT, G.A., 2011. Evaluation of infectivity of a canine lineage H3N8 influenza A virus in ponies and in primary equine respiratory epithelial cells. American Journal of Veterinary Research, 72(8), pp. 1071-1078.
50. RAJAO, D.S., ANDERSON, T.K., GAUGER, P.C. and VINCENT, A.L., 2014. Pathogenesis and vaccination of influenza A virus in swine. Influenza Pathogenesis and Control-Volume I. Springer, pp. 307-326.
51. RUSSELL, R.J., GAMBLIN, S.J. and SKEHEL, J.J., 2013. Influenza glycoproteins: hemagglutinin and neuraminidase. Textbook of Influenza, 2nd Edition, , pp. 67-100.
52. SCOCCO, P. and PEDINI, V., 2008. Localization of influenza virus sialoreceptors in equine respiratory tract. Histology and histopathology, 23(7-9), pp. 973-978.
53. SHIBUYA, N., GOLDSTEIN, I.J., BROEKAERT, W.F., NSIMBA-LUBAKI, M., PEETERS, B. and PEUMANS, W.J., 1987. The elderberry (Sambucus nigra L.) bark lectin recognizes the Neu5Ac(alpha 2-6)Gal/GalNAc sequence. The Journal of biological chemistry, 262(4), pp. 1596-1601.
54. SKEHEL, J.J. and WILEY, D.C., 2000. Receptor binding and membrane fusion in virus entry: the influenza hemagglutinin. Annual Review of Biochemistry, 69(1), pp. 531-569.
55. SONG, H., QI, J., KHEDRI, Z., DIAZ, S., YU, H., CHEN, X., VARKI, A., SHI, Y. and GAO, G.F., 2016. An open receptor-binding cavity of hemagglutinin-esterase-fusion glycoprotein from newly-identified influenza D virus: basis for its broad cell tropism. PLoS pathogens, 12(1), pp. e1005411.
56. SONG, D., KANG, B., LEE, C., JUNG, K., HA, G., KANG, D., PARK, S., PARK, B. and OH, J., 2008. Transmission of avian influenza virus (H3N2) to dogs. Emerging infectious diseases, 14(5), pp. 741-746.
57. SOVINOVA, O., TUMOVA, B., POUSKA, F. and NEMEC, J., 1958. Isolation of a virus causing respiratory disease in horses. Acta virologica, 2(1), pp. 52-61.
58. SUZUKI, Y., ITO, T., SUZUKI, T., HOLLAND, R.E.,Jr, CHAMBERS, T.M., KISO, M., ISHIDA, H. and KAWAOKA, Y., 2000. Sialic acid species as a determinant of the host range of influenza A viruses. Journal of virology, 74(24), pp.

11825-11831.
59. TREBBIEN, R., LARSEN, L.E. and VIUFF, B.M., 2011. Distribution of sialic acid receptors and influenza A virus of avian and swine origin in experimentally infected pigs. Virology journal, 8(1), pp. 434.
60. UIPRASERTKUL, M., PUTHAVATHANA, P., SANGSIRIWUT, K., POORUK, P., SRISOOK, K., PEIRIS, M., NICHOLLS, J.M., CHOKEPHAIBULKIT, K., VANPRAPAR, N. and AUEWARAKUL, P., 2005. Influenza A H5N1 replication sites in humans. Emerging infectious diseases, 11(7), pp. 1036-1041.
61. VAN POUCKE, S.G., NICHOLLS, J.M., NAUWYNCK, H.J. and VAN REETH, K., 2010. Replication of avian, human and swine influenza viruses in porcine respiratory explants and association with sialic acid distribution. Virology journal, 7(1), pp. 38.
62. WANG, M., TSCHERNE, D.M., MCCULLOUGH, C., CAFFREY, M., GARCIA-SASTRE, A. and RONG, L., 2012. Residue Y161 of influenza virus hemagglutinin is involved in viral recognition of sialylated complexes from different hosts. Journal of virology, 86(8), pp. 4455-4462.
63. WEBSTER, R., 1993. Are equine 1 influenza viruses still present in horses? Equine veterinary journal, 25(6), pp. 537-538.
64. WHITFORD, M., STEWART, S., KUZIO, J. and FAULKNER, P., 1989. Identification and sequence analysis of a gene encoding gp67, an abundant envelope glycoprotein of the baculovirus Autographa californica nuclear polyhedrosis virus. Journal of virology, 63(3), pp. 1393-1399.
65. WICKRAMASINGHE, I.N.A., DE VRIES, R.P., EGGERT, A.M., WANDEE, N., DE HAAN, C.A., GRÖNE, A. and VERHEIJE, M.H., 2015. Host tissue and glycan binding specificities of avian viral attachment proteins using novel avian tissue microarrays. PloS one, 10(6), pp. e0128893.
66. WICKRAMASINGHE, I.N., DE VRIES, R.P., GRONE, A., DE HAAN, C.A. and VERHEIJE, M.H., 2011. Binding of avian coronavirus spike proteins to host factors reflects virus tropism and pathogenicity. Journal of virology, 85(17), pp. 8903-8912.
67. XU, R., MCBRIDE, R., NYCHOLAT, C.M., PAULSON, J.C. and WILSON, I.A., 2012. Structural characterization of the hemagglutinin receptor specificity from the 2009 H1N1 influenza pandemic. Journal of virology, 86(2), pp. 982-990.
68. YAMANAKA, T., TSUJIMURA, K., KONDO, T., MATSUMURA, T., ISHIDA, H., KISO, M., HIDARI, K.I. and SUZUKI, T., 2010. Infectivity and pathogenicity of canine H3N8 influenza A virus in horses. Influenza and other respiratory viruses, 4(6), pp. 345-351.
69. YANG, G., LI, S., BLACKMON, S., YE, J., BRADLEY, K.C., COOLEY, J., SMITH, D., HANSON, L., CARDONA, C. and STEINHAUER, D.A., 2013. Mutation tryptophan to leucine at position 222 of haemagglutinin could facilitate H3N2 influenza A virus infection in dogs. Journal of General Virology, 94(12), pp. 2599-2608.
70. ZENG, Q., LANGEREIS, M.A., VAN VLIET, A.L., HUIZINGA, E.G. and DE GROOT, R.J., 2008. Structure of coronavirus hemagglutinin-esterase offers insight into corona and influenza virus evolution. Proceedings of the National Academy of Sciences of the United States of America, 105(26), pp. 9065-9069.
71. ZHU, H., HUGHES, J. and MURCIA, P.R., 2015. Origins and Evolutionary Dynamics of H3N2 Canine Influenza Virus. Journal of virology, 89(10), pp. 5406-5418.

	A	B	C	D	E	F
1	Upper Trachea	Duodenum	Nasopharynx	Conjuctiva	Cerebellum	Caecum
2	Kidney	Primary Bronchus	Colon	Cranial side epiglottis	Ovarium	Blader
3	Lower Trachea	Jejunum	Milt	Bulbus olfactorius	Pharyngeal tonsil	Sciatic nerve
4	Heart	Stomach	Oesophagus	Nasal epithelium	Hypofyse	Caudal side epiglottis
5	Liver	Ileum	Pancreas	Uterus	Adrenal gland	Brain stem
6	Lung	Lymphnode	Larynx	Cerebrum	Thymus	Soft palatum

Annex I, Table 1. Placement map of monospecies porcine TMA, containing various organs.

	A	B	C	D	E	F
1	37.1 Upper Trachea	38.1 Upper Trachea	39.1 Upper Trachea	40.1 Upper Trachea	41.1 Upper Trachea	42.1 Upper Trachea
2	37.2 Mid Trachea	38.2 Mid Trachea	39.2 Mid Trachea	40.2 Mid Trachea	41.2 Mid Trachea	42.2 Mid Trachea
3	37.3 Lower Trachea	38.3 Lower Trachea	39.3 Lower Trachea	40.3 Lower Trachea	41.3 Lower Trachea	42.3 Lower Trachea
4	37.4 Primary bronchus	38.4 Primary bronchus	39.4 Primary bronchus	40.4 Primary bronchus	41.4 Primary bronchus	42.4 Primary bronchus
5	37.5 Bronchioli	38.5 Bronchioli	39.5 Bronchioli	40.5 Bronchioli	41.5 Bronchioli	42.5 Bronchioli
6	37.6 Alveoli	38.6 Alveoli	39.6 Alveoli	40.6 Alveoli	41.6 Alveoli	42.6 Alveoli

Annex I, Table 2. Placement map of monospecies porcine TMA, containing respiratory organs from six different individuals.

	A	B	C	D	E	F
1	**EMPTY**	Canine Nasal epithelium	Canine Prim bronchus	Equine Nasal epithelium	Equine Prim bronchus	**EMPTY**
2	**EMPTY**	Canine Laryngeal epithelium	Canine Lung	Equine Laryngeal epithelium	Equine Lung	**EMPTY**
3	**EMPTY**	Canine oropharynx	Canine Bulbus olphactorius	Equine oropharynx	Equine Bulbus olphactorius	**EMPTY**
4	**EMPTY**	Canine Upper trachea	Canine Kidney	Equine Upper trachea	Equine Kidney	**EMPTY**
4	**EMPTY**	Canine Lower trachea	Canine Soft palate	Equine Lower trachea	**EMPTY**	**EMPTY**
6	**EMPTY**	**EMPTY**	**EMPTY**	**EMPTY**	**EMPTY**	**EMPTY**

Annex I, Table 3. Placement map of equine & canine respiratory organs TMA.

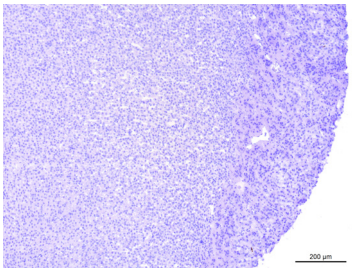

Adrenal gland

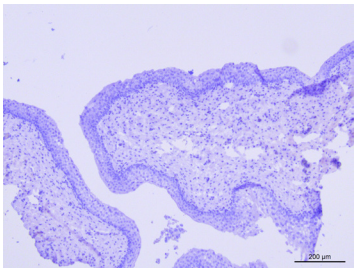

Bladder

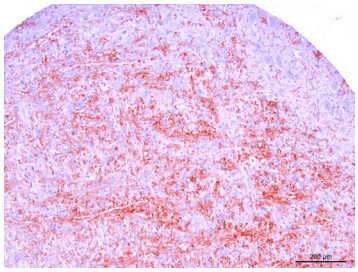

Brainstem

Damaged/unavailable core

Bulbus olphacto-rius

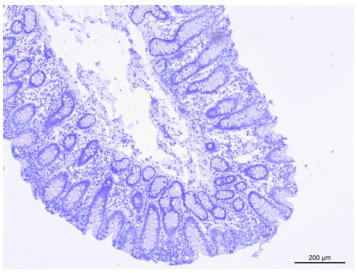

Caecum

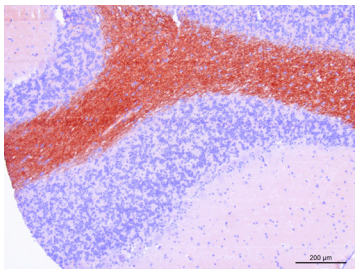

Cerebel-lum

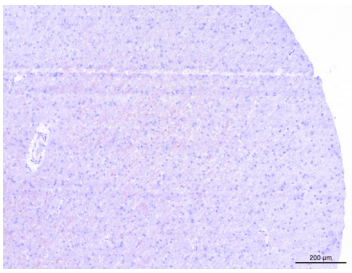

Cerebrum

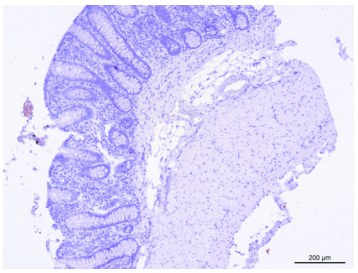

Colon

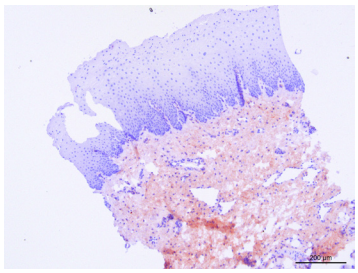

Conjuctiva

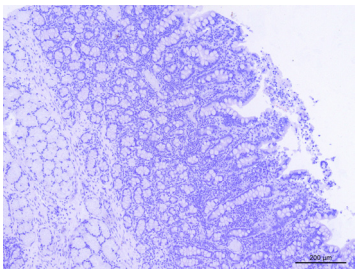

Duode-num

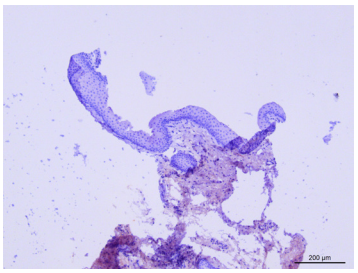

Epiglottis caudal side

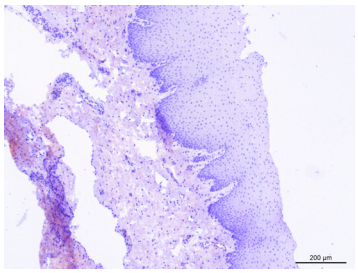

Epiglottis cranial side

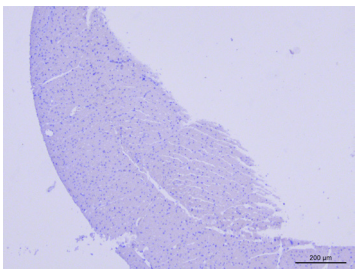

Heart

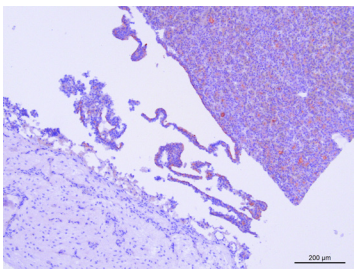

Hypofyse

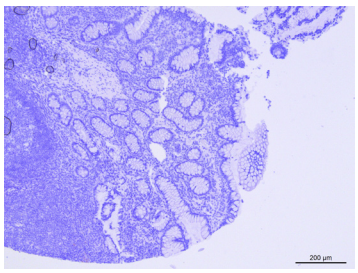

Ileum

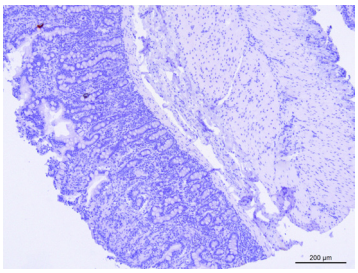

Jejunum

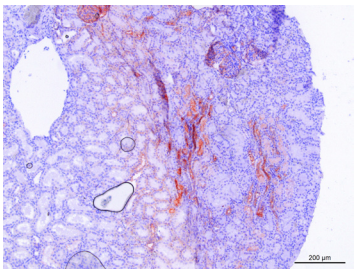

Kidney

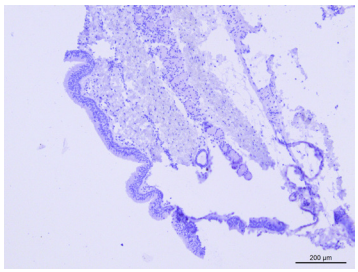

Larynx

Annex I, figure 1. MALI staining on the porcine TMA consinstig of multiple organs and tissues.

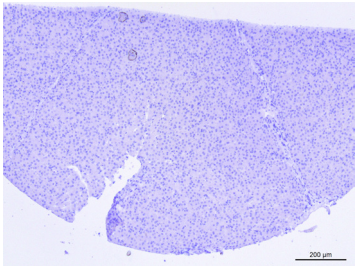

Liver

Damaged/unavailable core

Lower trachea

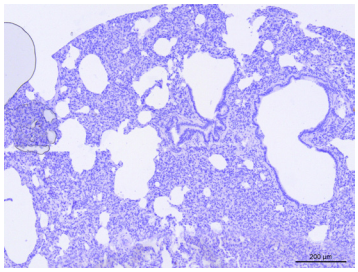

Lung

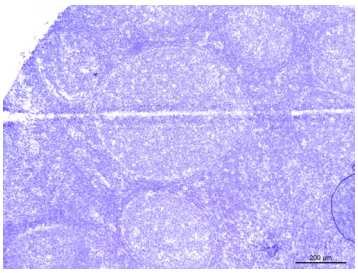

Lymph-node

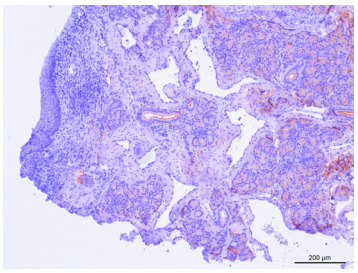

Nasal epi-thelium

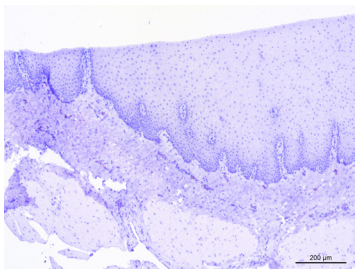

Oesoph-agus

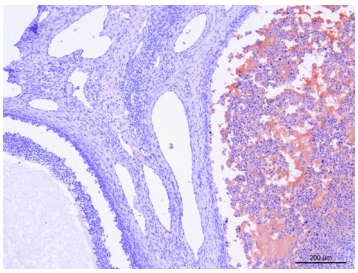

Ovarium

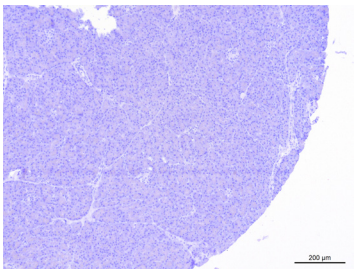

Pancreas

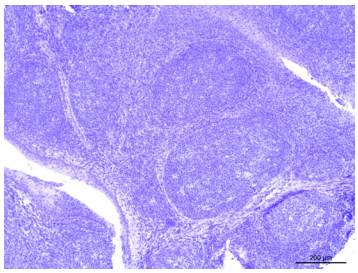

Pharyngeal tonsil

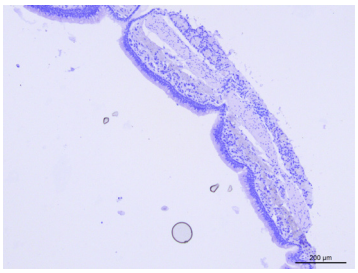

Primary bronchus

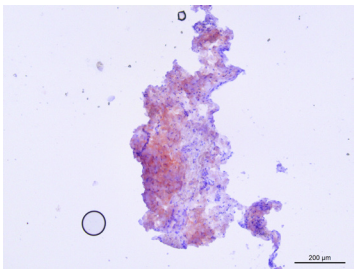

Sciatic nerve

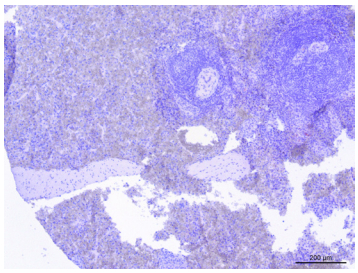

Spleen

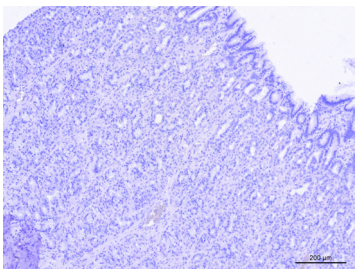

Stomach

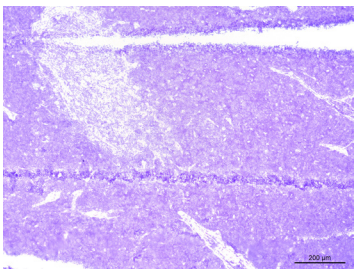

Thymus

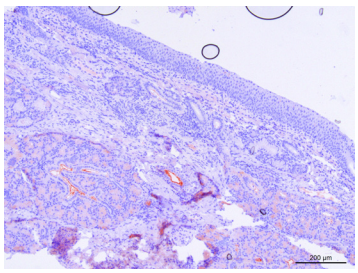

Nasophar-ynx

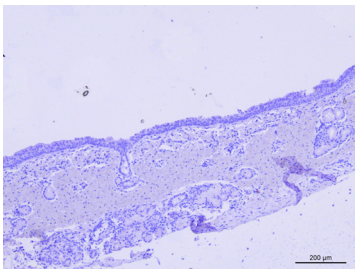

Upper trachea

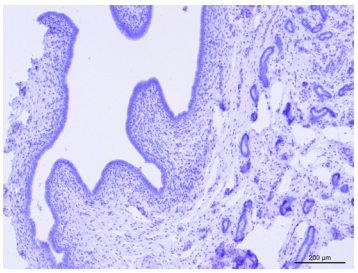

Uterus

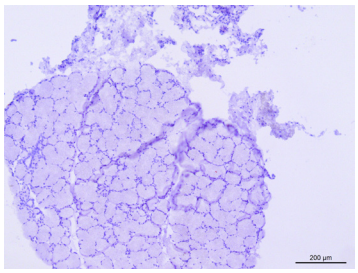

Soft palate

Annex I, figure 1 (continued). MALI staining on the porcine TMA consinstig of multiple organs and tissues.

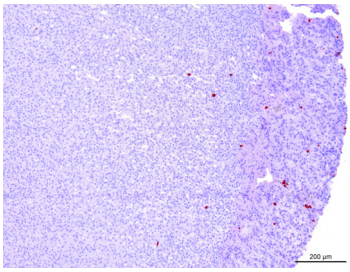

Adrenal gland

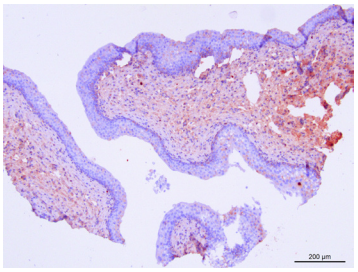

Bladder

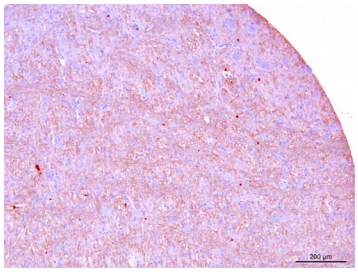

Brainstem

Damaged/unavailable core

Bulbus olphacto-rius

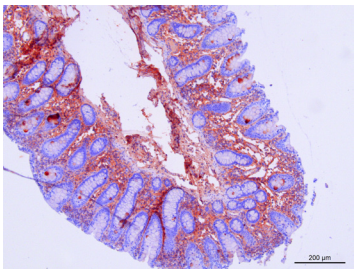

Caecum

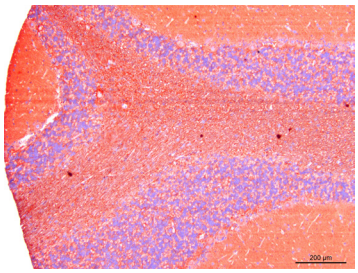

Cerebel-lum

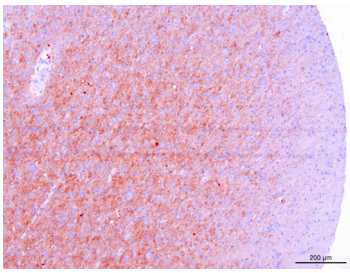

Cerebrum

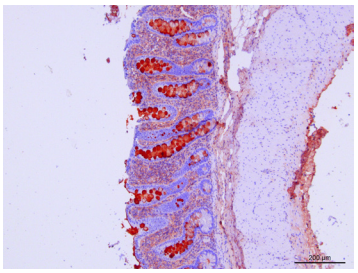

Colon

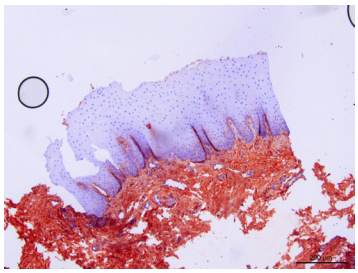

Conjuctiva

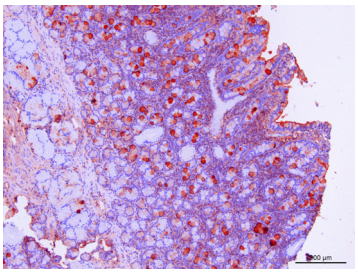

Duode-num

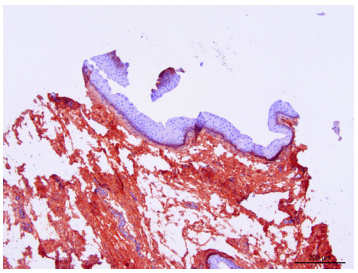

Epiglottis caudal side

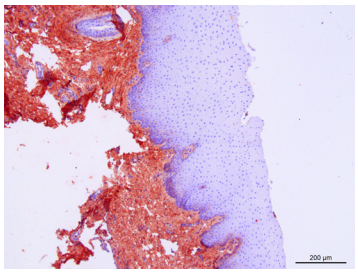

Epiglottis cranial side

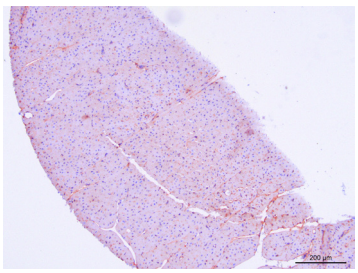

Heart

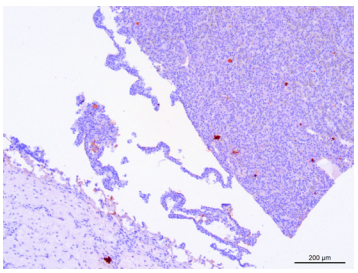

Hypofyse

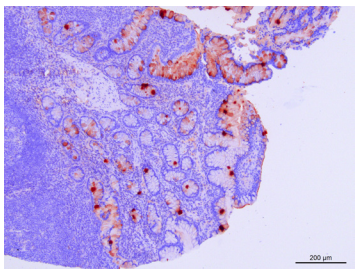

Ileum

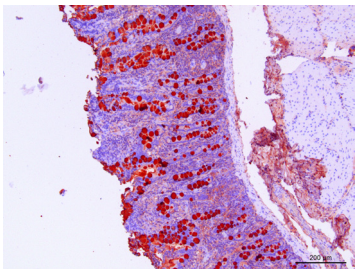

Jejunum

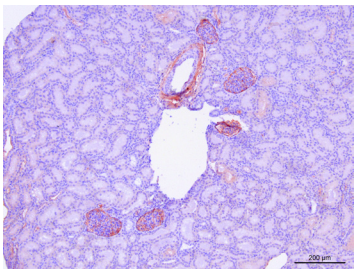

Kidney

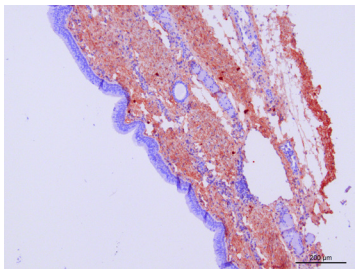

Larynx

Annex I, figure 2. MALII staining on the porcine TMA consinstig of multiple organs and tissues.

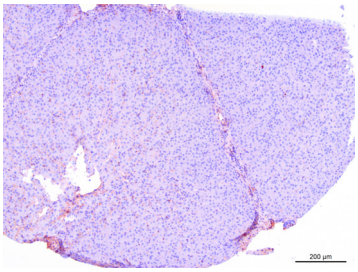
Liver

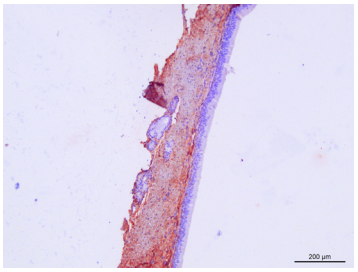
Lower trachea

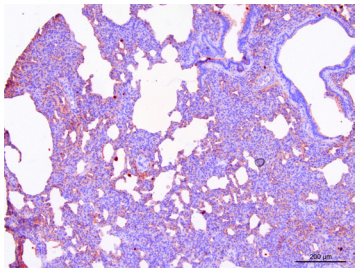
Lung

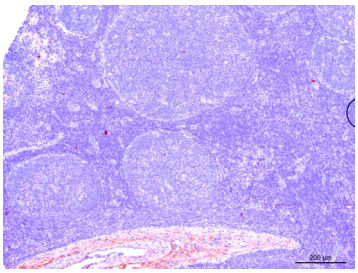
Lymph-node

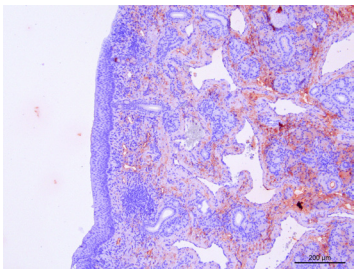
Nasal epi-thelium

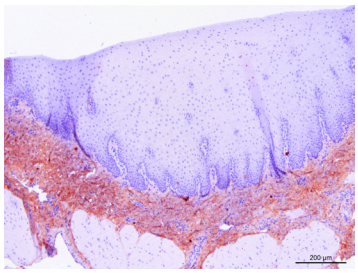
Oesoph-agus

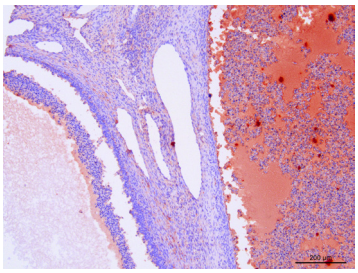
Ovarium

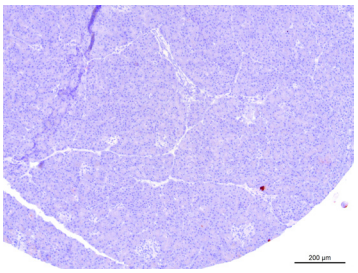
Pancreas

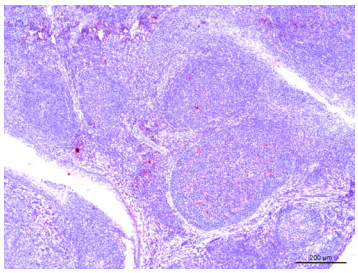
Pharyngeal tonsil

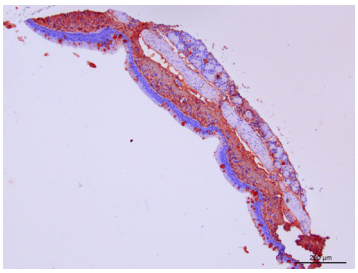
Primary bronchus

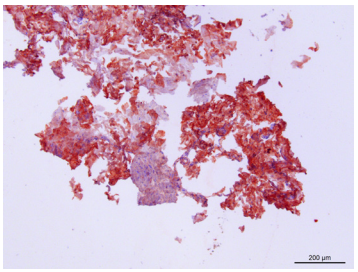
Sciatic nerve

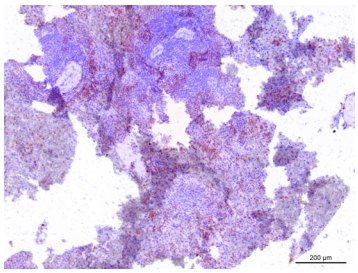
Spleen

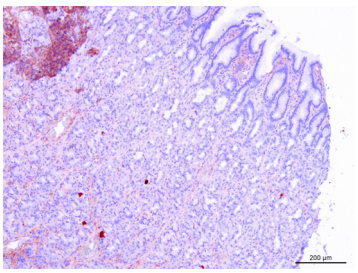
Stomach

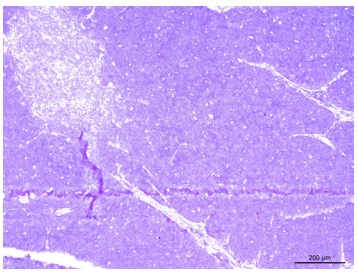
Thymus

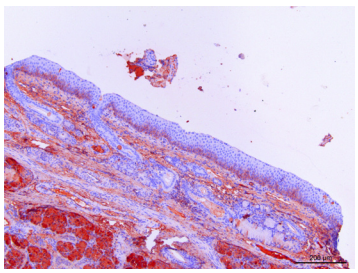
Nasophar-ynx

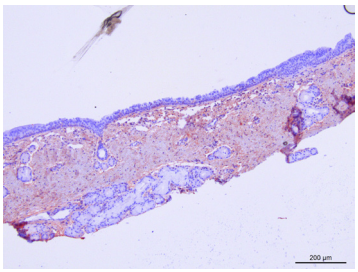
Upper trachea

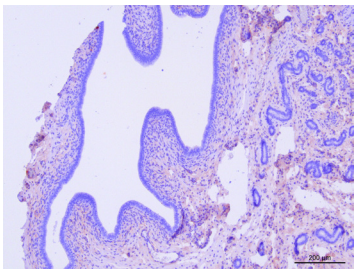
Uterus

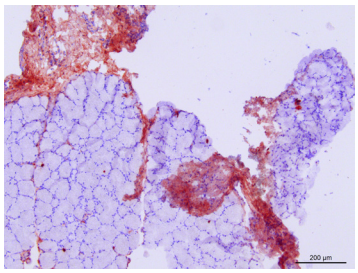
Soft palate

Annex I, figure 2 (continued). MALII staining on the porcine TMA consinstig of multiple organs and tissues.

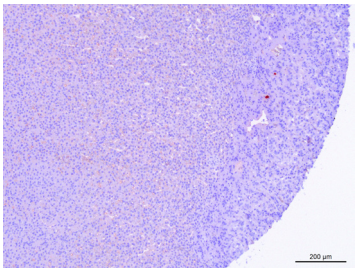

Adrenal gland

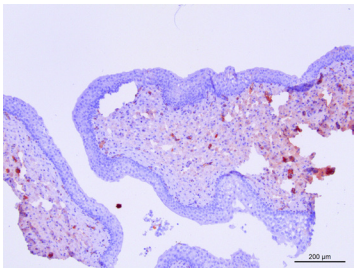

Bladder

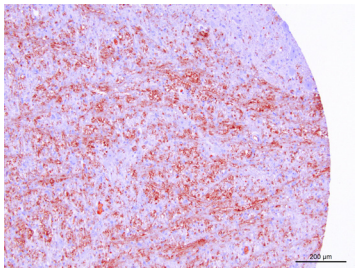

Brainstem

Damaged/unavailable core

Bulbus olphacto-rius

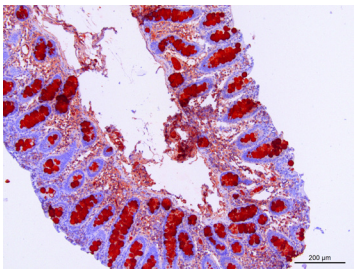

Caecum

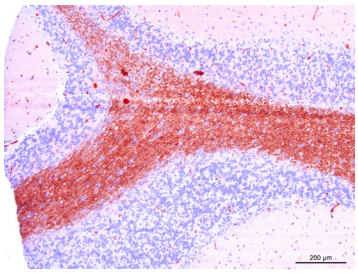

Cerebel-lum

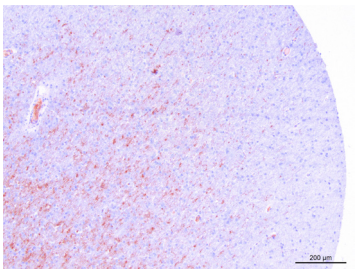

Cerebrum

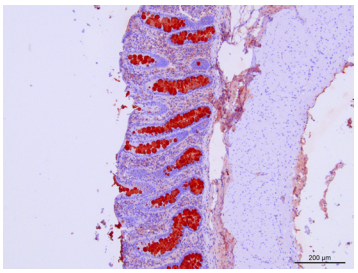

Colon

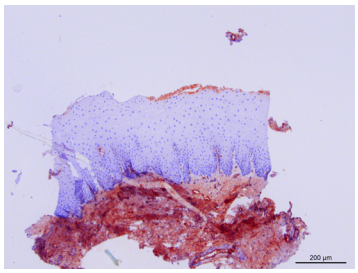

Conjuctiva

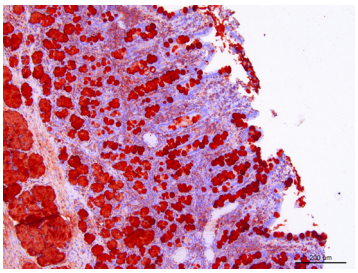

Duode-num

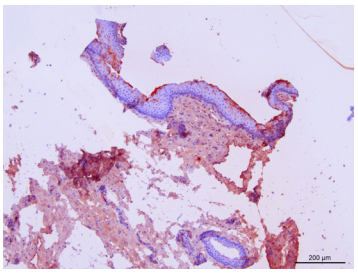

Epiglottis caudal side

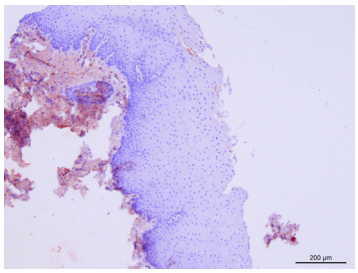

Epiglottis cranial side

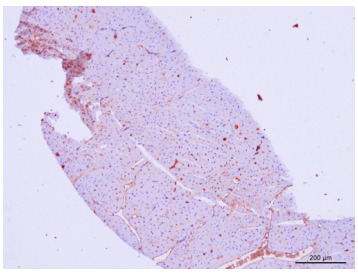

Heart

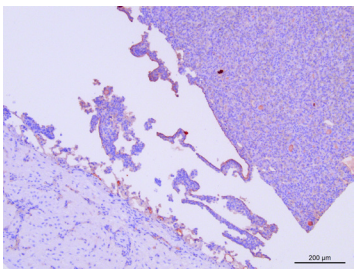

Hypofyse

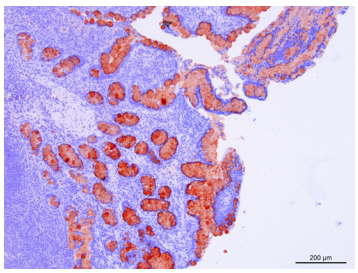

Ileum

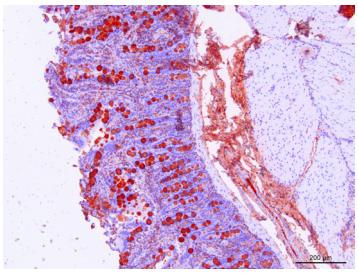

Jejunum

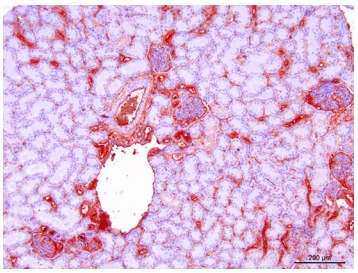

Kidney

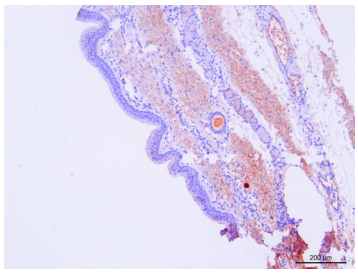

Larynx

Annex I, figure 3. SNA staining on the porcine TMA consinstig of multiple organs and tissues.

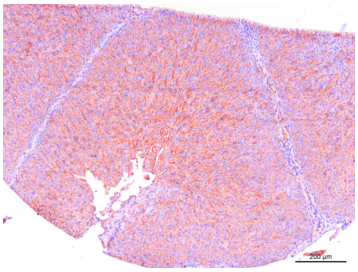
Liver

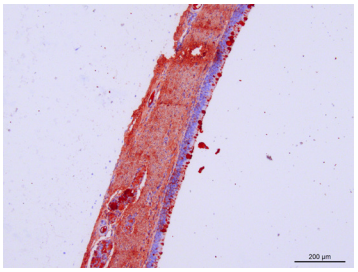
Lower trachea

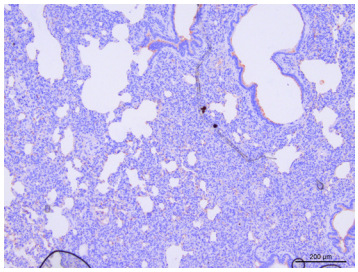
Lung

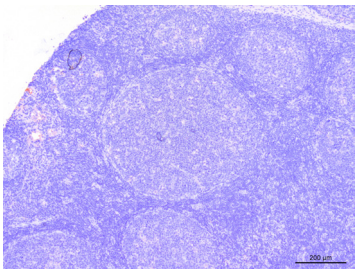
Lymph-node

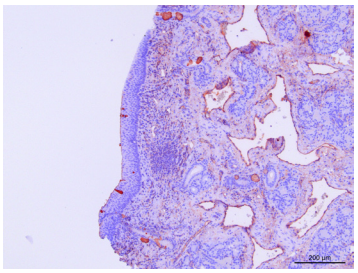
Nasal epi-thelium

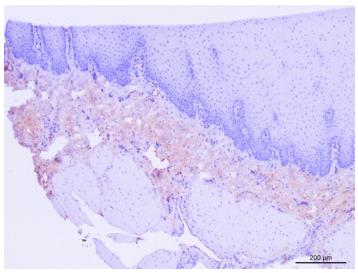
Oesoph-agus

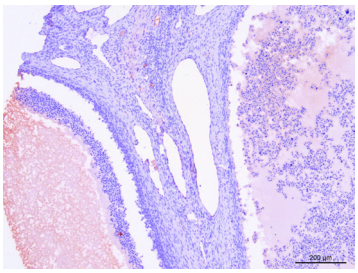
Ovarium

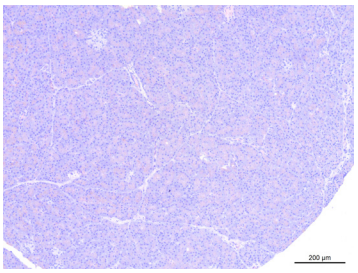
Pancreas

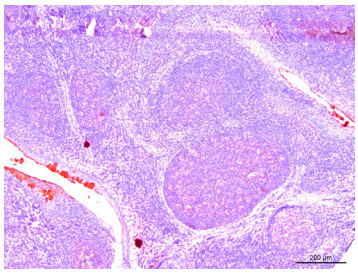
Pharyngeal tonsil

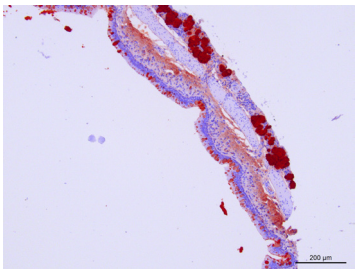
Primary bronchus

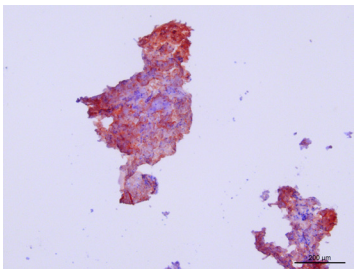
Sciatic nerve

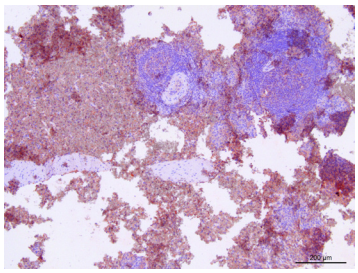
Spleen

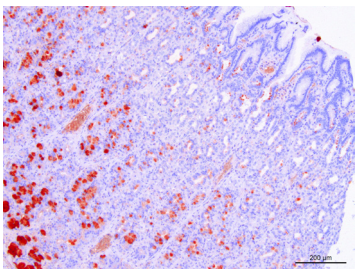
Stomach

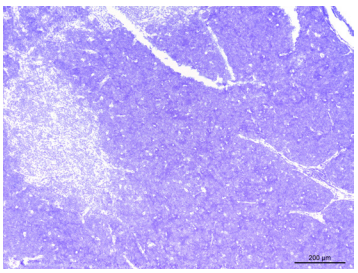
Thymus

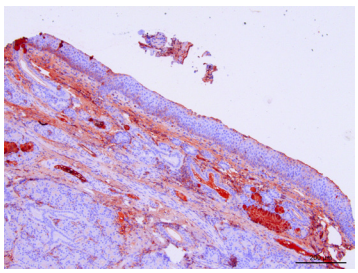
Nasophar-ynx

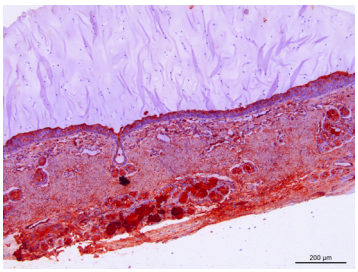
Upper trachea

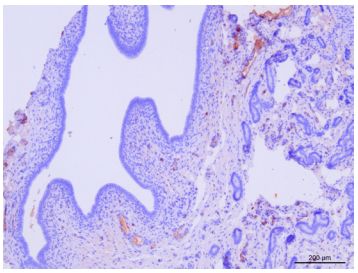
Uterus

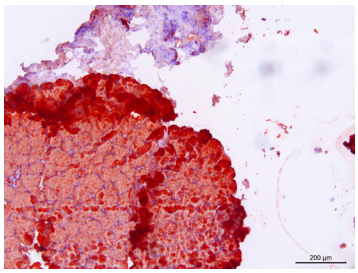
Soft palate

Annex I, figure 3 (continued). SNA staining on the porcine TMA consinstig of multiple organs and tissues.

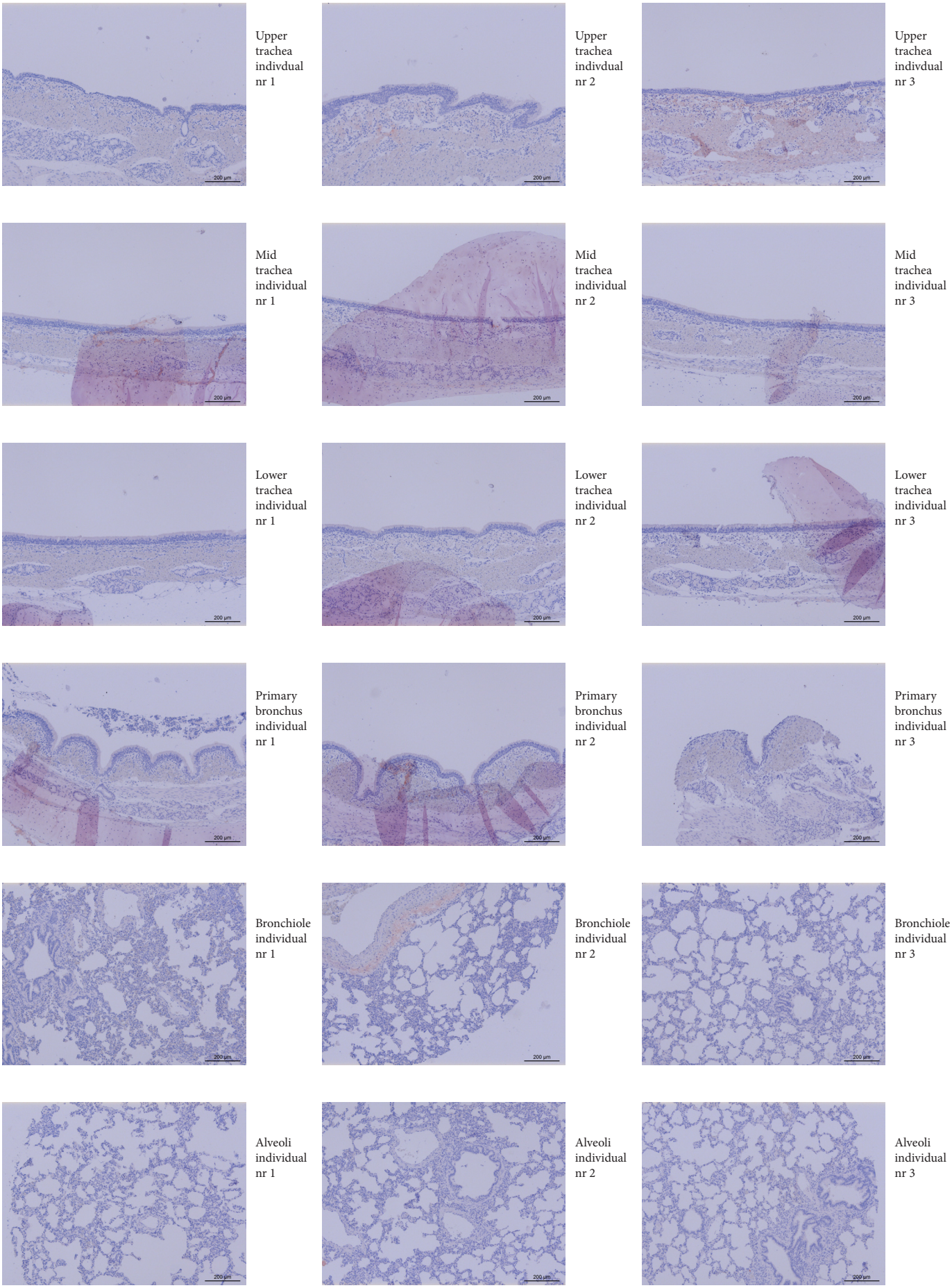

Annex I, figure 4. MALI staining on the porcine TMA consinstig of respiratory tract organs from six different individuals.

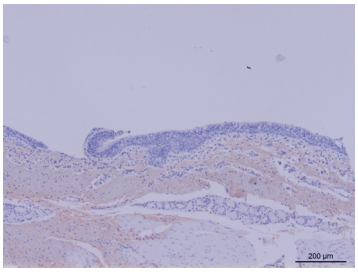

Upper trachea indivdual nr 4

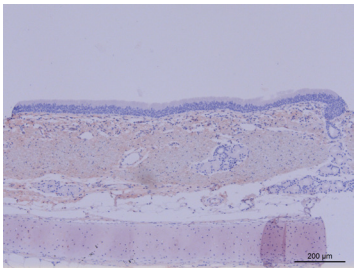

Upper trachea indivdual nr 5

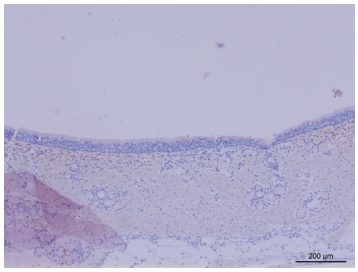

Upper trachea indivdual nr 6

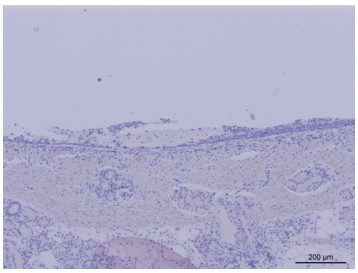

Mid trachea individual nr 4

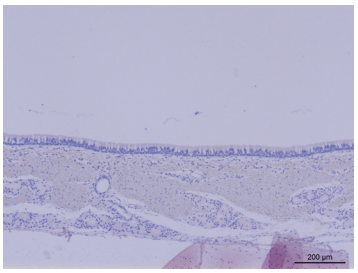

Mid trachea individual nr 5

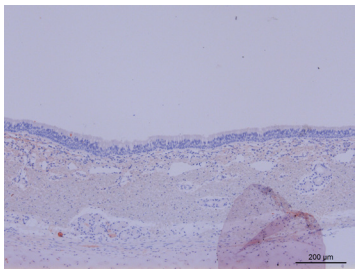

Mid trachea individual nr 6

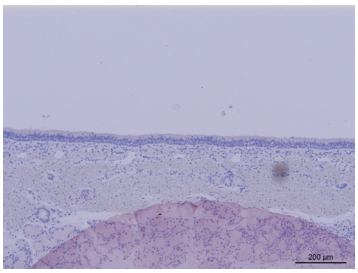

Lower trachea individual nr 4

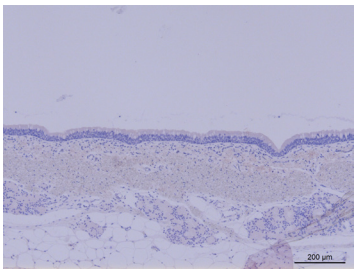

Lower trachea individual nr 5

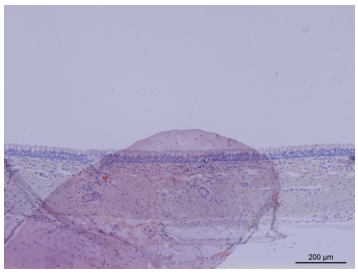

Lower trachea individual nr 6

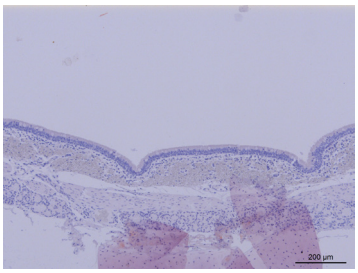

Primary bronchus individual nr 4

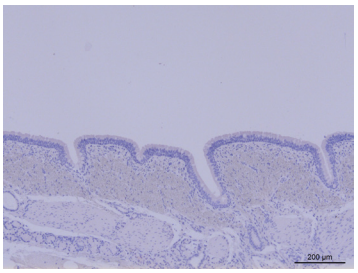

Primary bronchus individual nr 5

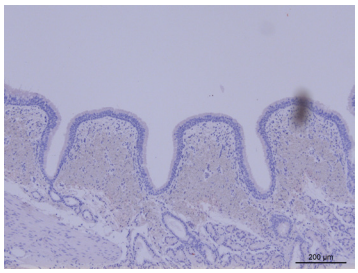

Primary bronchus individual nr 6

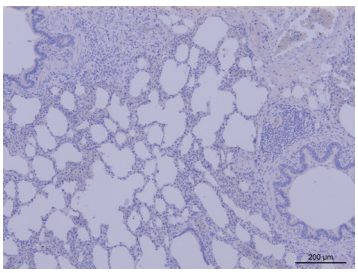

Bronchiole individual nr 4

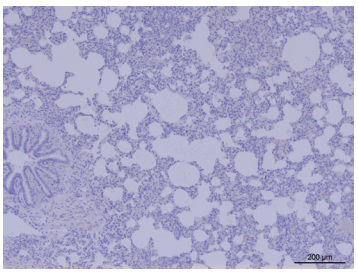

Bronchiole individual nr

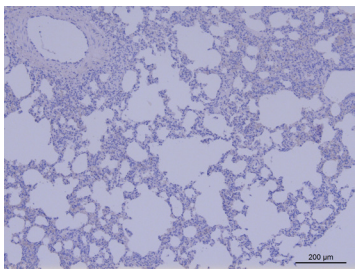

Bronchiole individual nr 6

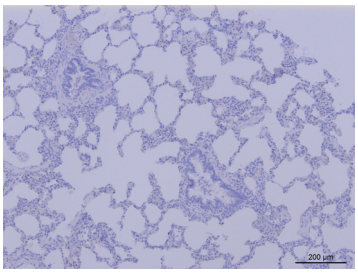

Alveoli individual nr 4

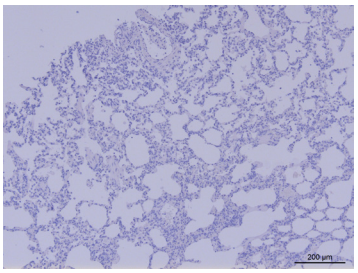

Alveoli individual nr 5

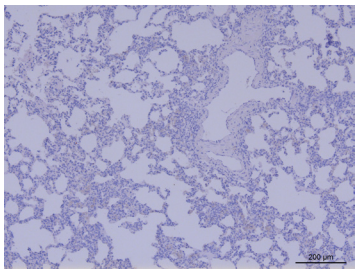

Alveoli individual nr 6

Annex I, figure 4 (continued). MALI staining on the porcine TMA consinstig of respiratory tract organs from six different individuals.

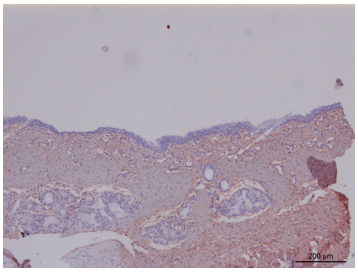

Upper trachea indivdual nr 1

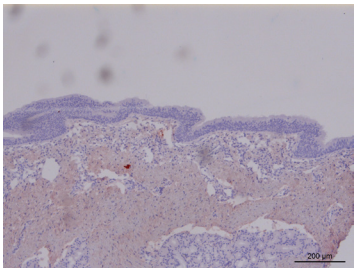

Upper trachea indivdual nr 2

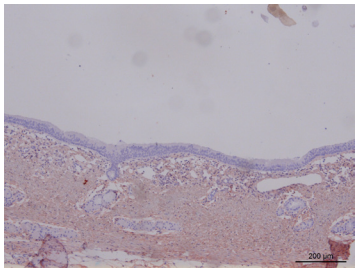

Upper trachea indivdual nr 3

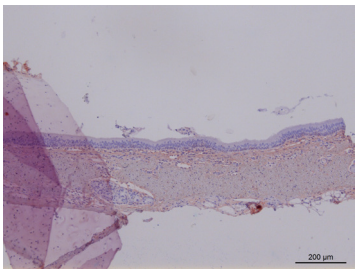

Mid trachea individual nr 1

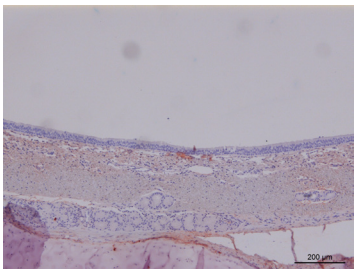

Mid trachea individual nr 2

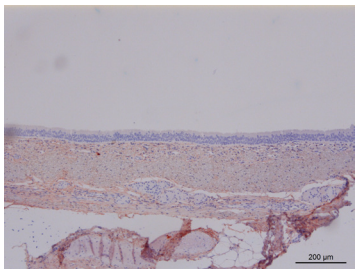

Mid trachea individual nr 3

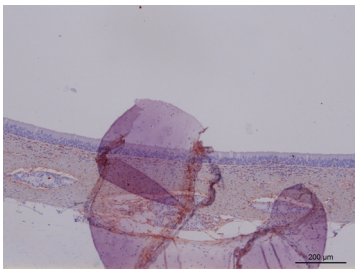

Lower trachea individual nr 1

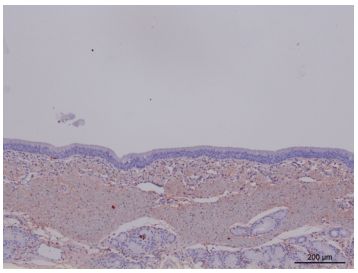

Lower trachea individual nr 2

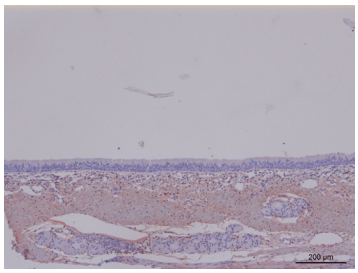

Lower trachea individual nr 3

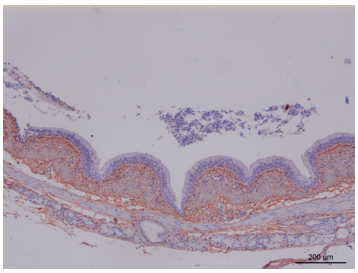

Primary bronchus individual nr 1

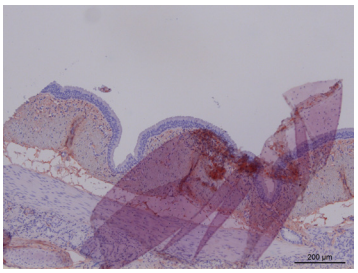

Primary bronchus individual nr 2

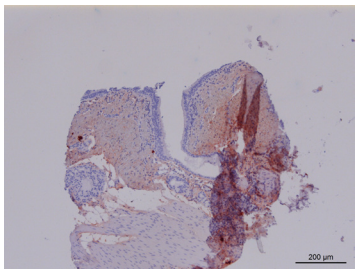

Primary bronchus individual nr 3

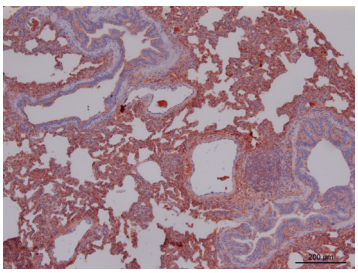

Bronchiole individual nr 1

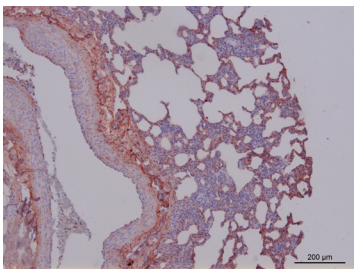

Bronchiole individual nr 2

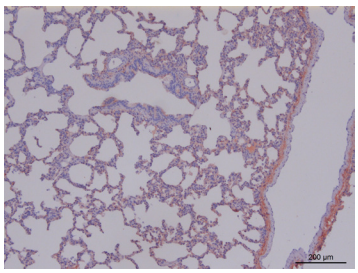

Bronchiole individual nr 3

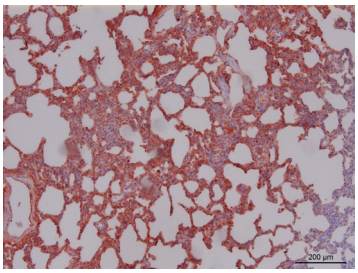

Alveoli individual nr 1

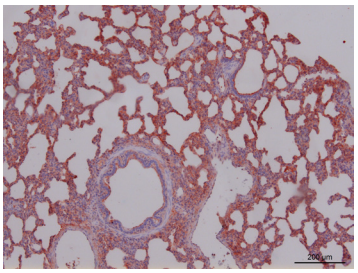

Alveoli individual nr 2

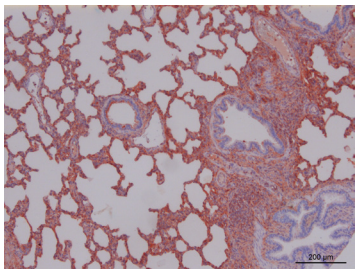

Alveoli individual nr 3

Annex I, figure 5. MALII staining on the porcine TMA consinstig of respiratory tract organs from six different individuals.

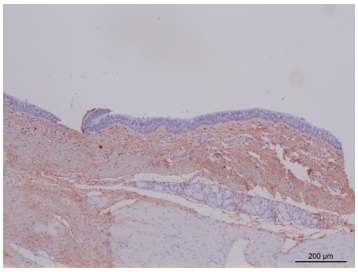

Upper trachea indivdual nr 4

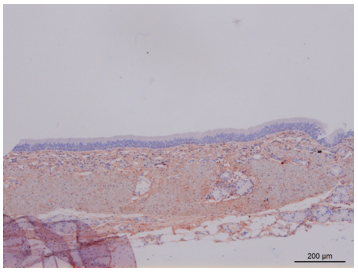

Upper trachea indivdual nr 5

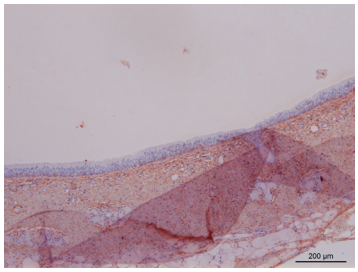

Upper trachea indivdual nr 6

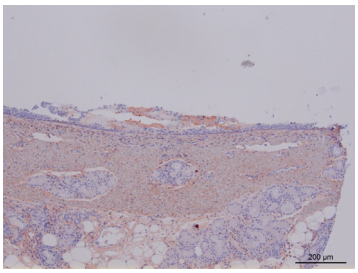

Mid trachea individual nr 4

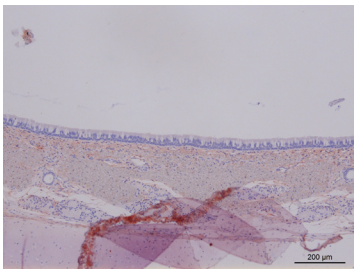

Mid trachea individual nr 5

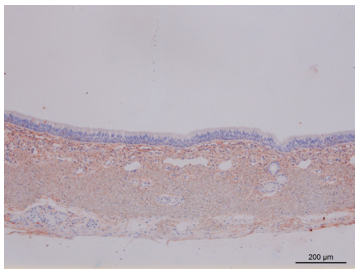

Mid trachea individual nr 6

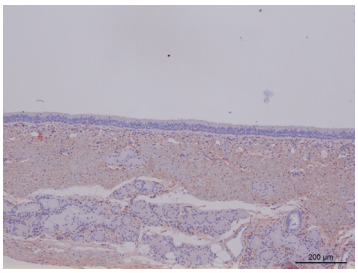

Lower trachea individual nr 4

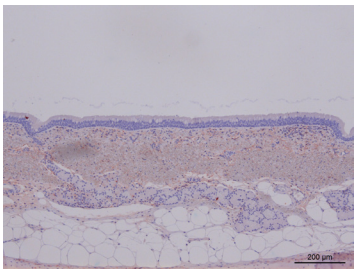

Lower trachea individual nr 5

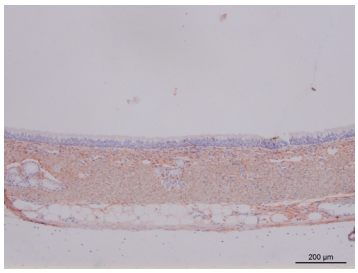

Lower trachea individual nr 6

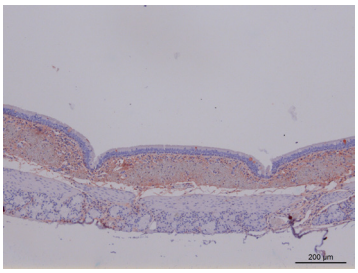

Primary bronchus individual nr 4

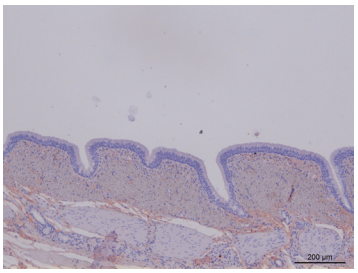

Primary bronchus individual nr 5

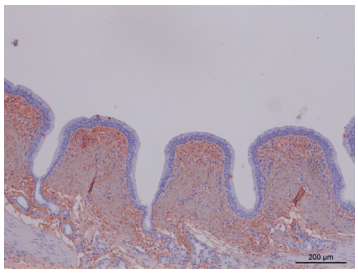

Primary bronchus individual nr 6

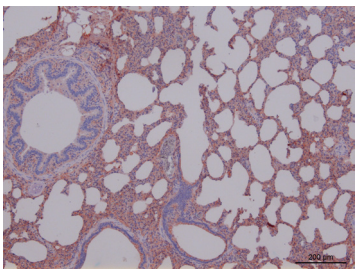

Bronchiole individual nr 4

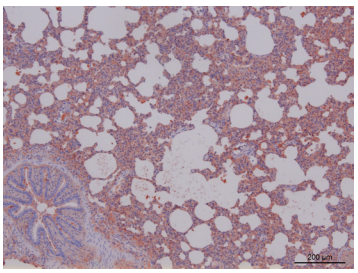

Bronchiole individual nr

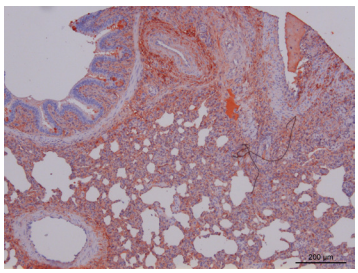

Bronchiole individual nr 6

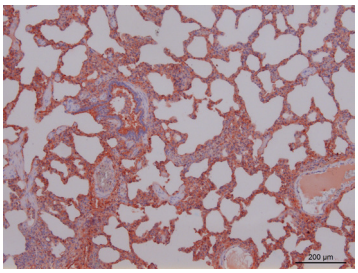

Alveoli individual nr 4

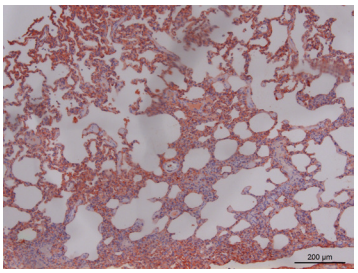

Alveoli individual nr 5

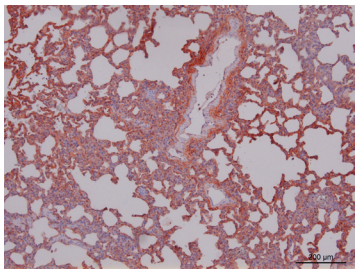

Alveoli individual nr 6

Annex I, figure 5 (continued). MALII staining on the porcine TMA consinstig of respiratory tract organs from six different individuals.

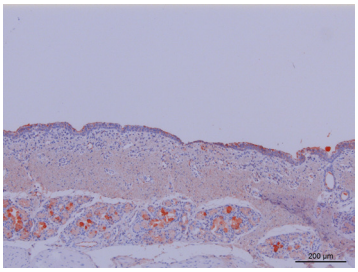

Upper trachea indivdual nr 1

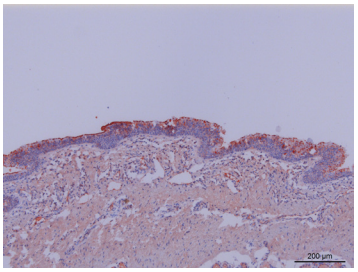

Upper trachea indivdual nr 2

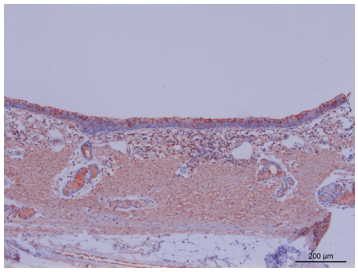

Upper trachea indivdual nr 3

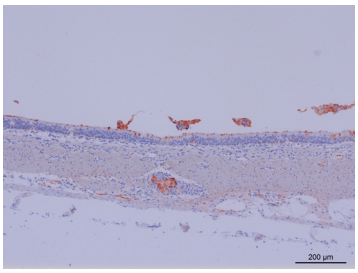

Mid trachea individual nr 1

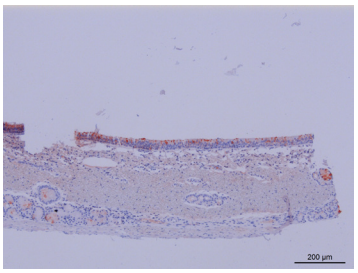

Mid trachea individual nr 2

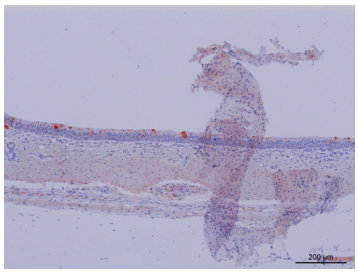

Mid trachea individual nr 3

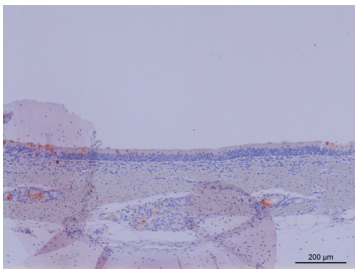

Lower trachea individual nr 1

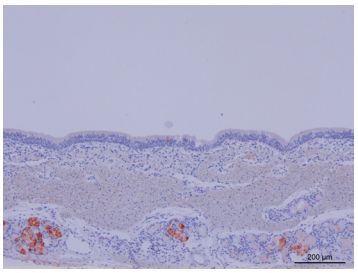

Lower trachea individual nr 2

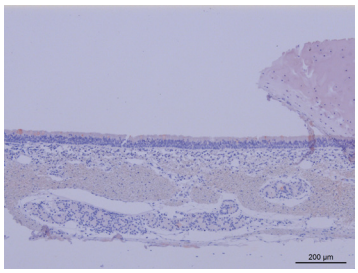

Lower trachea individual nr 3

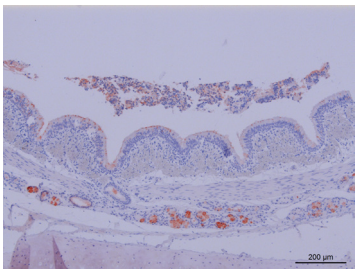

Primary bronchus individual nr 1

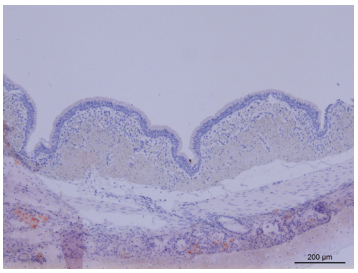

Primary bronchus individual nr 2

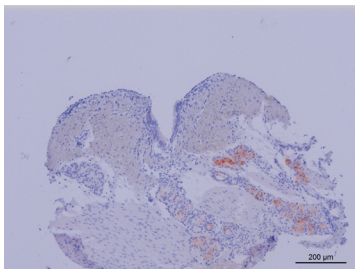

Primary bronchus individual nr 3

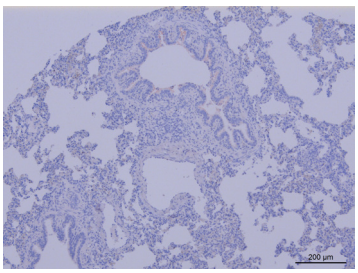

Bronchiole individual nr 1

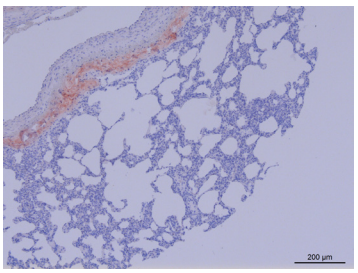

Bronchiole individual nr 2

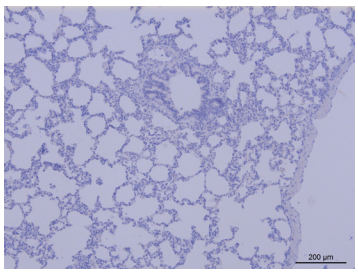

Bronchiole individual nr 3

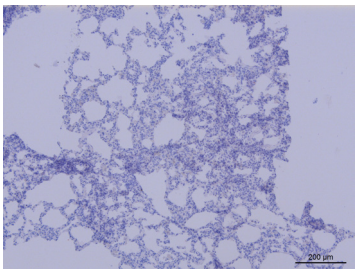

Alveoli individual nr 1

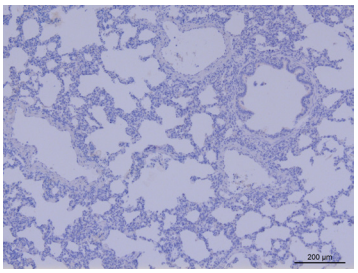

Alveoli individual nr 2

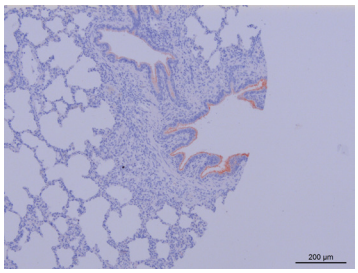

Alveoli individual nr 3

Annex I, figure 6. SNA staining on the porcine TMA consinstig of respiratory tract organs from six different individuals.

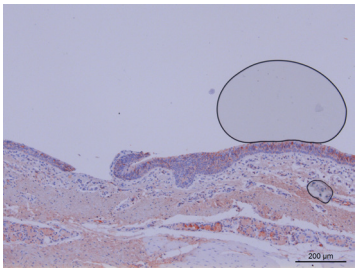

Upper trachea indivdual nr 4

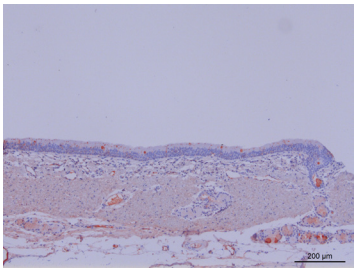

Upper trachea indivdual nr 5

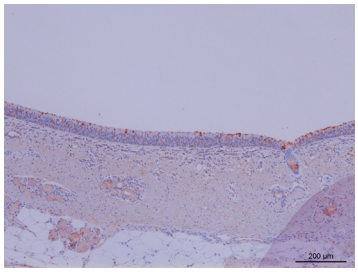

Upper trachea indivdual nr 6

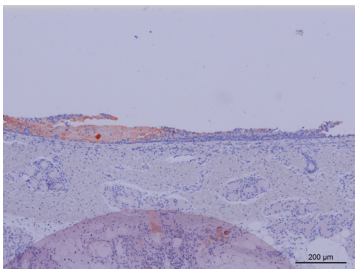

Mid trachea individual nr 4

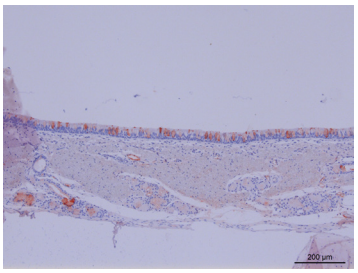

Mid trachea individual nr 5

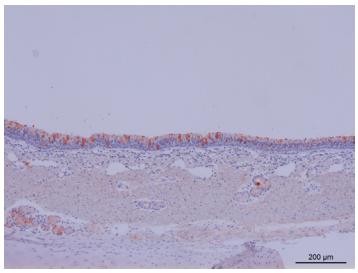

Mid trachea individual nr 6

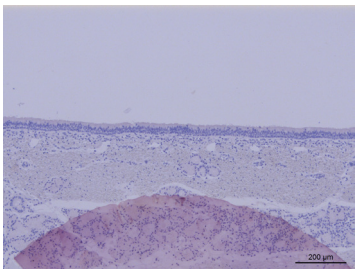

Lower trachea individual nr 4

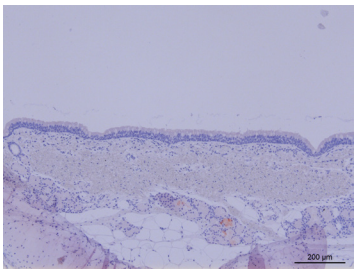

Lower trachea individual nr 5

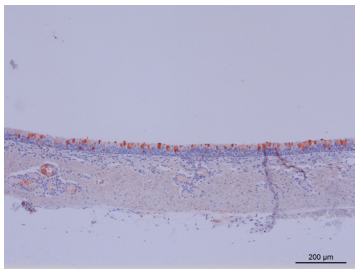

Lower trachea individual nr 6

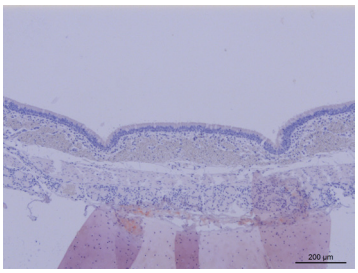

Primary bronchus individual nr 4

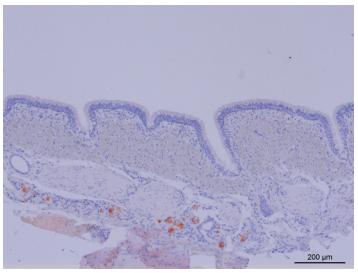

Primary bronchus individual nr 5

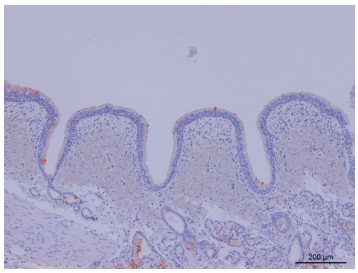

Primary bronchus individual nr 6

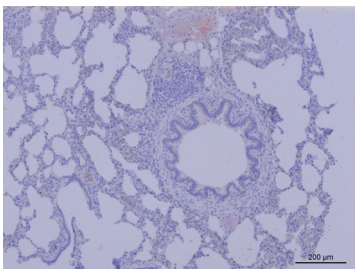

Bronchiole individual nr 4

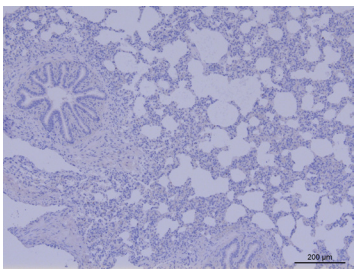

Bronchiole individual nr

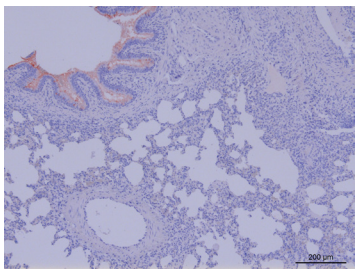

Bronchiole individual nr 6

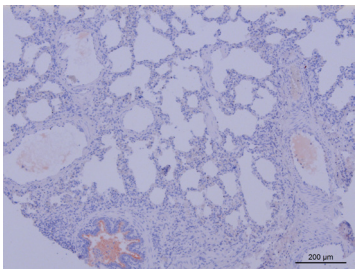

Alveoli individual nr 4

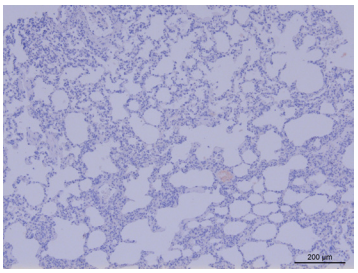

Alveoli individual nr 5

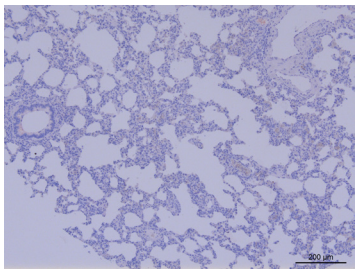

Alveoli individual nr 6

Annex I, figure 6 (continued). SNA staining on the porcine TMA consinstig of respiratory tract organs from six different individuals.

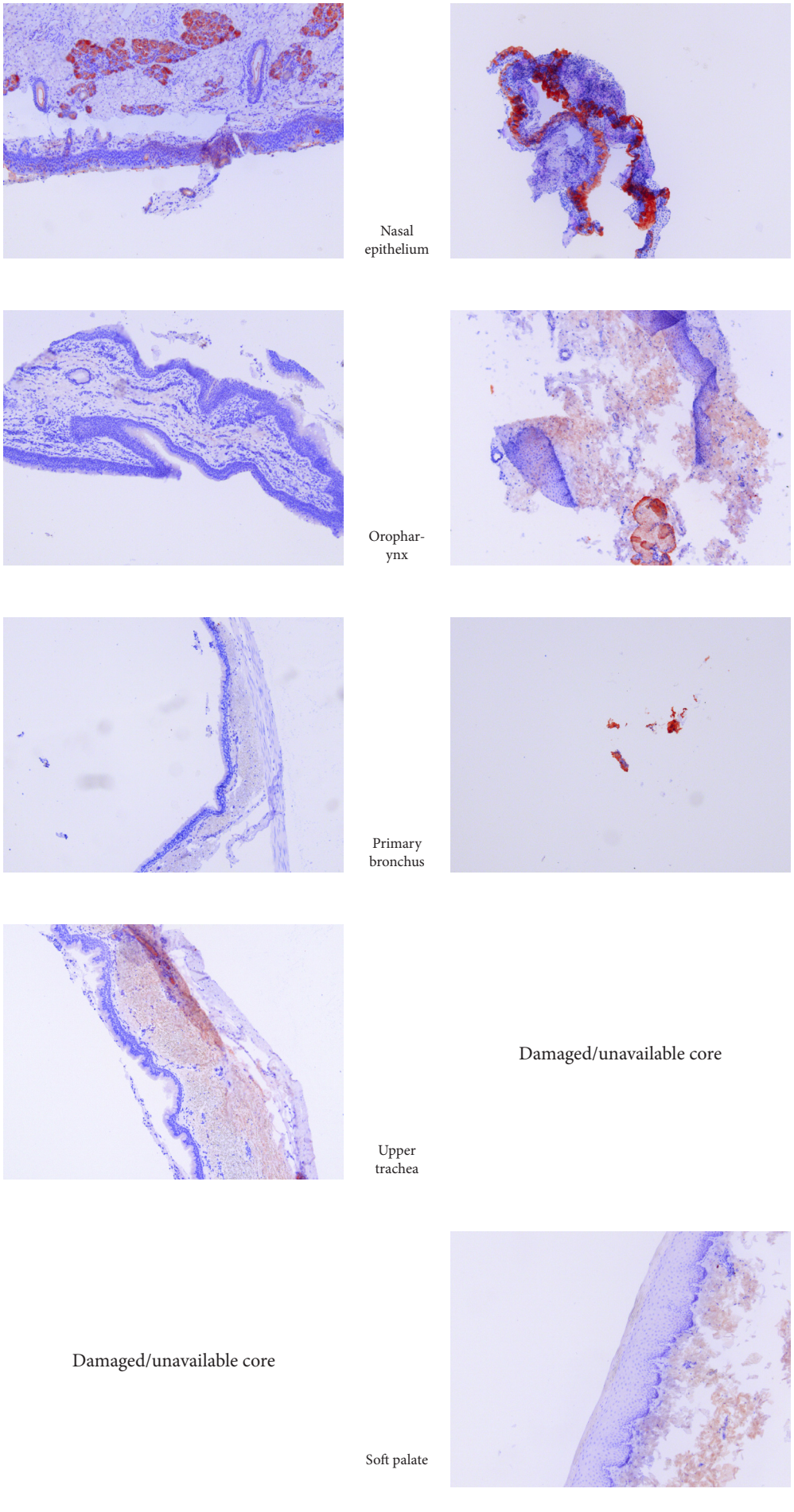

Annex I, figure 7. MALI staining on the respiratory tract tissues of equine and canine individuals.

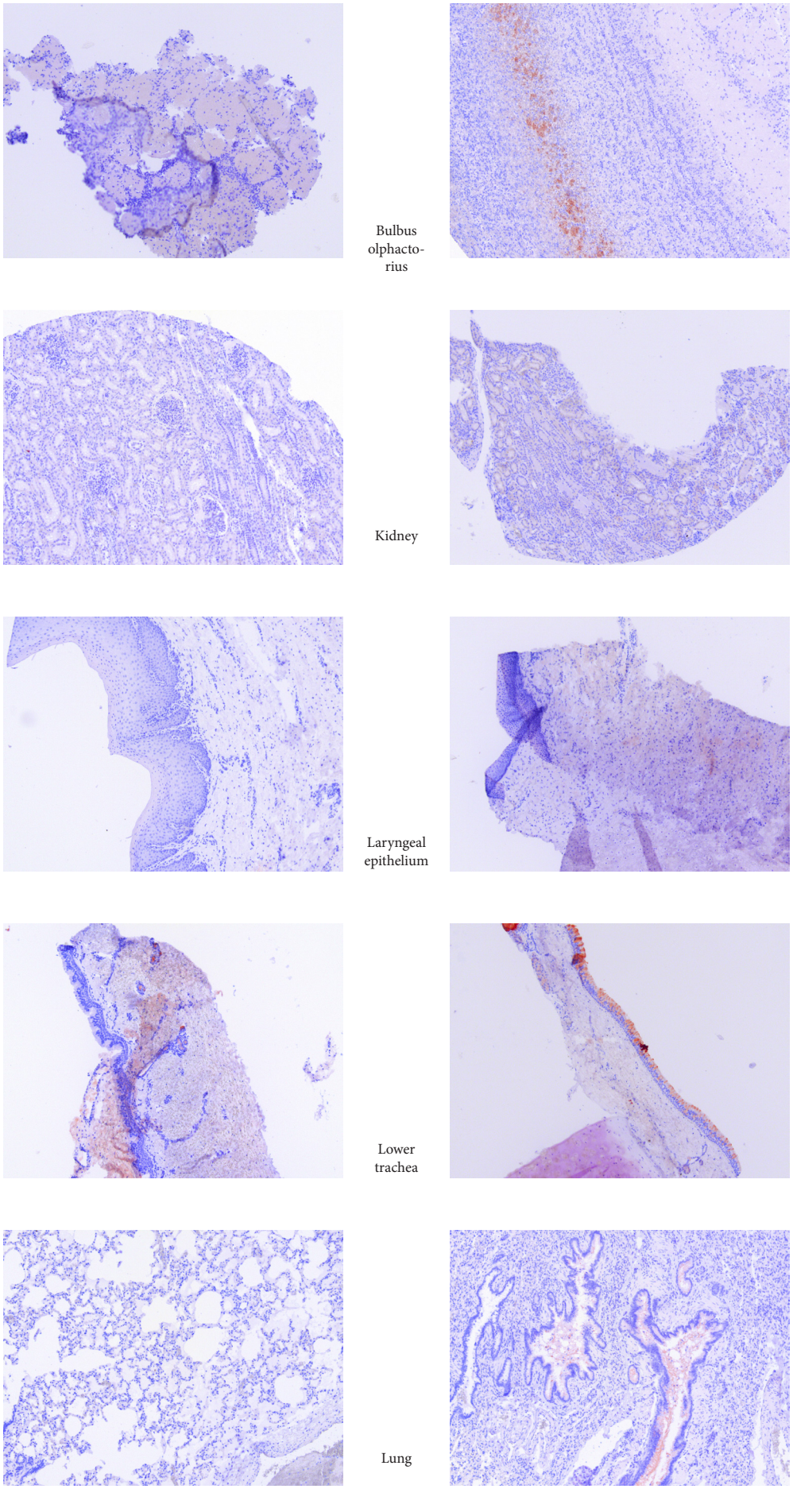

Annex I, figure 7 (continued). MALI staining on the respiratory tract tissues of equine and canine individuals.

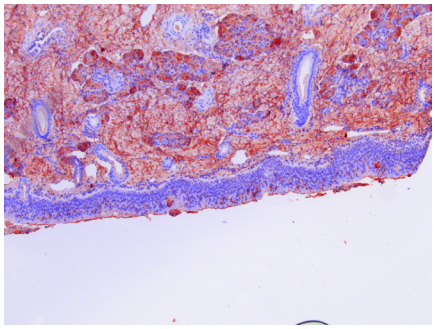

Nasal epithelium

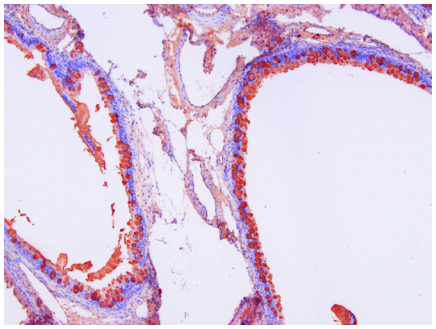

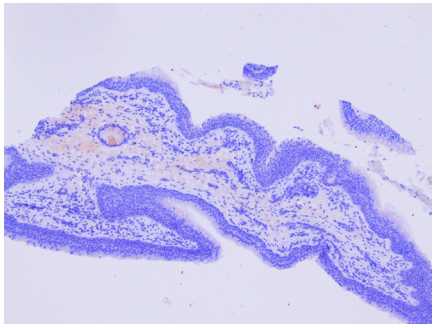

Orophar-ynx

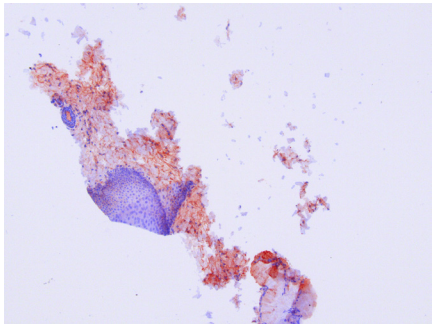

Equine

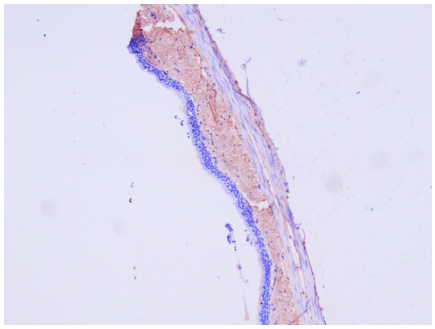

Primary bronchus

Damaged/unavailable core

Canine

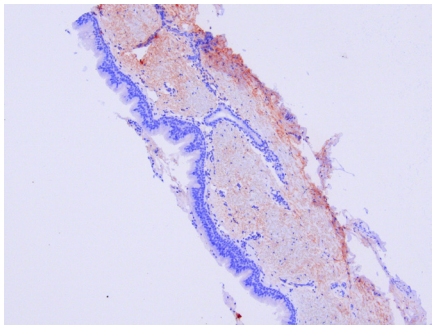

Upper trachea

Damaged/unavailable core

Damaged/unavailable core

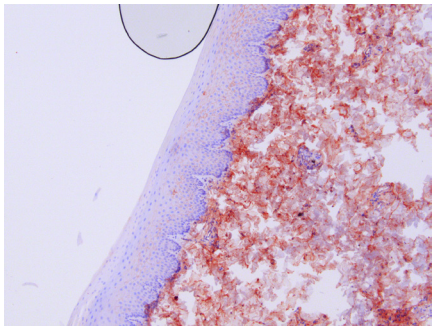

Soft palate

Annex I, figure 8. MALII staining on the respiratory tract tissues of equine and canine individuals.

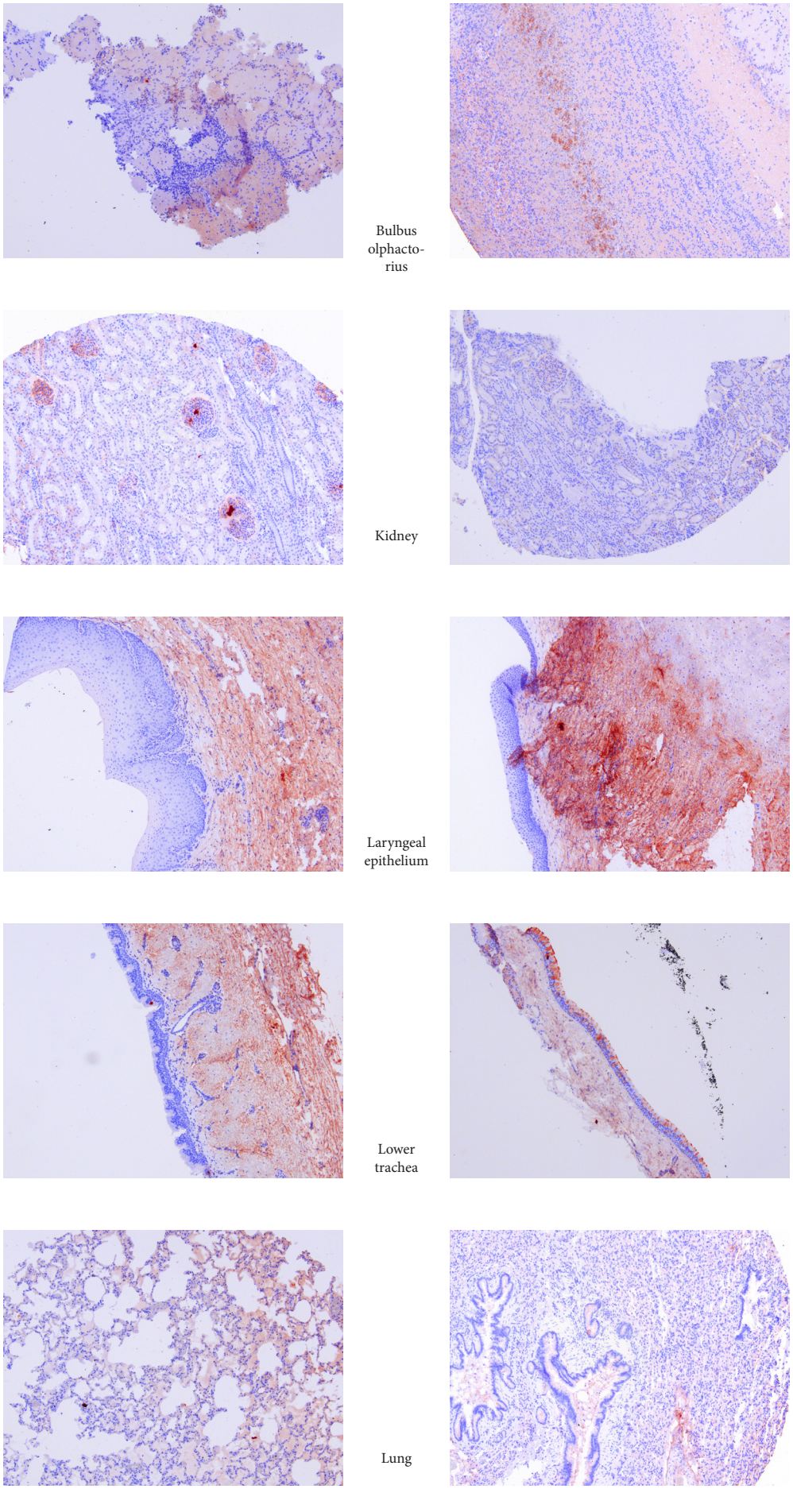

Annex I, figure 8 (continued). MALII staining on the respiratory tract tissues of equine and canine individuals.

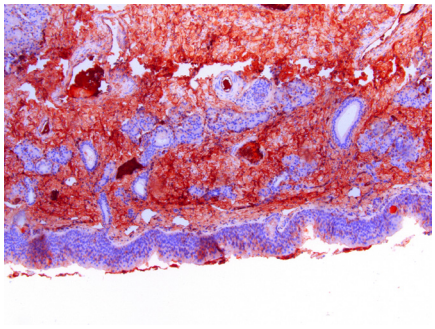

Nasal epithelium

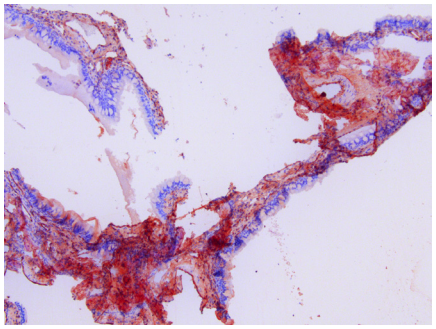

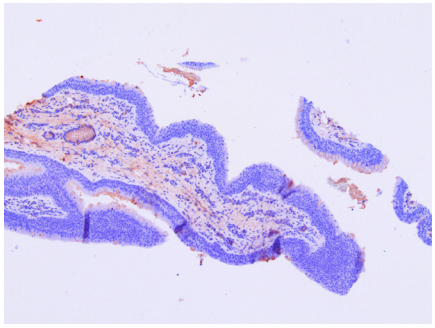

Orophar-ynx

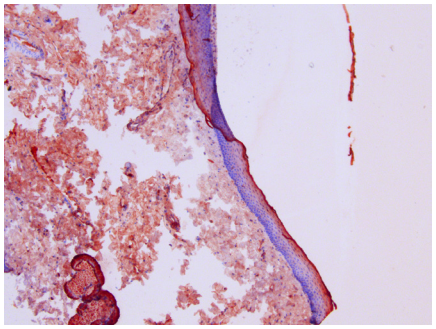

Equine

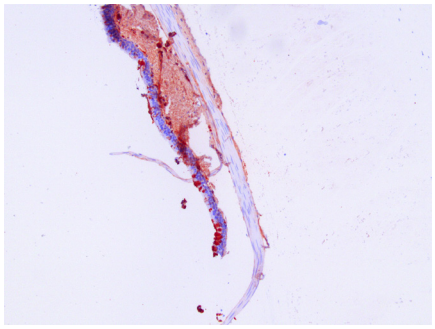

Damaged/unavailable core

Canine

Primary bronchus

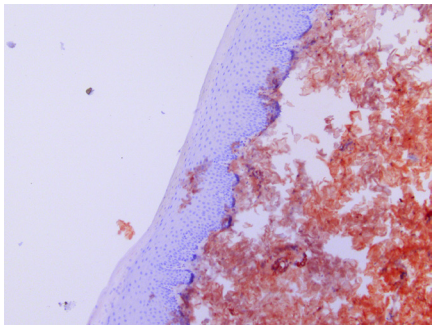

Damaged/unavailable core

Upper trachea

Damaged/unavailable core

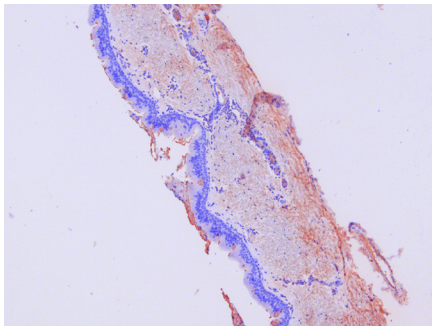

Soft palate

Annex I, figure 9. SNA staining on the respiratory tract tissues of equine and canine individuals.

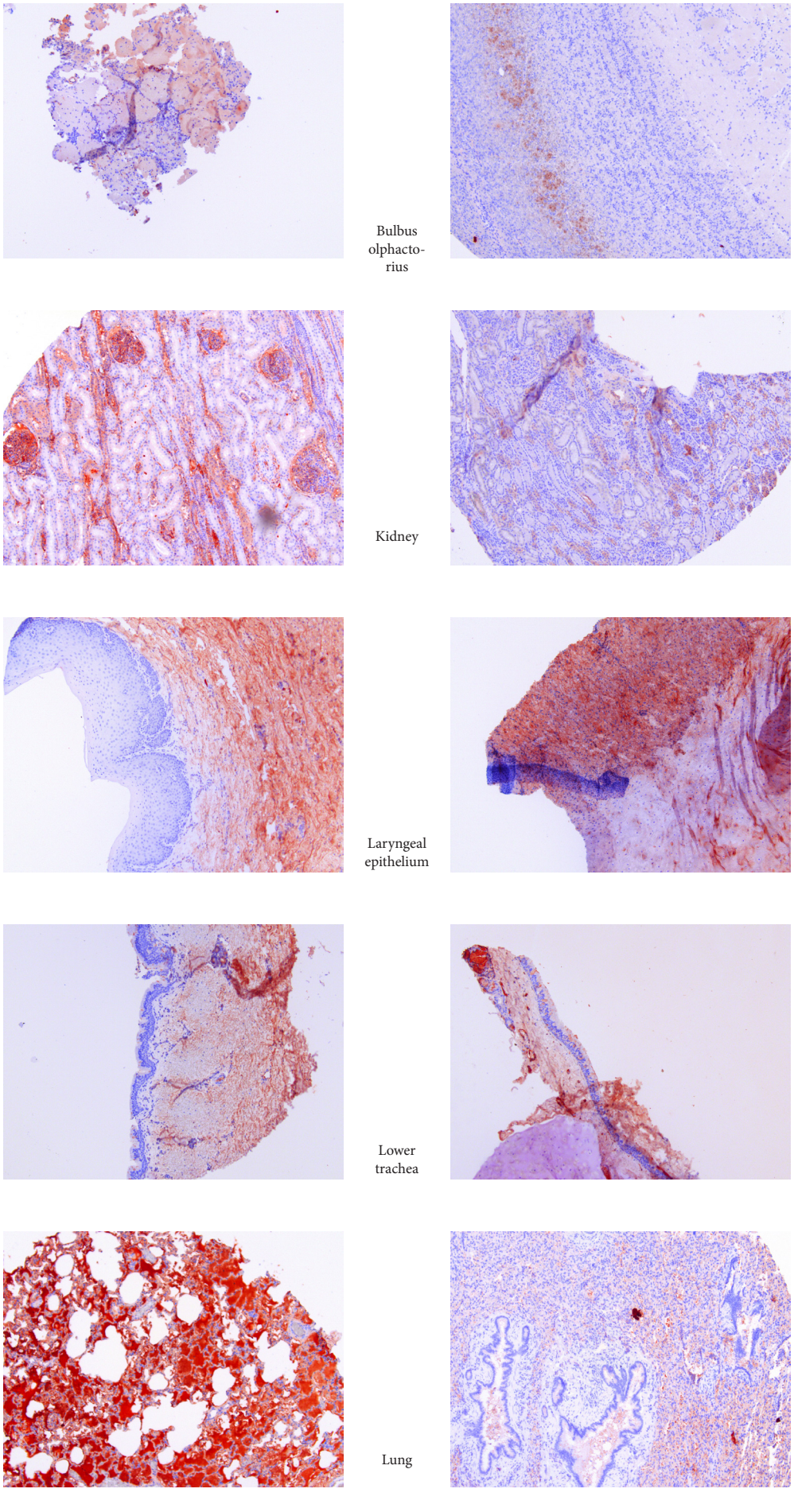

Annex I, figure 9 (continued). SNA staining on the respiratory tract tissues of equine and canine individuals.

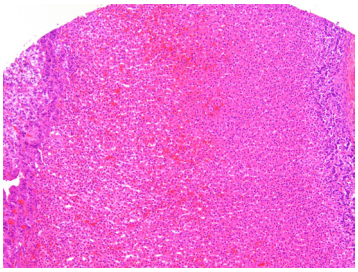

Adrenal gland

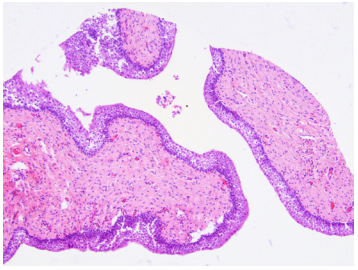

Bladder

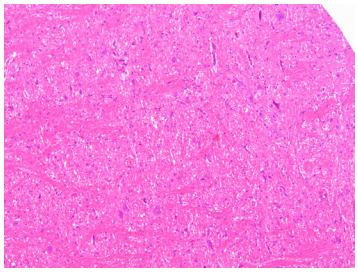

Brainstem

Damaged/unavailable core

Bulbus olphacto-rius

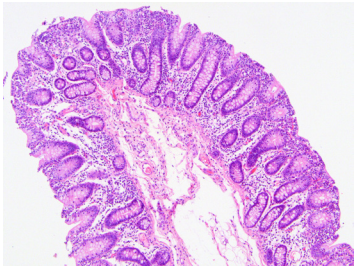

Caecum

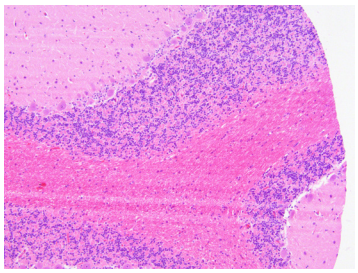

Cerebel-lum

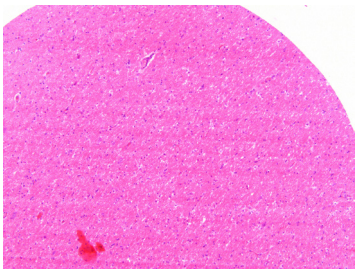

Cerebrum

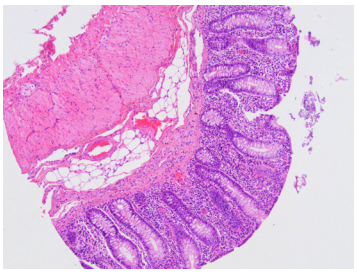

Colon

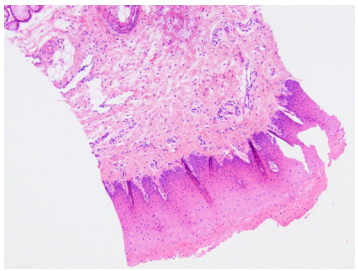

Conjuctiva

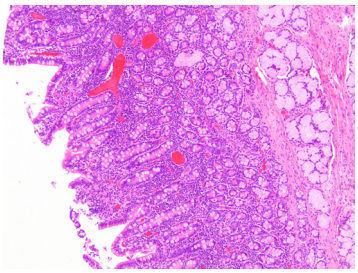

Duode-num

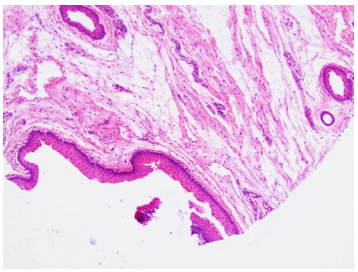

Epiglottis caudal side

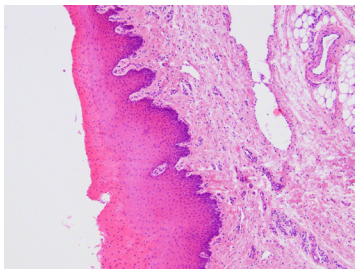

Epiglottis cranial side

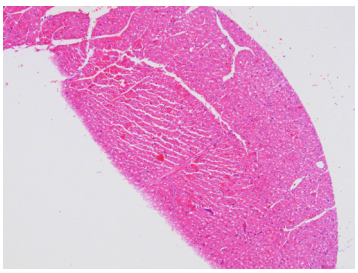

Heart

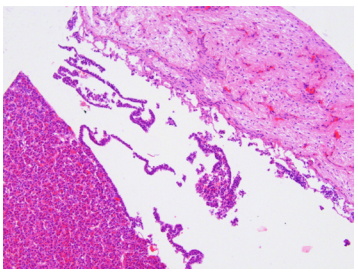

Hypofyse

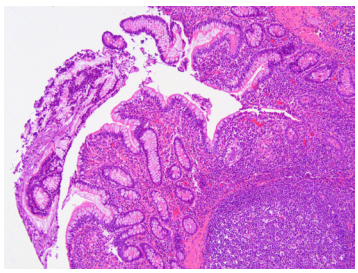

Ileum

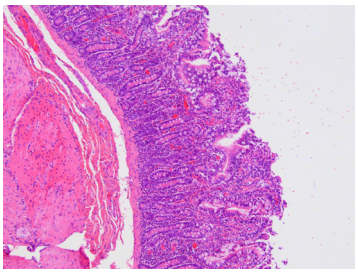

Jejunum

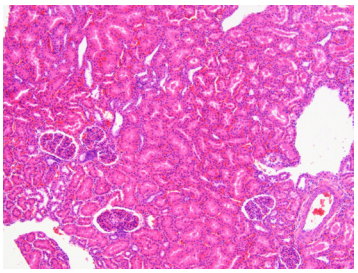

Kidney

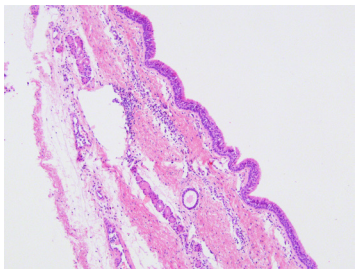

Larynx

Annex I, figure 10. H&E staining on the porcine TMA consinstig of multiple organs and tissues.

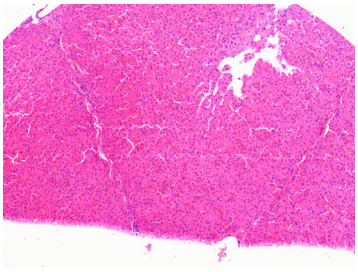

Liver

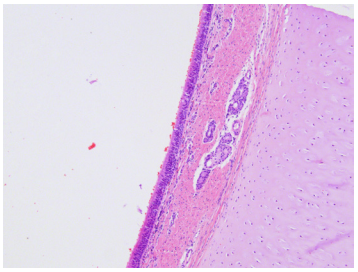

Lower trachea

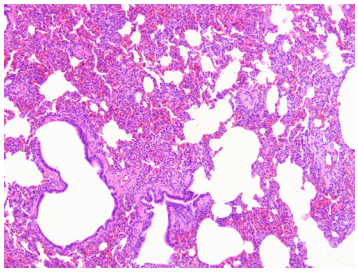

Lung

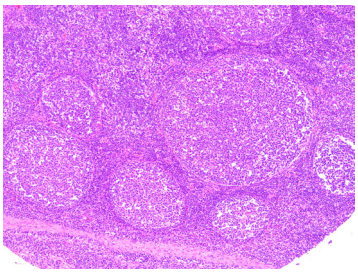

Lymph-node

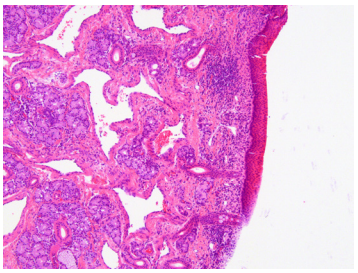

Nasal epi-thelium

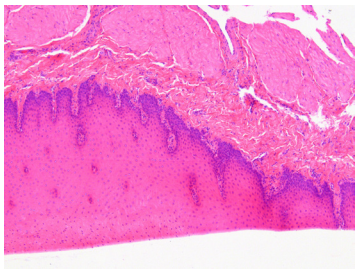

Oesoph-agus

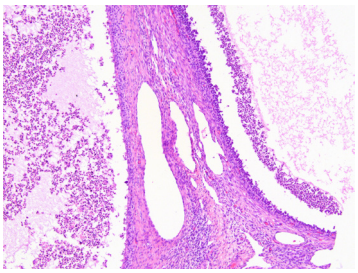

Ovarium

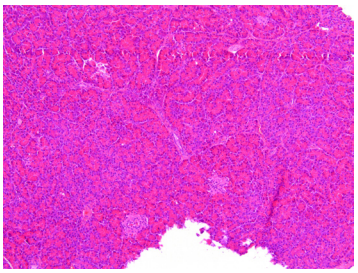

Pancreas

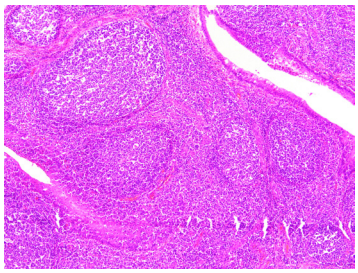

Pharyngeal tonsil

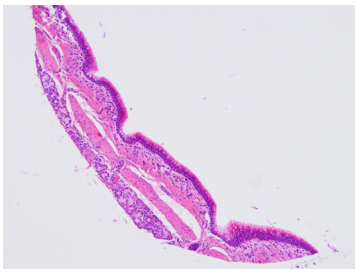

Primary bronchus

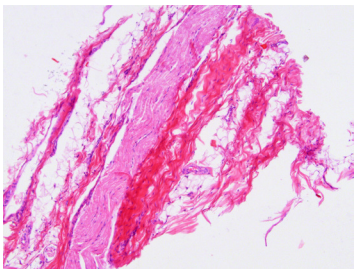

Sciatic nerve

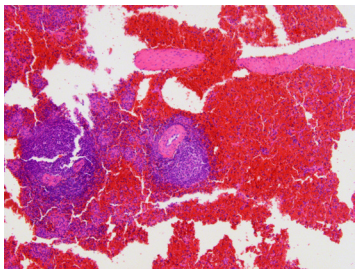

Spleen

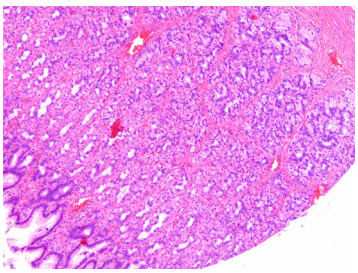

Stomach

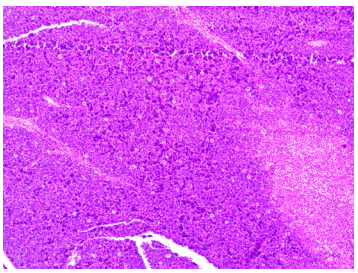

Thymus

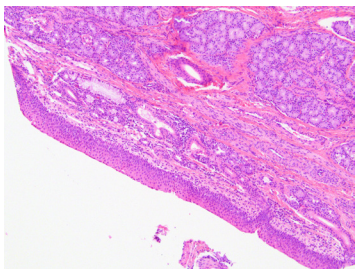

Nasophar-ynx

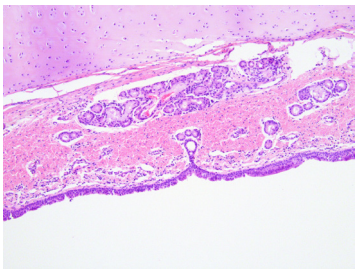

Upper trachea

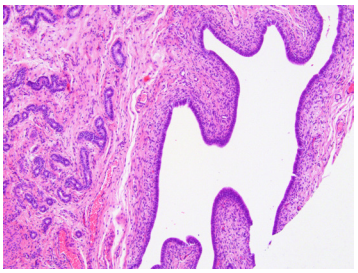

Uterus

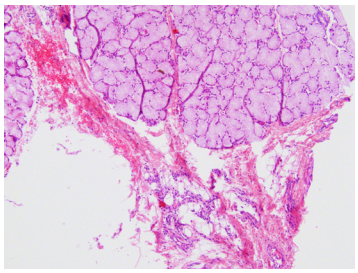

Soft palate

Annex I, figure 10 (continued). H&E staining on the porcine TMA consinstig of multiple organs and tissues.

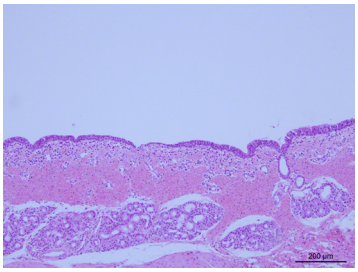

Upper trachea indivdual nr 1

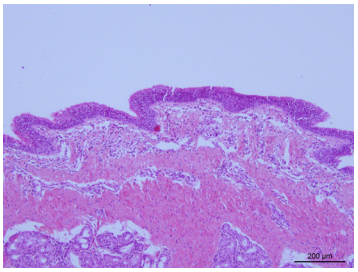

Upper trachea indivdual nr 2

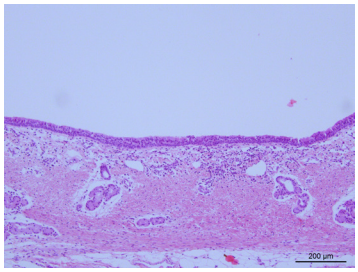

Upper trachea indivdual nr 3

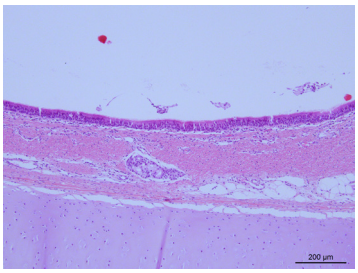

Mid trachea individual nr 1

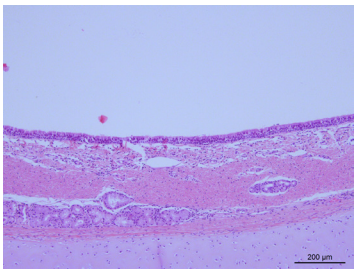

Mid trachea individual nr 2

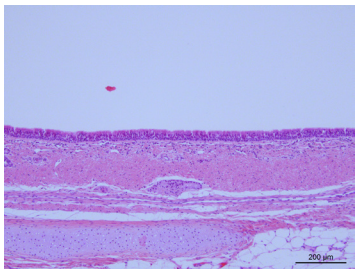

Mid trachea individual nr 3

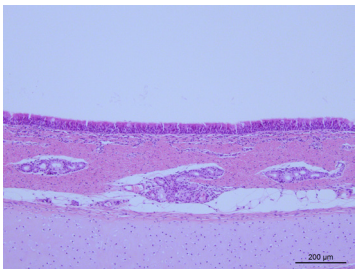

Lower trachea individual nr 1

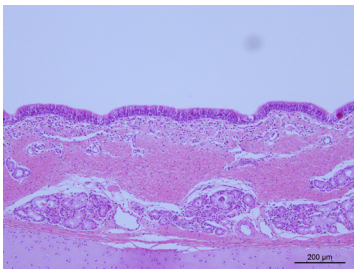

Lower trachea individual nr 2

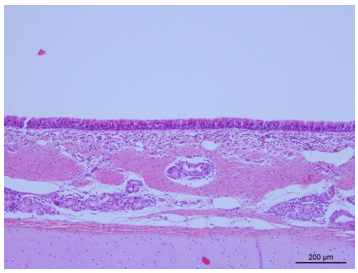

Lower trachea individual nr 3

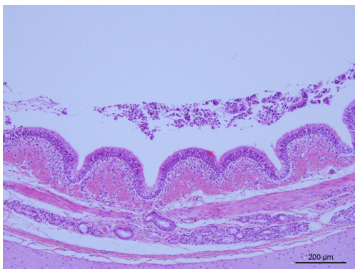

Primary bronchus individual nr 1

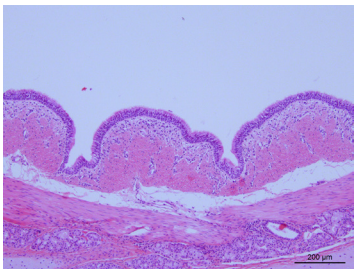

Primary bronchus individual nr 2

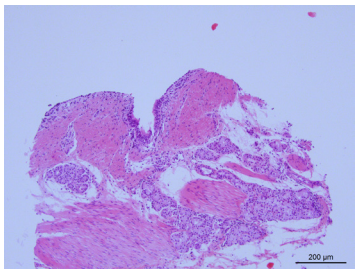

Primary bronchus individual nr 3

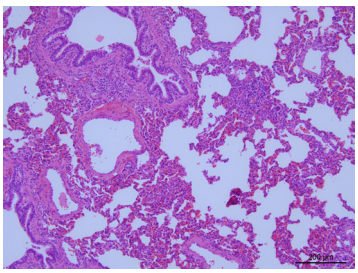

Bronchiole individual nr 1

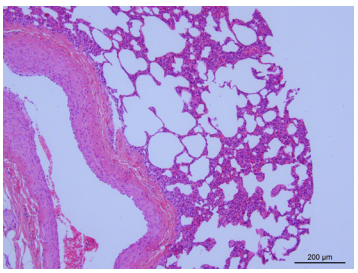

Bronchiole individual nr 2

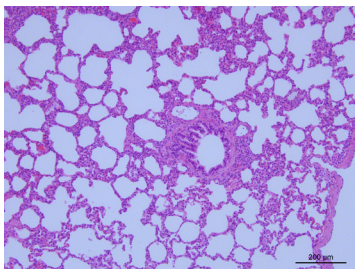

Bronchiole individual nr 3

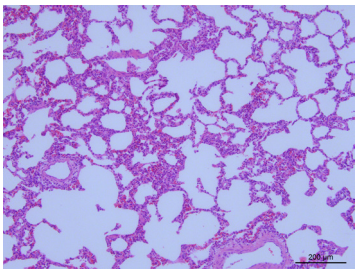

Alveoli individual nr 1

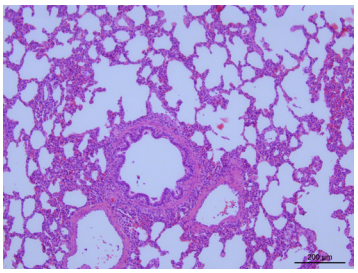

Alveoli individual nr 2

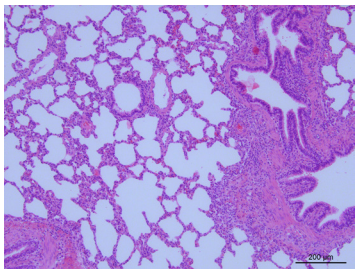

Alveoli individual nr 3

Annex I, figure 11. H&E staining on the porcine TMA consinstig of respiratory tract organs from six different individuals.

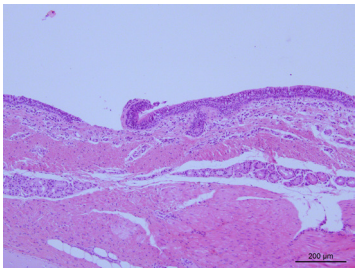

Upper trachea indivdual nr 4

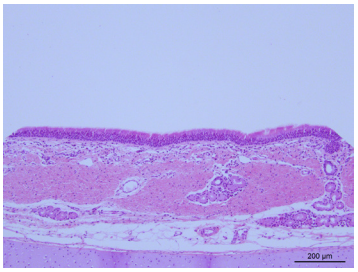

Upper trachea indivdual nr 5

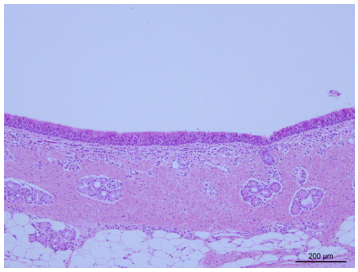

Upper trachea indivdual nr 6

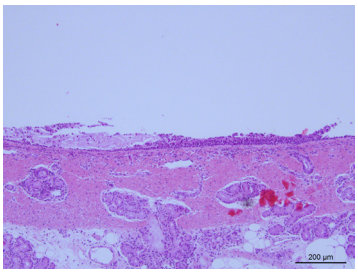

Mid trachea individual nr 4

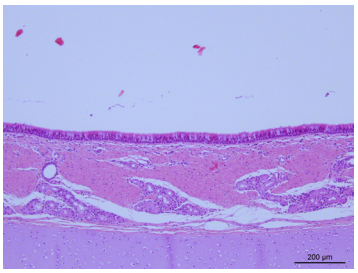

Mid trachea individual nr 5

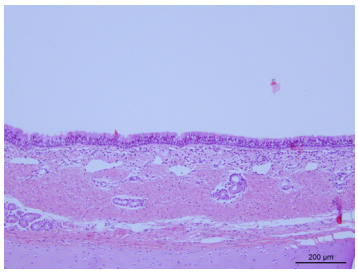

Mid trachea individual nr 6

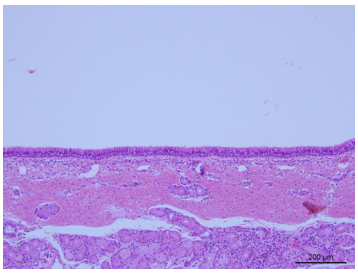

Lower trachea individual nr 4

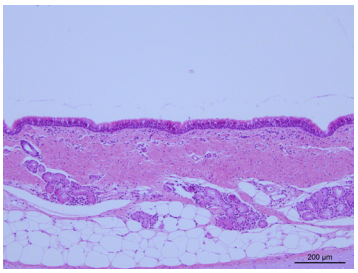

Lower trachea individual nr 5

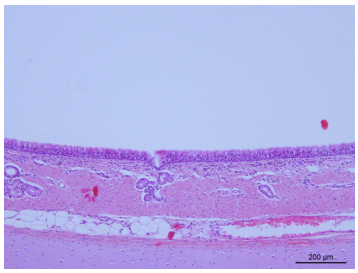

Lower trachea individual nr 6

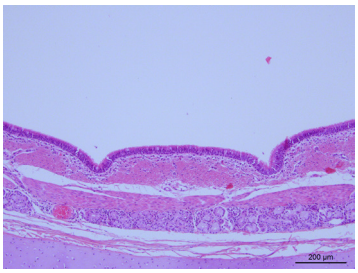

Primary bronchus individual nr 4

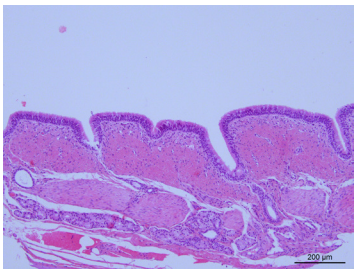

Primary bronchus individual nr 5

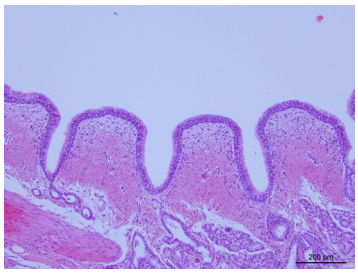

Primary bronchus individual nr 6

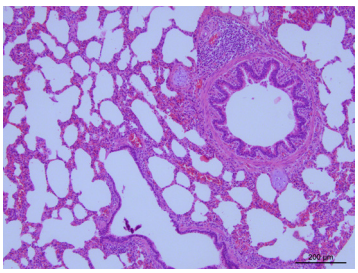

Bronchiole individual nr 4

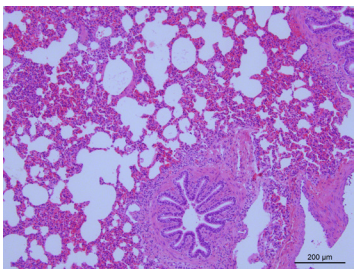

Bronchiole individual nr

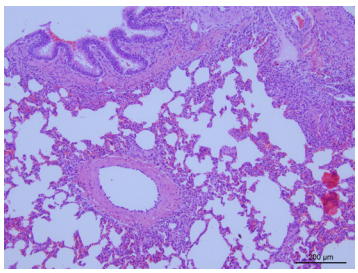

Bronchiole individual nr 6

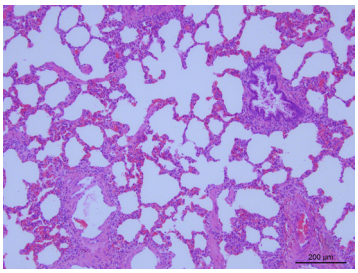

Alveoli individual nr 4

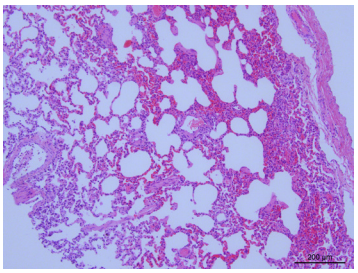

Alveoli individual nr 5

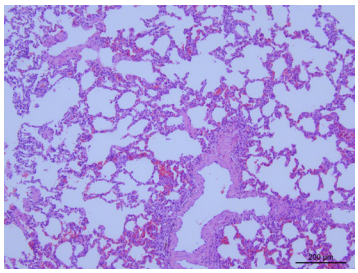

Alveoli individual nr 6

Annex I, figure 11 (continued). H&E staining on the porcine TMA consinstig of respiratory tract organs from six different individuals.

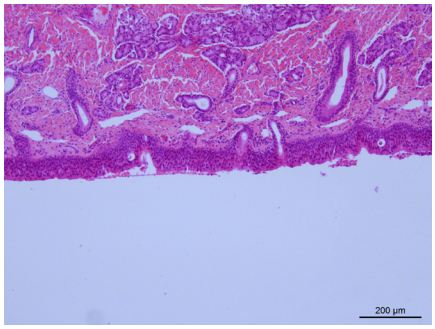

Nasal epithelium

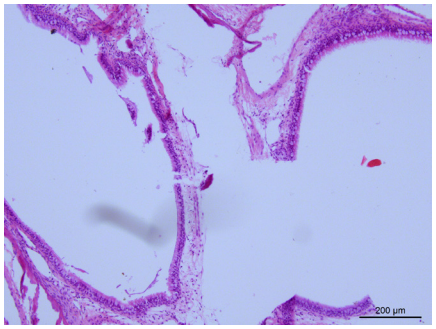

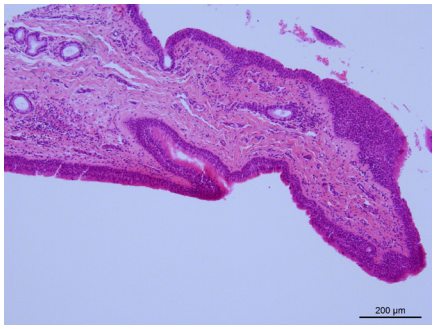

Orophar-ynx

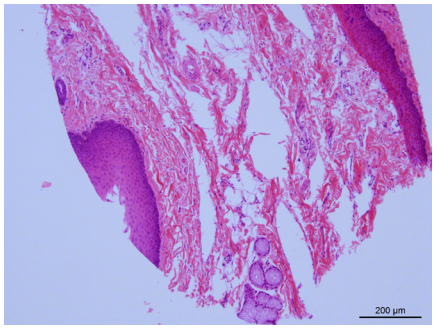

Equine

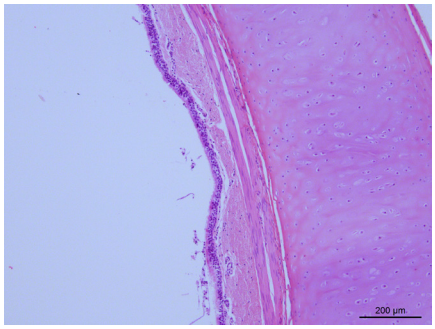

Primary bronchus

Damaged/unavailable core

Canine

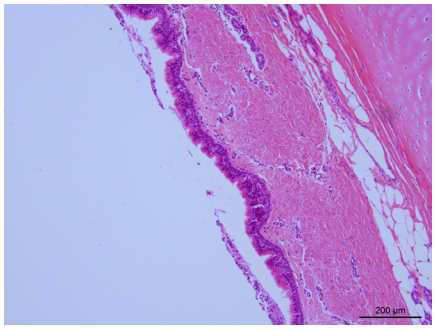

Upper trachea

Damaged/unavailable core

Damaged/unavailable core

Soft palate

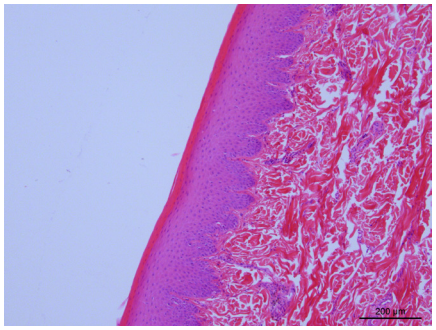

Annex I, figure 12. H&E staining on the respiratory tract tissues of equine and canine individuals.

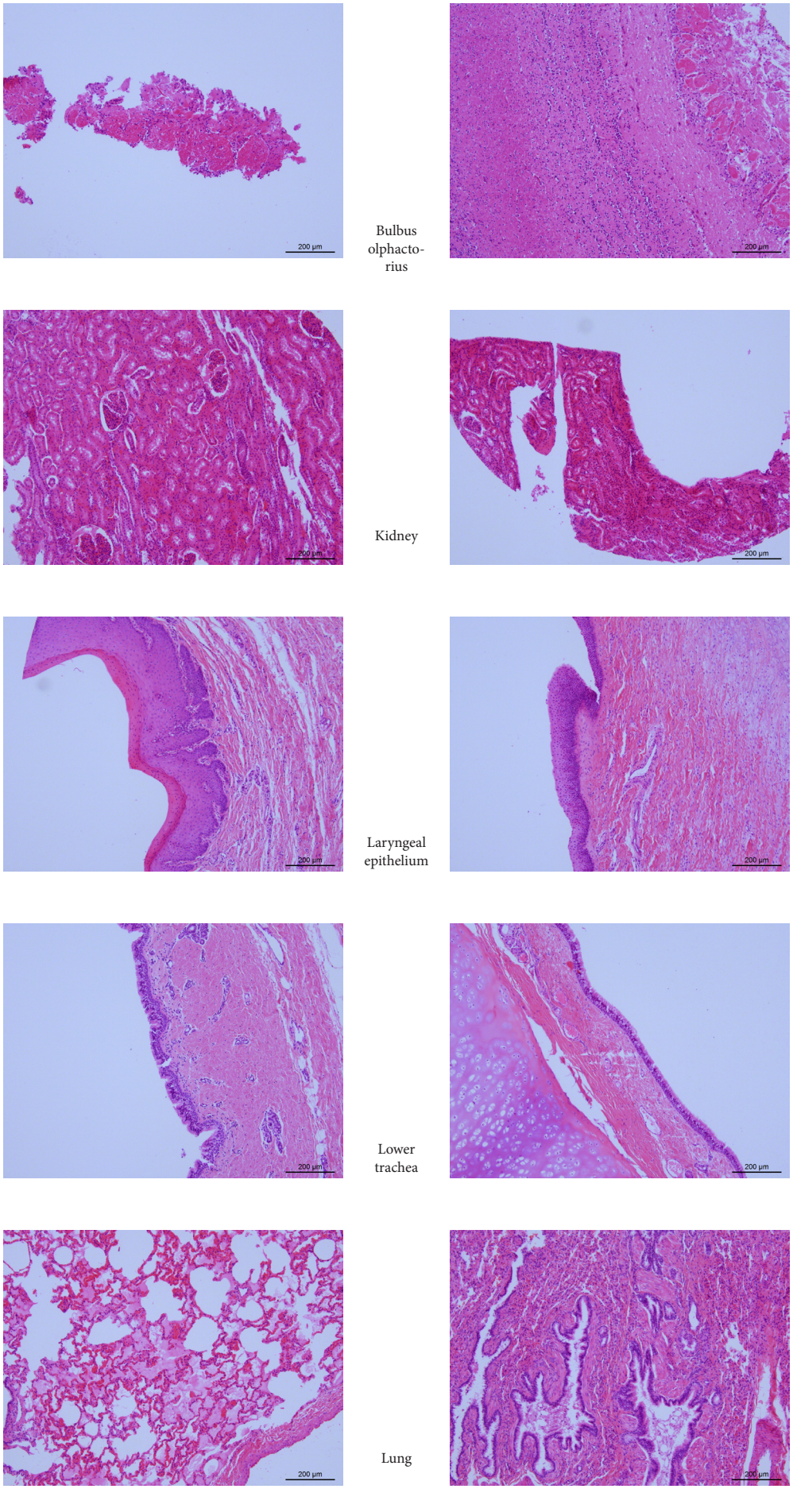

Annex I, figure 12 (continued). H&E staining on the respiratory tract tissues of equine and canine individuals.